School of Molecular and Life Sciences

Diagnostic Value of Multi-Slice CT Pulmonary Angiography in the Diagnosis of Pulmonary Embolism: An Investigation of Optimal Scanning Protocols in Terms of Image Quality, Contrast and Radiation Doses.

Sultan Aeyd Rashed Al-Dosari

This thesis is presented for the Degree of
Doctor of Philosophy
of
Curtin University

December 2018

Declaration

To the best of my knowledge and belief this thesis contains no material previously published by any other person except where due acknowledgment has been made.

This thesis contains no material which has been accepted for the award of any other degree or diploma in any university

The research presented and reported in this thesis was conducted in accordance with the National Health and Medical Research Council National Statement on Ethical Conduct in Human Research (2007) – updated March 2014. The proposed research study received human research ethics approval from the Curtin University Human Research Ethics Committee (EC00262), Approval Number HRE2016-0419

Signature 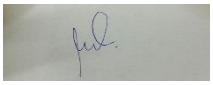

December 2018

Abstract

Computed tomography pulmonary angiography (CTPA) is currently the first line imaging modality for the diagnosis of patients with suspected pulmonary embolism (PE). However, radiation dose associated with CTPA still represents a major concern due to its potential risk of radiation-induced malignancy. Furthermore, use of contrast medium during CTPA is another concern because of contrast-induced nephropathy. Therefore, lowering radiation dose and contrast medium dose during CTPA examinations is the current research direction and this forms the focus of this study with the aim of addressing these issues through developing optimal CTPA protocols.

This research was performed in five stages with Stage 1 being a systematic review of the current double low-dose CTPA protocols to Stages 2-4 involving the design of a patient-specific 3D printed model and testing different CTPA protocols on the 3D printed pulmonary artery model with simulation of PE at the main and peripheral pulmonary arteries, while Stage 5 is a retrospective analysis of patients with confirmed PE by different CTPA protocols.

Stage 1 is a systematic review of studies reporting double low-dose CTPA protocols. Radiation dose reduction was found between 29.6 and 87.5% (range: 0.4 to 23.5 mSv) through analysis of 13 eligible studies. Use of low contrast medium volume was reported in 12 studies with reduction between 25 and 67% when compared to the standard protocol. Similar image quality (quantitative and qualitative assessments) was found in the low-dose group when compared to the standard group. This review shows the feasibility of using double low-dose CTPA in the diagnosis of PE.

Stage 2 involved development of a patient-specific 3D printed pulmonary artery. A realistic physical model was printed with the elastoplastic material with similar tissue property to that of arterial wall. The model was scanned on a 64-slice CT with 80, 100 and 120 kVp and pitch of 0.7, 0.9 and 1.2. Image quality analysis in terms of signal-to-noise ratio (SNR) was measured at the pulmonary trunk and main pulmonary arteries and compared between these protocols. The 3D printed model was found to be highly accurate in replicating normal anatomical structures with mean difference in diameter measurements <0.8 mm (<5% deviation in diameter). Up to 75% dose

reduction was noticed when kVp was lowered from 120 to 80 kVp without compromising image quality.

Stage 3 was conducted to identify optimal CTPA protocols by simulating PE in the main pulmonary arteries in the 3D printed model and test different scanning protocols on a 128-slice CT scanner. Simulation of PE was performed by inserting blood clots in the left and right main pulmonary arteries and the model was scanned with different kVp and pitch values, comprising 70, 80, 100 and 120 kVp, 0.9, 2.2 and 3.2 pitch. SNR was measured in the main pulmonary arteries to determine image quality corresponding to these protocols. Results showed no significant differences in image quality assessment when kVp was reduced from 120 to 80 kVp, or pitch was increased from 0.9 to 3.2 ($p>0.05$), indicating significant dose reduction of more than 80%. However, the CTPA protocol of 70 kVp and high pitch 3.2 led to suboptimal image quality with increased image noise, affecting visualisation of pulmonary artery wall and thrombus.

Stage 4 built up on the Stage 3's study by simulating PE in the peripheral arteries and tested different CTPA protocols on a latest CT scanner, 192-slice CT with images reconstructed with advanced iterative reconstruction (IR) model. Small blood clots were inserted into the peripheral pulmonary arteries with scans conducted using the same protocols as described in Stage 3. Further, qualitative assessment of image quality was performed by two experienced radiologists to score the images using a 5-point Likert scale. There were no significant differences in SNR across all CTPA protocols ($p>0.05$) with all images scored of 3 or more, indicating acceptable for diagnosis of PE. Results further confirmed the feasibility of low-dose CTPA protocols with images acceptable for detection of small emboli when kVp was reduced to 70 and pitch increased to 3.2, with resulting dose reduction of more than 80%. Findings concluded that low-dose CTPA protocol of 70 kVp and pitch of 2.2 or 3.2 is recommended with significant dose reduction while still producing diagnostic images.

Stage 5 is a retrospective study of double low-dose CTPA in patients with confirmed PE. Fifty-nine patients were recruited from a major tertiary hospital and patients were categorised into three groups: Group 1 comprised 23 patients who underwent CTPA of 100 kVp and pitch 0.9, Group 2 included 30 patients undergoing standard CTPA with 120 kVp and pitch 0.9, while group 3 consisting of 6 patients undergoing 120

kVp and high pitch 3.2. Qualitative and quantitative assessments (SNR and contrast-to-noise ratio-CNR) of image quality were performed and compared between these groups, while radiation dose and contrast medium volume were also compared to determine the dose reduction. No significant differences were found in SNR or CNR between the low kVp and standard kVp or high-pitch CTPA protocols ($p>0.05$). The effective dose for the 100 kVp CTPA protocol was highly significant lower than that for the 120 kVp and high-pitch protocols (2.43 ± 0.41 vs 4.66 ± 1.76 and 3.33 ± 0.60 mSv, $p<0.001$). The contrast medium was between 35-45 ml for the 100 and 120 kVp protocols, and 20-30 ml for the 120 kVp flash mode protocol. Subjective assessment shows good agreement between the two observers ($k=0.78$).

In summary, this project has shown that it is feasible to use low-dose CTPA protocols for the diagnosis of pulmonary embolism based on phantom experiments and patient data analysis. Lowering kVp from 120 to 70 and 80 and increasing pitch to 2.2 or 3.2 is possible with significant dose reduction of more than 80%, while maintaining diagnostic image quality. In the meantime, contrast medium volume can be reduced to 20 or 30 ml with acquisition of diagnostic images.

Acknowledgements

First and foremost, I am duty bound to express my enormous gratitude to Almighty Allah for His Infinite support and guidance.

In the same time, I would like to express indebtedness to my supervisor Professor Zhonghua Sun for his consistent support and availability throughout my study at Curtin University to guide me, address my inquiries and most importantly, teaching me how to write and prepare manuscripts, and vividly explaining certain concepts during the course of my research. His informed suggestion and criticism have indeed added value to the work, hence making it rigorous and productive.

Many thanks go to Prof Shirley Jansen as my PhD co-supervisor for her support and valuable advice from a clinical perspective. I would also like to show my solemn appreciation to all my bosom academic and professional colleagues- Dr Ali Al-Montashri, Dr Mansour Al-Moudi, Dr Mohamed Ramadan, Mr Philippe Elkhoury, Ali Al-Mary and Shag Alotabi for their tremendous support and encouragement.

I am grateful to my sponsor- Saudi Health Ministry. I have to thank them for supporting me and offering me the opportunity to pursue PhD at Curtin University.

Deep thanks go to my family and specifically my mother and late father. Words expressions will not suffice. Their encouragement has resulted in modest achievements. Last but not least, I would like to thank my siblings for their unwavering support and encouragement which was highly commendable.

List of publications included as part of the thesis

1. **Aldosari S**, Sun Z. A systematic review of double low-dose CT pulmonary angiography in pulmonary embolism. Curr Med Imaging Rev 2018 (Epub ahead of print) (IF=0.299)
2. **Aldosari** S, Jansen S, Sun Z. Optimization of computed tomography pulmonary angiography protocols using 3D printed model with simulation of pulmonary embolism. Quant Imaging Med Surg 2019;9: 53-62 (IF=2.231)
3. **Aldosari S,** Jansen S, Sun Z. Patient-specific 3D printed pulmonary artery model with simulation of peripheral pulmonary embolism for developing optimal computed tomography pulmonary angiography protocols. 2018 Quant Imaging Med Surg 2019;9: 75-85 (IF=2.231)
4. **Aldosari S**, Squelch A, Sun Z. Patient-specific three-dimensional printed pulmonary artery model: A preliminary study. Digital Med 2017;3(4):170-7.

Statements of contributions of others

Sultan aldosari input into this study and the associated papers include the execution of all the experimental work as well as a dominant contribution to the intellectual input involved in the project. As is almost always the case in conducting research studies with assistance by collaborators, other researchers made contributions to the work that were significant enough to warrant co-authorship on the resulting journal articles.

Sultan Al-Dosari 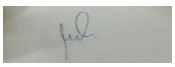 Prof. Zhonghua Sun 

List of additional publications relevant to the thesis but not forming part of it

1. Sun Z, **Aldosari S**. Three-dimensional printing-generated realistic anatomy models and virtual endoscopy-enhanced intravascular assessment of pathologies. Heart Res Open J 2018;5(1):e1-e4.
2. **Aldosari** S, Al-Moudi M and Sun Z. Double-low dose protocol of computed tomography pulmonary angiography (CTPA) in the diagnosis of pulmonary embolism: A feasible approach for reduction of both contrast medium and radiation doses, Heart Res Open J 2017; 4(2):33-38.

List of conference presentations

International conferences

1. **Al-Dosari** S, Sun Z. Optimisation of computed tomography pulmonary angiography protocols using 3D printed model with simulation of pulmonary embolism. 18th Asia-Oceania Congress of Medical Physics (AOCMP) in conjunction with the 16th South-East Asia Congress of Medical Physics (SEACOMP), 11–14 Nov 2018, Kuala Lumpur, Malaysia. Oral presentation.

2. **Al-Dosari** S, Sun Z. Patient-specific three-dimensional printed pulmonary artery model: A preliminary study. 18th Asia-Oceania Congress of Medical Physics (AOCMP) in conjunction with the 16th South-East Asia Congress of Medical Physics (SEACOMP), 11–14 Nov 2018, Kuala Lumpur, Malaysia. Poster presentation.
3. **Al-Dosari** S, Sun Z. Double low-dose CT pulmonary angiography in the diagnosis of pulmonary embolism. 18th Asia-Oceania Congress of Medical Physics (AOCMP) in conjunction with the 16th South-East Asia Congress of Medical Physics (SEACOMP), 11–14 Nov 2018, Kuala Lumpur, Malaysia. Poster presentation.
4. **Aldosari S**, Sun Z. Patient-specific 3D printed pulmonary artery model: A preliminary study. World Congress of Medical Physics and Biomedical Engineering, June 3-8, 2018, Prague, Czech Republic.
5. **Al-Dosari S**, Sun Z. CT pulmonary angiography in the diagnosis of pulmonary embolism: A systematic review of feasibility of using low-dose and low-contrast medium protocols. BIT"s 1st international biotechnology Congress, 26 April 2017, China. Oral presentation.
6. **Al-Dosari S**, Sun Z. 3D virtual intravascular endoscopy in the visualisation of aortic aneurysm and aortic dissection. The 11th Congress of the Asian Society of Cardiovascular Imaging, 11–13 Nov 2017, Kuala Lumpur, Malaysia. Poster presentation.
7. Sun Z, **Aldosari S,** Xu L, Fan Z. Left coronary bifurcation angle variation during cardiac cycle between coronary CT and invasive coronary angiography. ASMMIRT, Perth, 24-26, March, 2017. Poster presentation.
8. **Aldosari S**, Sun Z. A systematic review of feasibility of using double low dose protocol by coronary CT angiography. ASMMIRT, Perth, 24-26, March, 2017. Poster presentation.
9. **Al-Dosari** S, Sun Z. CT pulmonary angiography in the diagnosis of pulmonary embolism: A systematic review of feasibility of using low-dose and low-contrast medium protocols. The 72th Korean Congress of Radiology and Annual Delegate meeting of the Korean Society of Radiology October 2016, Coex, Seoul, Korea. Poster presentation.

National conferences

1. **Al-Dosari** S, Sun Z. Optimisation of computed tomography pulmonary angiography protocols using 3D printed model with simulation of pulmonary embolism. Annual Scientific Meeting of Medical Imaging and Radiation Therapist Conference (ASMMIRT), 20-21 Oct 2018, Perth. Oral presentation.
2. **Al-Dosari** S, Sun Z. Computed tomography pulmonary angiography-generated 3D virtual intravascular endoscopy in the diagnosis of pulmonary embolism. Annual Scientific Meeting of Medical Imaging and Radiation Therapist Conference (ASMMIRT), 06 June 2017, Perth. Oral presentation.

Table of Contents

List of abbreviations

ADMIRE	Advanced modelled iterative reconstruction
AIDR-3D	Adaptive iterative dose reduction 3D
ASIR	Adaptive statistical iterative reconstruction
ALARA	As Low as Reasonably Achievable
AEC	Automatic exposure control
ATCM	Automatic tube current modulation
BMI	Body mass index
CIN	Contrast-induced nephropathy
CNR	Contrast−to-noise ratio
CT	Computed tomography
CTPA	Computed tomography pulmonary angiography
CTDI	CT dose index
CTDIvol	Volume CT dose index
CTDIW	Weighted CT dose index
CXR	Chest x-ray
DICOM	Digital imaging and communications in medicine
DECT	Dual energy computed tomography
DECTPA	Dual energy computed tomography pulmonary angiography
DLP	Dose-length product
DSA	Digital subtraction angiography
DSCT	Dual-source computed tomography
DS-DECT	Dual-source dual energy computed tomography
ED	Effective dose
FBP	Filtered back projection
HU	Hounsfield unit

ICRP	International Commission on Radiological Protection
IR	Iterative reconstruction
IRIS	Iterative reconstruction in image space
kVp	Peak kilovoltage
LPA	Left pulmonary artery
mA	Milliampere
mAs	Milliampere second
MBIR	Model based iterative reconstruction
MDCT	Multidetector computed tomography
mGy	Milligray
MRI	Magnetic resonance imaging
MPA	Main pulmonary artery
MRPA	Magnetic resonance pulmonary angiography
mSv	Millisieverts
PE	Pulmonary embolism
PIOPED	Prospective investigation of pulmonary embolism diagnosis
ROI	Region of interest
RPA	Right pulmonary artery
SAFIRE	Sinogram affirmed iterative reconstruction
SD	Standard deviation
SNR	Signal-to-noise ratio
STL	Stereolithography
VIE	Virtual intravascular endoscopy
V/Q	Ventilation/perfusion
VSD	Ventricular septal defect
2D	Two dimensional

3D Three dimensional

List of Tables

List of Figures and Figure Legends

Chapter 1

Background and Introduction

1.1 Introduction

Pulmonary embolism (PE) represents a common cardiovascular disorder that is commonly encountered in clinical practice, especially for patients presenting to the emergency department (1). PE is a potentially fatal and life-threatening situation because if it is left unchecked without appropriate treatment, chronic PE could result in morbidity and mortality. PE presentations could vary from dyspnoea to pleuritic chest pain. It has been reported that the incidence of PE is 0.6–1.2 (1).

Diagnostic imaging plays a significant role in the diagnosis or exclusion of patients with suspected PE. Over the last decade, rapid progress has taken place in the use of various imaging modalities for diagnosis of PE, with improved diagnostic performance. Further, selection of appropriate imaging modalities may contribute only high diagnostic value, but also effective patient management and reduction of mortalities associated with PE (2).

1.2 Imaging diagnosis of pulmonary embolism

A variety of imaging techniques are involved in the diagnostic assessment of patients with suspected PE, including general chest x-ray (CXR), CT pulmonary angiography (CTPA) magnetic resonance angiography (MRA), nuclear medicine ventilation/perfusion (V/Q) scan, and invasive pulmonary angiography. Of these imaging modalities, CTPA is currently the method of choice for diagnosis of PE with sufficient evidence to support its clinical value in the literature. In the following sections, discussion of each imaging modality is reviewed with a focus on CTPA in the diagnosis of PE(3).

1.2.1 Chest x-ray

In the past (and for a significantly long time period) diagnosing PE was conducted using a thoracic imaging technique (CXR). CXR is widely known as a recommendable thoracic imaging technique and while there are better alternatives that have come into use in recent years, CXR is still performed often for the initial imaging test in a patient whose symptoms are associated with the chest. Of note is that CXR's contribution in diagnosis of PE is in provision of options (that are clear and diverse) of diagnosis of

symptoms in patients. Common abnormalities that include basal atelectasis, small pleural effusions as well as dilated pulmonary trunk (that occurs in central PE) and pulmonary infarct secondary to PE are difficult to be detected on CXR. There is a need for thoracic imaging that is more precise and highly accurate for diagnosis of PE (3, 4).

1.2.2 Pulmonary angiography

The imaging technique that was originally utilized in diagnosing PE was pulmonary angiography. However, this technique had a major limitation – it is invasive. When applying the technique, a specialized medical team as well as a catheter lab are needed to enhance proper functioning and in limiting its hazard. Additionally, the technique is linked with significantly mortality and morbidity. Over 1000 patients participated in a trial study that evaluated PIOPED (prospective investigation of pulmonary embolism diagnosis) and findings showed that pulmonary angiography is linked with a mortality rate of 0.5%. While pulmonary artery pressure contributes to the identified mortality rate, the degree of severity of the patient's clinical status also has a contribution (3, 5).

Conventional pulmonary angiography has come to be termed 'the gold standard' and evidence from studies such as the one conducted in 2005 and is cited in Yin et al (6). In the 2005 study, CTA's clinical value is found to be fundamentally identical to the one in conventional pulmonary angiography. Currently, CTA dominates as the preferred method in confirming or exclusion of PE. Preference of the approach is found on the high specificity, sensitivity as well as possession of overall predictive value that is associated with the approach to allow for clear diagnosis of acute PE. CTA can be easily accessed and promptly conducted although a limitation is patients may be exposed to radiation and in other cases intravenous contrast. The estimated number of patients who get exposed to contrast-induced nephropathy ranges between 6.5 to 19% of the patients who have undergone CTA(7) .

1.2.3 Nuclear scintigraphy

Beginning the 1960s, studies have been conducted on perfusion lung scintigraphy. Since perfusion lacks specificity, prompt identification of defects for pulmonary embolism would occur. Addition of ventilation scintigraphy with caution to ensure that any discrepancies between ventilation and perfusion (V/Q) are narrowed down to PE to cover potential synchronized abnormalities that may be suggestive for an alternative diagnosis (3). The initial imaging modality that is invasive was the V/Q scan and the approached performed almost similar to pulmonary angiography in the PIOPED study. In the context of a Ventilation phase that is based on ^{133}Xe and that includes a perfusion phase that employs $1.5x10^{8}$ Bq on ^{99m}Tc macro-aggregated albumin, a number of planar views are pointed out (3, 5).

A high percentage regarding inconclusiveness in results raises concerns as of the case in the PIOPED study (70% of conclusive results and 54% in another study) (8). It is primarily based on the V/Q study scan therefore the diagnostic harvest of the approach or method as a standalone test is severely curtailed. Even after considering the inconclusiveness of V/Q scan results, there is also an issue on the approach being integrated into diagnostic methods such as D-dimer measurement, and pre-test probability assessment whereby an estimated 95 percent of patients can be excluded from PE diagnosis (3).

1.2.4. MR pulmonary angiography

MR has limited value in the diagnostic assessment of PE. A comparison of two approaches gadolinium-enhanced MR angiography and reference standard – V/Q scan, D-dimer and CTPA was conducted according to the trial on PIOPED. The finding indicated the inadequacy of MRA (technical inadequacy) in a majority of the patients that participated (25%of the patients) (3).

In recent years, the occurrence of technological developments on pulmonary MR angiography has significantly influenced diagnosis of PE and other related medical

procedures. There have been improvements such as parallel imaging, pulmonary perfusion and view-sharing being applied. As a result of the improvements, the acquisition time of MR angiography has declined significantly. Additionally, spatial resolution has improved and the outcomes are not as highly vulnerable to motion artefacts. Other sequence types have also evolved and that enhance acquisition of image as well as introducing other functional information (5, 9).

Based on the information reviewed and the findings made, the overall sensitivity with regards to detecting thrombi within the pulmonary vasculature that supplies lingula is found to be 43% (that equals three of seven) for the entire imaging techniques that have been applied for MR. In the event that the approach is placed in contrast, embolus detection sensitivity that is detected in the segmental pulmonary vessels that remain and in association with MR imaging evaluation, the sensitivity ranges between 80 and 93%. Variations in sensitivity regarding detection of emboli in the lingula when comparison is made with pulmonary vascular anatomic segments that are also available show no significant difference ($p= 0.07$) (10).

1.2.5 CT pulmonary angiography

Multi-detector computed tomography angiography (MDCTA) is the preferred imaging modality for the diagnosis of patients suspected of PE, due to its less invasiveness, wide availability and high diagnostic accuracy(11). With 64- and post-64 slice CT widely available in clinical practice, CT pulmonary angiography (CTPA) has shown high diagnostic value in the detection of segmental and sub-segmental PE because of improved spatial and temporal resolution (12-14).

Due to advancements in technology, there has been widespread application of approaches such as MDCT. The objective of technicians (or specialists in development, design and sale of technological devices) has been to make improvements on image resolution, image thickness and allow for small and peripheral arteries to be better visualized (3, 5).

1.2.5.1 4 to 16-slice CT pulmonary angiography

MDCTA has become a popular and an excellent choice to use in the examination of pulmonary arteries. Emboli detection has traditionally been left to single slice imaging that has long been constrained by limitations found when scanning the pulmonary central vessels to segmental levels. Multi-slice CTA has been able to provide practitioners with a much needed solution with a greater ability in the detection of sub-segmental vessels when high resolution algorithms are applied (15).

The key factor for the detection of peripheral emboli is determined by the use of high spatial resolution. In the current study, PE has been detected in more selected patients with a 16-slice scanner which renders a 1 mm thickness. The study showed better results with this device compared to results from the 4-slice using 2-3 mm thickness scanner. However, the results of the study did not render significant differences. Instead, this study is comparable to the more positive resulting previous cases (16).

While studying the single-slice scanner with the multi-slice CTA method, noticeable differences could be seen in the visual quality of the pulmonary arteries. Sub-segmental and segmental arteries were better observed using 4 slice CTA with collimation settings at 1.25 mm. Both 4-slice and 16-slice CTA also perform additional tests to determine the possibility of pulmonary embolism (17).

1.2.5.2 16-64-slice CT pulmonary angiography

With the next generation CT scanners becoming more widely available such as the 16-64 slice MDCT and the even-slice MDCT, more patients are being correctly diagnosed particularly for those who have smaller isolated peripheral emboli which has been traditionally harder to detect with earlier model scanners (18).

MDCT devices were first introduced in 1998. Since the implementation of better CT scanners, non-invasive forms of vascular imaging is continuously improving. The current generation of MDCT scanners provides professionals with a simultaneous acquisition technique. The improved devices can perform scans from 16 to 64 sub-millimeter slices. The rotation time of the gantry is as low as 330 milliseconds. The spatial and temporal resolutions are also improving scanning times and are greatly

reduced when compared to the traditional 1 and 4-slice MDCT devices. The use of the MDCT modality has become the industry standard in the identification of chronic and acute PE due to its speed and nearly isotropic resolution (19).

Current models of MDCT scanners show improvements in visualization of arteries using thin slice collimation as its primary protocol. One of the limitations of CT was its inability to identify certain sub-segmental PE. However, innovation in the next generation of scanners has attempted to overcome this problem and can now provide more comprehensive diagnostic images (19).

1.2.5.3 Post 64-slice CT pulmonary angiography

While devices with the ability to scan with up to 320 and 640 rows are currently available, optimal detection for PE is mainly dependent upon the type of device available at the imaging facility. In the use of 4 to 8 row scanners, a compromise must be made between collimation and scan duration. However, with 16 to 64 row devices, the entire chest can be imaged in under 5 seconds while the collimation is set at 1 mm or less. Scanners with even faster scanning periods can image the whole chest in under a second (20).

The current generation of CT scanners not only bring better spatial resolution at faster scanning periods, but also deliver more enhanced images with fewer noise artefacts. The improvements provide higher sensitivity and become successful in the detection of distal PE in sub-segmental arteries. Newer CT scanners also provide practitioners with better reconstruction of images with optimal contrast media dynamics. The improvement in image quality allows for less noise artefacts and decreased dosages of radiation. Differences between the traditional single row scanners and the newer generations are greater than the 64-MDCT and multi-source 320-MDCT (12,21). The 320-MDCT uses a cone-beam acquisition which can cover an area of 160 mm. Improved CT technology can provide diagnostic accuracy with sensitivities of 92% with specificities reaching 95% (22).

Current CT image acquisition can provide a view of 0.5 to 1 mm thick depending upon the multi-detector modality chosen. The decreased thickness view can provide a more accurate image of PE with the decrease in volume averaging (20). In thin-slice images of the lungs taken to provide a view of the pulmonary arteries, the need of more images is required compared to the traditional single-slice CT scanners influencing the time duration of images (19).

1.3. Double low-dose CT pulmonary angiography

The double low-dose CTPA method is chosen by professionals in assessing PE using lower kV voltage and lower contrast dosages. While a number of techniques are used to lower the dosages of radiation, low voltage kV is the most widely selected. The method is preferred in cardiovascular and angiographic imaging. As recommended by the Society of Cardiovascular CT guidelines, the kV voltage tube selection should be made according to the patient's body mass index (BMI) (14). Lower kV settings of under 100 kV should be used on patients with smaller BMI. Decreased kV voltage values has proven to be highly useful in CT angiography because of the enhanced visualization of vessels while using contrast media. As observed in Boos' research, increased vascular attenuation can be achieved with lower voltage in kV selected group (23). The method of lower kV also provides an ability to use lower dosages of contrast media when compared to the use of other CT techniques for pulmonary angiography. The study also observed that higher image quality could be achieved in patients with higher BMI (23).

The Boos et al research provides a good example of the results of lowered kV tube voltage to achieved quality images for the diagnosis of PE. In one group, a setting of 70 kV during a simultaneous dual-source CTPA was used with patient's BMI lower than 35 kg/m^2 (23). In a number of other studies, further reduction in contrast media during CTPA has shown not to compromise image quality (24, 25). It can be thus assumed that the best method of reducing radiation dosages during image acquisition would be to employ reduced kV tube voltage and lower amounts of

contrast agents (26). Other methods of achieving quality imaging while using lower contrast dosages include faster injections velocity during the first pass exam (27).

1.3.1 CT pulmonary angiography-low radiation dose protocol

Medical Physicist and clinical professionals have agreed that the common goal of reduction in radiation exposure in the diagnosis of PE is to develop protocols, methods and technology to reduce the amount required (24). CT modality still requires the use of high radiation dose. However, constant research and developments are taking place each year to identify and implement methods and strategies that can decrease the volume and exposure times. In cardiovascular CT such as coronary angiography or CTPA, practitioners are constantly developing methods to reduce radiation exposure (23). Because of the risks that radiation exposure could potentially cause in certain patients, such as younger aged patients, medical imaging professionals are constantly seeking better alternatives in further radiation exposure reduction. A number of studies have revealed that CTPA protocols that employ 80 kV tube voltage have achieved 50 to 70% reductions when compared to the traditional 120 kV settings (24, 28).

Overall, it has been the success of the medical imaging industry from practitioners to manufacturers that efforts to lower the amount of radiation needed to perform methods of CT have been reduced to its current levels. The "As Low as Reasonably Achievable" (ALARA) principle has become the standard in medical imaging. With the age of patients becoming younger for the potential diagnosis for PE, imaging professionals are attempting to make every change available to them in the reduction of radiation (20). New techniques are being developed that can further reduce radiation by making the current and potential of tube kV selectable according to BMI. The addition of lower kV requirements and further decreases in the volumes of contrast media may not only assist in the achievement of lower dosages, but also improve image quality. With higher imaging reconstruction algorithms that deliver images with fewer noise artefacts, fewer images are required, thus a decrease in dose can be achieved. For example, the automatic exposure control (AEC) or tube current modulation algorithm found in a number of CT scanners are able to use 3D Smart mA which is used in radiology to perform a scout view (29).

1.3.2 CT pulmonary angiography-low contrast medium protocol

A number of studies have focused on the protocols of delivery of contrast media to meet enhanced attenuation while still decreasing the dosage (30, 31). The concern of researchers is to identify a technique that can decrease the amount of exposure to radiation and the major cause of contrast-induced nephropathy (CIN). Studies have argued that decreasing the amount and dose would decrease the chances of CIN (32). The BMI of 100 kg has been observed to display positive results in decreased tube voltage to 80 kV during CTPA (33). Further reduction in contrast doses are also shown to be effective in decreasing the risks of CIN (34).

1.4. Dual-Energy CT scan

Another medical imaging development in CT is the dual-energy CT or the DECT. The DECT method provides two datasets known as the quasi-simultaneous and the double simultaneous when using different energy levels. Normal radiation doses have been observed to be at standard levels in single energy CTPA. However, dual-energy module provides a number of advantages. The advantages include material differentiation with greater ability in reconstructing virtual monoenergetic images for better images. The differences that are observed in perfusion maps provide greater viewing of pulmonary arteries leading to a decrease in contrast doses (30).

With the advantages provided by DECT, a number of studies have emerged in acute PE since its introduction. With the use of two X-ray tubes that employ high and low peak kilovolt levels, better images can provide more optimal representation when used in imaging lung parenchymal perfusion. Research suggests that the presence of perfusion defects may be used as prognostic markers in certain patients (3). Newer scanners equipped with dual-source technology offer more functional data in images of lung perfusion in detecting the presence of PE. As CT technology progresses,

software packages are becoming better at detecting PE and other anomalies in shorter imaging periods. The current advancements in technology has been vast in recent years. However, much more research needs to be completed in the diagnostic algorithms of acute PE detection (20). The least amount of time required in each imaging period also leads to the advantage of lowering the radiation dose exposure to patients (35).

However, in studies with patients who are suspected to have PE, the proposed benefits of CTPA would outweigh potential hazards. Mortality rates for patients with untreated PE often undocumented. However, estimates suggest that the mortality rate for PE may be as much as 30%. Risks associated with radiation dose levels during diagnostic CT have not been fully studied. Hypothetically, reported risks in cancer due to radiation exposure during diagnostics may be less than 1%. When comparing the risk of radiation during diagnostic imaging and occurrence of cancer in high risk groups such as younger women, identification of PE seems to be the most likely choice. The typical percent of the population that undergo CT pulmonary angiographies are normally the aging. This group is generally viewed to be at a lower risk of developing cancer from radiation dosages associated to imaging modules (12).

The next generation model CT scanners are equipped with higher isotropic spatial imaging capabilities. Newer models allow radiologist to take faster images with more enhanced quality and decreased artifacts associated with motion. When considering corollary, newer technology provide higher sensitivity in the detection of distal PE. Another advantage that has been observed in the newest models of CT scanners is the availability of optimization selection in contrast bolus dynamics. The improvements in optimization would provide higher imaging reconstruction options with better quality images with decreased noise artifacts and lower radiation dosages (12).

1.5. Low kVp CT pulmonary angiography

Once imaging professionals deploy more advanced techniques in dose modulation such as modulating tube currents, peak voltage switching and beam geometry settings, better results can be observed. Radiologist using quicker high-pitch imaging available in dual-source devices and better reconstruction methods that decrease noise effects are able to lower dosages of radiation and achieve images without significant loses to quality (12).

It is also important to note the advantages to expanding upon more automatic techniques that sustain consistent attempts in the reduction of radiation dosages. The AEC is normally available from major scanner manufacturers and provides a solution by adjustable tube currents for x-ray beam attenuation according to body tissue and mass (36).

One notable factor in CT scanners and low kV, is that traditionally, lower kV is shown to increase noise. However, it is observed that contrast-to-noise ratio (CNR) is also enhanced. Lower kV has been associated with improvements in intravascular CT values under CTA as increased photoelectric effects also increase detection rating in iodine contrast materials. Studies have suggested that decreases in kV from 120 to 100 volts, CT values of contrast in materials such as iodine have been observed to increase up to 17%. With this factor in mind, low kV and the addition of lower concentrated contrast materials may provide similar results in CT values of traditional modules. Lower kV requires a lower concentration of contrast, otherwise the use of higher concentration would increase banded artifacts leading to limited image quality. In the current study, no major differences were observed in CT values in group using 100 kV and different groups suggesting that low kV may lead to enhanced intravascular CT values (37).

In traditional methods, decreasing the tube voltage in CT is the method most often attributed to decreasing radiation dosages in patients despite the increase of noise. In virtual monoenergetic methods, low voltages tend to lead to higher attenuation of contrast. The loss of tissue penetration added with higher photoelectric effects observed in low x-rays cause contrast enhancements which also decrease the need to use higher volumes of contrast material. A number of studies have provided evidence that contrast-associated kidney injuries during CT are considered low. However,

standard practice of decreased volumes of contrast medium is still an important objective among imaging professionals (30). It is also important to remember that lower tube voltages on average to small body mass patients can lead to more improvements in images associated with CT angiograms and other methods which use high amounts of contrast such as diagnostic images for renal stones (38).

A variety of tube voltages are available to be selected for CT imaging in accordance with the patient body size or specific to CT modulation. It has been observed that decreasing the tube voltage by as much as between 120 kV to 80 kV may provide an overall decrease in the exposure of radiation in small and average sized patients and should be a goal of imaging professionals (38).

There are currently a number of studies that have focused on contrast medium injection protocols under lower tube voltage scenarios. In examining reduction in the standard 120 kV, a reduction of 100 kV has led to discoveries of reduced exposure and the need for large amounts of contrast by 33% (30). Research has also observed lower tube voltage for CTPA may increase visualization of the peripheral and central arteries while sustaining quality images and diagnostic accuracy. Additionally, the use of automated tube voltage algorithms can be selected for the most optimal dose-efficient setting for patients according to the individuals size and anatomy when planning the range of image acquisition (30).

Studies suggest that the use of a lower setting for kVp leads to a number of advantages. Research in CTPA protocols propose limiting the volume of contrast media while decreasing the patients risk to contrast related injury such as nephropathy. Lower dose of radiation can be achieved by lower contrast amounts. These CTPA protocols could potentially be useful in the search for methods of minimizing risks of exposure and solutions in the prevention of contrast induced events (39).

As the continued improvements in the developments of imaging methods and technologies accelerate, more advantages are being discovered. Low peak kVp methods ranging between 70-80 kV added to high-pitch imaging has led to major reduction of contrast for CTPA down to 9-21g. Lower kVp is currently set at 70-80 kVp as a standard shared between manufacturers because of the efficiency in X-ray

tubes that have insufficient photon emission causing imaging noise during lower kVp settings (40).

There are a number of methods that demand reduction of radiation when dealing with CT angiography. For example, attenuation of tube voltage shows promising reduction in radiation exposure. Exposure generally increases with the amount of voltage. Imaging methods which are taken at low voltages increase clarity because of the k-edge in iodine reducing the amount of contrast needed. High-pitch imaging also provides a method of lowering radiation exposure during CT angiography(32).

1.6. Use of iterative reconstruction in CTPA

The method of filtered back projection (FBP) is considered the more widely used technique in CT reconstruction. However, the recently widespread use of iterative reconstruction (IR) such as adaptive statistics iterative reconstruction (ASIR) has been developed as a means to decrease noise. The method was developed to reconstruct projected data using the FBP technique and showed improvements from 25 to 50% dosage reduction (41, 42).

Algorithms have been introduced in IR which have added to the strategy of reducing noise while enhancing the quality of images with lower dosages. Combinations of high-pitch low kV and IR for CTPA have been observed to reduce dosages of radiation up to 52% with contrast media of 20 mL and lower protocol dosages. Researchers are optimistic that further reduction of dosages and CTPA can be achieved (43).

Model-based iterative reconstruction (MBIR) is a popular technique in iterative reconstruction as it tends to model the x-ray beam, when traveling from the cathode to detectors. The modeling changes the shape of the focal spot on the anode and as it emerges from the anode, 3-dimensional interaction with the voxel and 2-dimensional interaction in the detector. Through modeling optical constructs, MBIR can be sustained while providing improvements in quality of images by the spatial resolution and lower noise artifacts (41).

While the demand for CT continues, the search for lower dose techniques are increasing. However, FBP reconstruction introduces limits in reducing radiation dosage. This is the case with higher spatial resolution and smaller image slice thickness are attempted. The reduction of dosage in CT has therefore shifted its focus away from hardware and tube current to the current development of reconstruction algorithms. Noise model-based IR such ASIR, iDose and sinogram affirmative iterative reconstruction (SAFIRE) are new software types of CT algorithms that use statistical models to reduce the noise in the image and with good image quality(44). The new IR techniques are becoming commonplace in clinical practices and demonstrate acceptable clinical imaging with reduced dosage from 32 to 65% (45).

1.7. Low tube current in CTPA

Tube current adjustments have become a system which prefers to use automatic techniques that vary according to the types of scanners used the level of kV settings (36). At the beginning of this research it was discussed that current dose modulation software provided by most imaging device manufacturers is considered among professionals as the standard versions. Software is designed to control the tube current while dosage can be adjusted according to the patient's body mass, geometry and rate of absorption during acquisition. The software replenishes and can even compensate according to the different dose requirements across the different body types and cross-sections like shoulder areas and air-filled chests. To ensure that the image quality is maintained among the different body types and images, adaptive tube current modulation can be used to reduce dosages even further up to 10 to 50 percent according to the area of the body being imaged such as chest, diaphragm or shoulder regions (20).

Automatic exposure control for X-ray modalities have been around for a number of years. Tube-current modulation is currently undergoing a number of developments to further be able to reduce the amount of dose radiation. However, there are still a number of limited options currently available. For example, in the *z*-direction of mA measurements still depend on scout views in both lateral and AP. Dose modulation in the tube currents in *x*-*y*-plane imaging by rotation tube while dealing

with attenuation in patient body mass different projections. Modulation in automatic tube-current was also a high point address by the International Commission on Radiological Protection (ICRP) and addressed by it was currently the best way to reduce radiation dose during CT scans compared to other options currently available (46). Modulation in the x-ray beam is also based on attenuation of body mass and tissues acquired in x-ray projection radiographs or SPRs while attempting to maintain quality images. Adjustments of the x-ray tube during rotation with smaller diameter anterior-posterior direction while using lower exposures than what is seen in the lateral position has also shown promising results. Adjustments can also be made during the scans progression using high tube current for thicker regions such as lateral shoulder or hip areas. Reduction in the tube current in areas of soft tissue attenuation is also ideal in abdomen and chest regions. Automatic tube current modulation (ATCM) systems are observed to be able to change exposure levels in accordance with patient's size and gives an advantage of a more uniform level of quality for patients as seen in the employment of automatic exposure control currently available in radiographic systems (47-49).

Tube current modulation is one of the most important parameters according to practitioners in the more modern models of CT scanners for the purpose of reduction of radiation dosages in patients. The methods available for adjusting the tube current are considered important to the ability to maintain a constant in noise levels of images according to the patient's body mass, profile x-ray and other parameters including the kilovolt, pitch beam coverage area, table speed and the rotation time. It can be noted that the modulation methods that include dose and tube current can be decreased through automatic models in accordance with the patient's imaged areas using low attenuation and still maintain a focus on noise levels while imaging quality is attended. Techniques or methods which use the angular modulation is sure to include major variables. The variables include tube current during the rotation around the patient even though modulation in the z-axis includes the variable mAs as directed along the z-axis (50).

1.8 Aim and objectives

The research project is designed to assess the image quality, radiation dose and the volume of contrast medium associated with CT pulmonary angiography with the latest CT scanners in patients with suspected pulmonary embolism. The study is expected to achieve the following objectives:

1. To identify factors that affect image quality, radiation and contrast doses of CT pulmonary angiography in pulmonary embolism.
2. To develop optimal scanning protocols of CT pulmonary angiography based on 3D printing physical pulmonary artery model with simulation of thrombus in the pulmonary arteries.
3. To implement the optimal scanning protocols of CT pulmonary angiography in clinical settings with the aim of determining clinical value of optimal CT pulmonary angiography.

1.9 Thesis Outline

This thesis is composed of seven chapters with each chapter presenting individual contents. This chapter (Chapter 1) is a general introduction and background of various imaging modalities in the diagnosis of pulmonary embolism with a focus on CT pulmonary angiography and associated dose-reduction strategies.

Chapter 2 is a systematic review of double low-dose CT pulmonary angiography protocols through analysis of 13 studies with the aim of reducing radiation dose and contrast medium dose. Chapter 3 consists of study design of a patient-specific 3D printing pulmonary artery model with testing various CT pulmonary angiography protocols. Quantitative assessment of image quality and model accuracy in terms of replicating normal pulmonary artery anatomy are assessed in this chapter with results published in a refereed journal, Digital Medicine.

Chapter 4 tests different CT pulmonary angiography protocols on the developed 3D printed pulmonary artery model on 128-slice dual-source CT scanner with simulation of thrombus in the main pulmonary arteries. A series of scans comprising different kVp and pitch values are performed on the model with optimal CT scanning protocols identified through quantitative assessment of image quality. Chapter 5 focuses on simulation of peripheral emboli in the distal pulmonary arteries on the 3rd generation dual-source CT scanner with use of the same scanning protocols as used in Chapter 4, with the aim of determining optimal scanning protocols for detection of peripheral pulmonary embolism based on qualitative and quantitative assessments. Chapter 6 involves recruitment of patients with confirmed pulmonary embolism who undergo different CT pulmonary angiography protocols including 100 and 120 kVp with standard pitch, and 120 kVp with high pitch of 3.2 with use of different contrast volumes. Quantitative assessments of image quality are included for comparison of these protocols. Chapter 7 is a summary of key findings and future research directions with regard to CT pulmonary angiography in the diagnosis of pulmonary embolism.

1.10 References

1. Chen H, Chen R-c, Guan Y-b, Li W, Liu Q, Zeng Q-s. Correlation of Pulmonary Function Indexes Determined by Low-Dose MDCT With Spirometric Pulmonary Function Tests in Patients With Chronic Obstructive Pulmonary Disease. American Journal of Roentgenology. 2014;202(4):711-8.
2. Stein PD, Athanasoulis C, Alavi A, Greenspan RH, Hales CA, Saltzman HA, et al. Complications and validity of pulmonary angiography in acute pulmonary embolism. Circulation. 1992;85(2):462-8.
3. Robert-Ebadi H, Le Gal G, Righini M. Evolving imaging techniques in diagnostic strategies of pulmonary embolism. Expert Review of Cardiovascular Therapy. 2016;14(4):495-503.
4. Sherk WM, Stojanovska J. Role of Clinical Decision Tools in the Diagnosis of Pulmonary Embolism. American Journal of Roentgenology. 2016;208(3):W60-W70.
5. Righini M, Robert-Ebadi H, Le Gal G. Diagnosis of pulmonary embolism. La Presse Médicale. 2015;44(12, Part 2):e385-e91.
6. Yin F, Wilson T, Della Fave A, Larsen M, Yoon J, Nugusie B, et al. Inappropriate Use of D-Dimer Assay and Pulmonary CT Angiography in the Evaluation of Suspected Acute Pulmonary Embolism. American Journal of Medical Quality. 2012;27(1):74-9.
7. KOOIMAN J, KLOK FA, MOS ICM, VAN DER MOLEN A, DE ROOS A, SIJPKENS YWJ, et al. Incidence and predictors of contrast-induced nephropathy following CT-angiography for clinically suspected acute pulmonary embolism. Journal of Thrombosis and Haemostasis. 2010;8(2):409-11.
8. Anderson DR, Kahn SR, Rodger MA, Kovacs MJ, Morris T, Hirsch A, et al. Computed tomographic pulmonary angiography vs ventilation-perfusion lung scanning in patients with suspected pulmonary embolism: a randomized controlled trial. Jama. 2007;298(23):2743-53.
9. Hochhegger B, Ley-Zaporozhan J, Marchiori E, Irion K, Soares Souza A, Moreira J, et al. Magnetic resonance imaging findings in acute pulmonary embolism. The British Journal of Radiology. 2011;84(999):282-7.
10. Kalb B, Sharma P, Tigges S, Ray GL, Kitajima HD, Costello JR, et al. MR Imaging of Pulmonary Embolism: Diagnostic Accuracy of Contrast-enhanced 3D MR Pulmonary Angiography, Contrast-enhanced Low–Flip Angle 3D GRE, and Nonenhanced Free-Induction FISP Sequences. Radiology. 2012;263(1):271-8.
11. Martini K, Meier A, Higashigaito K, Saltybaeva N, Alkadhi H, Frauenfelder T. Prospective Randomized Comparison of High-pitch CT at 80 kVp Under Free Breathing with Standard-pitch CT at 100 kVp Under Breath-Hold for Detection of Pulmonary Embolism. Academic Radiology. 2016;23(11):1335-41.
12. Araoz PA, Haramati LB, Mayo JR, Barbosa EJM, Rybicki FJ, Colletti PM. Panel Discussion: Pulmonary Embolism Imaging and Outcomes. American Journal of Roentgenology. 2012;198(6):1313-9.
13. Wittram C, Maher MM, Yoo AJ, Kalra MK, Shepard JAO, McLoud TC. CT angiography of pulmonary embolism: diagnostic criteria and causes of misdiagnosis. RadioGraphics. 2004;24:1219.
14. Raff GL, Chinnaiyan KM, Cury RC, Garcia MT, Hecht HS, Hollander JE, et al. SCCT guidelines on the use of coronary computed tomographic angiography for patients presenting with acute chest pain to the emergency department: a report of

the Society of Cardiovascular Computed Tomography Guidelines Committee. Journal of cardiovascular computed tomography. 2014;8(4):254-71.
15. Prokop M. Multislice CT angiography. European Journal of Radiology. 2000;36(2):86-96.
16. Ritchie G, McGurk S, McCreath C, Graham C, Murchison JT. Prospective Evaluation of Unsuspected Pulmonary Embolism on Contrast Enhanced Multidetector CT (MDCT). Thorax. 2006.
17. Stein PD, Fowler SE, Goodman LR, Gottschalk A, Hales CA, Hull RD, et al. Multidetector Computed Tomography for Acute Pulmonary Embolism. New England Journal of Medicine. 2006;354(22):2317-27.
18. Douma R, Hofstee H, Schaefer-Prokop C, Lely R, Kamphuisen P, Gerdes V, et al. Comparison of 4-and 64-slice CT scanning in the diagnosis of pulmonary embolism. Thrombosis and haemostasis. 2010;103(1):242-6.
19. Heuschmid M, Mann C, Luz O, Mahnken AH, Reimann A, Claussen CD, et al. Detection of pulmonary embolism using 16-slice multidetector-row computed tomography: evaluation of different image reconstruction parameters. Journal of computer assisted tomography. 2006;30(1):77-82.
20. Hartmann IJC, Wittenberg R, Schaefer-Prokop C. Imaging of acute pulmonary embolism using multi-detector CT angiography: An update on imaging technique and interpretation. European Journal of Radiology. 2010;74(1):40-9.
21. Kroft LJM, Roelofs JJH, Geleijns J. Scan time and patient dose for thoracic imaging in neonates and small children using axial volumetric 320-detector row CT compared to helical 64-, 32-, and 16- detector row CT acquisitions. Pediatric Radiology. 2010;40(3):294-300.
22. Sauter A, Koehler T, Fingerle AA, Brendel B, Richter V, Rasper M, et al. Ultra Low Dose CT Pulmonary Angiography with Iterative Reconstruction. PLOS ONE. 2016;11(9):e0162716.
23. Boos J, Kröpil P, Lanzman RS, Aissa J, Schleich C, Heusch P, et al. CT pulmonary angiography: simultaneous low-pitch dual-source acquisition mode with 70 kVp and 40 ml of contrast medium and comparison with high-pitch spiral dual-source acquisition with automated tube potential selection. The British journal of radiology. 2016;89(1062):20151059.
24 Aldosari S, Al-Moudi M, Sun Z. Double-Low Dose Protocol of Computed Tomography Pulmonary Angiography (CTPA) in the Diagnosis of Pulmonary Embolism: A Feasible Approach for Reduction of Both Contrast Medium and Radiation Doses. Heart Research Open Journal. 2017;4(2):33-8.
25. Hu X, Ma L, Zhang J, Li Z, Shen Y, Hu D. Use of pulmonary CT angiography with low tube voltage and low-iodine-concentration contrast agent to diagnose pulmonary embolism. Scientific Reports. 2017;7(1):12741.
26. Laqmani A, Kurfürst M, Butscheidt S, Sehner S, Schmidt-Holtz J, Behzadi C, et al. CT Pulmonary Angiography at Reduced Radiation Exposure and Contrast Material Volume Using Iterative Model Reconstruction and iDose4 Technique in Comparison to FBP. PLOS ONE. 2016;11(9):e0162429.
27. Aschoff AJ, Catalano C, Kirchin MA, Krix M, Albrecht T. Low radiation dose in computed tomography: the role of iodine. The British Journal of Radiology. 2017;90(1076):20170079.
28. Duan X, Wang J, Christner JA, Leng S, Grant KL, McCollough CH. Dose reduction to anterior surfaces with organ-based tube-current modulation: evaluation of performance in a phantom study. American Journal of Roentgenology. 2011;197(3):689-95.

29. Zhao YX, Zuo ZW, Suo HN, Wang JN, Chang J. A Comparison of the Image Quality and Radiation Dose Using 100-kVp Combination of Different Noise Index and 120-kVp in Computed Tomography Pulmonary Angiography. Journal of computer assisted tomography. 2016;40(5):784-90.
30. Albrecht MH, Bickford MW, Nance JW, Zhang L, De Cecco CN, Wichmann JL, et al. State-of-the-Art Pulmonary CT Angiography for Acute Pulmonary Embolism. American Journal of Roentgenology. 2017;208(3):495-504.
31. Mitchell AM, Jones AE, Tumlin JA, Kline JA. Prospective Study of the Incidence of Contrast-Induced Nephropathy Among Patients Evaluated for Pulmonary Embolism by Contrast-Enhanced Computed Tomography. Academic emergency medicine : official journal of the Society for Academic Emergency Medicine. 2012;19(6):618-25.
32. Suntharalingam S, Mikat C, Stenzel E, Erfanian Y, Wetter A, Schlosser T, et al. Submillisievert standard-pitch CT pulmonary angiography with ultra-low dose contrast media administration: A comparison to standard CT imaging. PLoS ONE. 2017;12(10):e0186694.
33. Szucs-Farkas Z, Megyeri B, Christe A, Vock P, Heverhagen JT, Schindera ST. Prospective randomised comparison of diagnostic confidence and image quality with normal-dose and low-dose CT pulmonary angiography at various body weights. European Radiology. 2014;24(8):1868-77.
34. Sodickson A, Weiss M. Effects of patient size on radiation dose reduction and image quality in low-kVp CT pulmonary angiography performed with reduced IV contrast dose. Emergency Radiology. 2012;19(5):437-45.

35. Sabel BO, Buric K, Karara N, Thierfelder KM, Dinkel J, Sommer WH, et al. High-Pitch CT Pulmonary Angiography in Third Generation Dual-Source CT: Image Quality in an Unselected Patient Population. PLOS ONE. 2016;11(2):e0146949.
36. Iezzi R, Larici AR, Franchi P, Marano R, Magarelli N, Posa A, et al. Tailoring protocols for chest CT applications: when and how? Diagnostic and Interventional Radiology. 2017;23(6):420-7.
37. Zhang H, Ma Y, Lyu J, Yang Y, Yuan W, Song Z. Low kV and Low Concentration Contrast Agent with Iterative Reconstruction of Computed Tomography (CT) Coronary Angiography: A Preliminary Study. Medical Science Monitor : International Medical Journal of Experimental and Clinical Research. 2017;23:5005-10.
38. Mayo-Smith WW, Hara AK, Mahesh M, Sahani DV, Pavlicek W. How I Do It: Managing Radiation Dose in CT. Radiology. 2014;273(3):657-72.
39. Viteri-Ramírez G, García-Lallana A, Simón-Yarza I, Broncano J, Ferreira M, Pueyo JC, et al. Low radiation and low-contrast dose pulmonary CT angiography: Comparison of 80 kVp/60 ml and 100 kVp/80 ml protocols. Clinical Radiology. 2012;67(9):833-9.
40. Meyer M, Haubenreisser H, Schabel C, Leidecker C, Schmidt B, Schoenberg SO, et al. CT pulmonary angiography in patients with acute or chronic renal insufficiency: Evaluation of a low dose contrast material protocol. Scientific Reports. 2018;8:1995.
41. Ichikawa Y, Kitagawa K, Nagasawa N, Murashima S, Sakuma H. CT of the chest with model-based, fully iterative reconstruction: comparison with adaptive statistical iterative reconstruction. BMC Medical Imaging. 2013;13(1):27.

42. Hara AK, Paden RG, Silva AC, Kujak JL, Lawder HJ, Pavlicek W. Iterative Reconstruction Technique for Reducing Body Radiation Dose at CT: Feasibility Study. American Journal of Roentgenology. 2009;193(3):764-71.
43. Gill MK, Vijayananthan A, Kumar G, Jayarani K, Ng K-H, Sun Z. Use of 100 kV versus 120 kV in computed tomography pulmonary angiography in the detection of pulmonary embolism: effect on radiation dose and image quality. Quant Imaging Med Surg. 2015;5(4):524-33.
44. Lee SH, Kim M-J, Yoon C-S, Lee M-J. Radiation dose reduction with the adaptive statistical iterative reconstruction (ASIR) technique for chest CT in children: an intra-individual comparison. European journal of radiology. 2012;81(9):e938-e43.
45. Sun J, Yu T, Liu J, Duan X, Hu D, liu Y, et al. Image quality improvement using model-based iterative reconstruction in low dose chest CT for children with necrotizing pneumonia. BMC Medical Imaging. 2017;17:24.
46. Martin CJ, Sookpeng S. Setting up computed tomography automatic tube current modulation systems. Journal of Radiological Protection. 2016;36(3):R74.
47. Althén JN. Automatic tube-current modulation in CT—a comparison between different solutions. Radiation Protection Dosimetry. 2005;114(1-3):308-12.
48. Redžić M, Beganović A, Čiva L, Jašić R, Skopljak-Beganović A, Vegar-Zubović S, editors. Quality control of angular tube current modulation2017; Singapore: Springer Singapore.
49. Sookpeng S, Martin CJ, Gentle DJ. Influence of CT automatic tube current modulation on uncertainty in effective dose. Radiation Protection Dosimetry. 2016;168(1):46-54.
50. Livingstone RS, Pradip J, Dinakran PM, Srikanth B. Radiation doses during chest examinations using dose modulation techniques in multislice CT scanner. The Indian journal of radiology & imaging. 2010;20(2):154.

Chapter 2

A systematic review of double low-dose CT pulmonary angiography in pulmonary embolism

2.1 Introduction

Computed tomography pulmonary angiography (CTPA) is currently the preferred imaging modality in the diagnosis of patients with suspected pulmonary embolism who present to the emergency department (1-5). Although CTPA has high diagnostic value in detecting pulmonary embolism owing to rapid developments in CT scanning techniques in recent years, it is associated with high radiation dose. Further, CTPA requires injection of contrast medium which represents another limitation with a potential risk of contrast-induced nephropathy or acute kidney injury (6, 7). Therefore, reduction of both radiation and contrast medium doses during CTPA, or briefly defined as double low-dose CTPA is the current research direction with the aim of minimising risks from both radiation exposure and use of contrast medium.

Some recent studies have shown that it is feasible to implement double low-dose CTPA protocol without compromising image quality in the diagnosis of pulmonary embolism (8-13). In their recent study, Boos et al compared the low dose protocol comprising 70 kVp and 40 ml of contrast medium with a low-pitch of 0.9 in 35 patients with another group comprising 35 patients who were scanned with 100 and 120 kVp and 70 ml of contrast medium with a pitch of 2.2 (11). Reduction in radiation dose and contrast medium dose by 50% and 40% was achieved in the low-dose protocol group with similar diagnostic image quality between the two groups. Further reduction of contrast medium to 20 ml with use of 80 kVp was reported in another study leading to 50% dose reduction without comprising image quality (13).

Reduction of contrast medium in CT angiography (CTA) has attracted strong interests recently due to the increased contrast enhancement at low tube voltage levels because of an approximation to the k-edge of iodine, thus promoting double low-dose CTPA protocol in the current clinical practice. Although Shen et al (14) conducted a systematic review of double low-dose CTA in body examinations, authors briefly summarised the application of double low-dose CTPA without providing detailed analysis of the feasibility and image quality associated with the use of double low-dose protocol. Thus, the purpose of this review is to analyse the current literature with regard to the diagnostic performance of double low-dose CTPA in diagnosing pulmonary embolism. We strictly limit our analysis to only studies providing evidence of reductions in both radiation dose and contrast medium dose during CTPA

examinations, with the aim of determining the usefulness of double low-dose CTPA protocol.

2.2 Materials and Methods

This review was performed in accordance with the Preferred Reporting Items for Systematic Reviews and Meta-Analysis (PRISMA) guidelines (15). The PRISMA guidelines allow researchers to develop powerful search strategy for identifying and examining quantitative medical studies. A search of the literature using databases consisting of Medline/Pubmed, Scopus and ScienceDirect was conducted to identify studies reporting double low-dose CTPA. The following search terms were used to obtain relevant articles: "double low-dose CT pulmonary angiography"; "CT pulmonary angiography AND low dose protocol"; "CT pulmonary angiography AND low radiation dose AND low contrast medium"; "low dose AND CT pulmonary angiography". The search was limited to articles that were published in English within the last ten years (last search 19 July, 2018) to ensure the currency of these studies and also the use of latest CT scanning techniques to achieve low dose purpose.

2.2.1 Inclusion and exclusion criteria

Studies were included for analysis if they met the following criteria: (1): studies are published with both low kVp and low contrast medium (either low contrast volume or low concentration) used; (2): results on reductions in both radiation and contrast medium doses must be reported; (3): studies must be CTPA scans or CTA scans that involved analysis of pulmonary arteries for detection/diagnosis of pulmonary embolism. Studies were excluded from the analysis without providing details on dose reductions despite the use of double low-dose CTPA protocol. Studies were still included in the analysis even if no details of radiation dose or contrast medium dose were provided, as long as the percentage of dose reduction was available. Further, studies that were conducted on phantom experiments, or conference abstracts, editorials or review articles were excluded.

2.2.2 Data extraction

The two assessors (SA and ZS) conducted the searching process using the same search terms separately. They both screened the titles and abstracts of all identified references independently with any disagreements resolved by consensus. Data extraction includes the following details: year of publication, sample size in each group (low dose vs standard dose group), radiation dose in terms of effective dose and contrast medium dose values on both low dose and standard group, kVp ranges (70, or 80, or 100 vs 120 kVp), quantitative and qualitative assessments of image quality, as well as the differences (increased or decreased or no significant difference) in image quality assessments between the low dose and standard dose groups.

2.2.3 Statistical analysis

Due to heterogeneity in the study design in terms of methods and data analysis, results were entered into MS Excel 2013 for comparing the percentage calculations between the double low-dose and standard CTPA groups in terms of dose reductions in radiation dose and contrast medium dose. Box plots were generated using SPSS (SPSS 24.0, IBM Corporation, Armonk, NY, USA) to demonstrate the mean effective radiation dose and contrast medium volume between these two groups. Continuous values were expressed as mean and standard deviation, while categorical variables were shown as percentages. A paired samples T test was used to determine the significant difference between standard and low-dose CTPA groups, with p value less than 0.05 indicating significant difference.

2.3 Results

2.3.1 Study selection

The initial literature research retrieved 554 articles from three different databases, with 527 excluded because of irrelevance to the topic. Twenty-seven full-text articles were reviewed with further 12 studies excluded because of 11 studies focusing on single low-dose protocol, and the remaining one being a review article. Two studies were further excluded because 1 study did not provide information of assessing pulmonary arteries, although the double low-dose protocol was used in examining the whole body

CTA, and another study did not report the use of low kVp. Thus, a total of 13 studies were eligible for inclusion in the analysis (9, 11, 13, 16-25). Figure 2.1 is the flow chart showing search strategy to identify eligible studies.

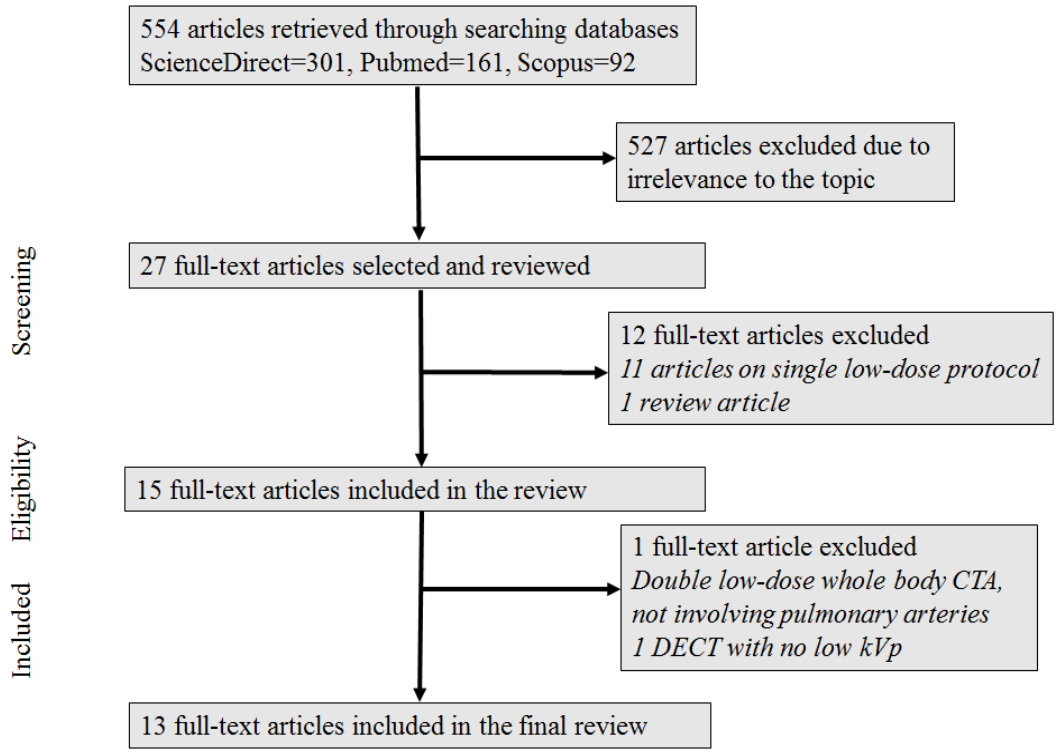

Figure 2.1 Flow chart shows search strategy to identify eligible studies for the systematic review.

2.3.2 Study characteristics

The study characteristics are provided in Table 2.1. Of 13 studies, 10 were published in the last five years (2013-2017), while the remaining three studies were published between 2011 and 2012 (9, 23, 25). In 10 studies, both low dose (low kVp such as 70 or 80 kVp versus 100 or standard 120 kVp) and low contrast medium (different volumes of contrast medium) protocols were used for comparison of the feasibility of using double low-dose protocol. In the remaining three studies, although low kVp and low contrast medium were included in the CTPA protocols, some details were not provided. Details of different kVp values were not available in two studies (9, 23),

however, percentage of radiation dose reduction was provided. In the remaining study, although the same volume (40 ml) of contrast medium was used in the two groups, different contrast medium concentrations were applied, thus percentage of contrast medium reduction was available (18).

Table 2.1Baseline characteristics of studies involving comparison of double low-dose CT pulmonary angiography protocols

Author/ year of publication	Total No. of patients	Radiation dose values (mSv)			Dose decrease (%)	Contrast medium (ml)		CM decrease (%)
		70/80 kVp	100 kVp	120 kVp		Low dose CTPA group	Standard CTPA group	
Boos et al 2016 (11)	70 (35 in each group)	2.0 ± 0.6*	ATPS 3.9 ± 1.1 (120 kVp in 29, 100 kVp in 6)		48.7	40	70	42.8
Chen et al 2015 (16)	108 (60 in group A, 48 in group B)	-	2.7 ± 0.7	21.6 ± 6.0	87.5	74	101	26.7
Dong et al 2013 (17)	86 (41 in CTPA, 45 in DECT)	5.74 ± 0.5#	-	3.32 ± 0.6	-42.1	20	50	60
Hu et al 2017 (18)	382 (192 in each group)	2.0 ± 0.9	-	5.5 ± 0.8	63.6	40 (270 mg I/ml)	40 (350 mg I/ml)	22.9
Kidoh et al 2014 (19)	60 (30 in each TRO group)	-	23.5 ± 2.6	33.4 ± 1.4	29.6	60.1 ± 0.6	91.8 ± 22.6	34.5
Kilic et al 2014 (20)	24 (12 in TB and 12 in BT groups)	-	3.75 ± 0.8	5.84 ± 2.1	35.8	38.5 ± 3.9	70 ± 0.0	45
Li et al 2015 (21)	80 (40 in each group)	0.4 ± 0.1*	2.0 ± 0.4	-	80	40	60	33
Lu et al 2014 (13)	100 (50 in each group)	0.9 ± 0.5	1.7 ± 0.2	-	47	20	60	66.7
Moynihan et al 2017 (22)	150 (50 each for 3 groups)	-	2.92 ± 0.75	4.88 ±1.77 5.1 ± 1.5	40-42.7	54.08 ± 9.26 58.46 ± 8.78	80	27.5-32.5

Sodickson et al 2012 (23)	152 (53 in 100 kVp and 99 in 120 kVp)	-	NA	NA	33	50	75	33.3
Szucs-Farkas et al 2011 (9)	80 (40 in normal dose and 40 in low dose groups)	NA	-	NA	57	75	100	25
Suntharalingam et al 2017 (24)	100 (50 in each group)	0.7	2.4	-	70.8	25	60	58.3
Viteri-Ramirez et al 2012 (25)	70 (35 in each group)	1.1 ± 0.74	2.7 ± 1.2	-	59.2	60	80	25

ATPS: automatic tube potential selection. CTPA-CT pulmonary angiography, NR-not available, RC-reduced volume of contrast media, RT-routine thoracic CT scans, BT-bolus tracking, CM-contrast medium, CNR-contrast-to-noise ratio, SNR-signal-to-noise ratio, TB-test bolus, TRO-triple rule-out protocol. ↓: lower with double low-dose protocol; ↑: improved with double low-dose protocol, = equal with double low-dose protocol.

* 70 kVp was used in the low dose study group. # In Dong et al study, DECT (80/140 kVp) was compared with the standard 120 group.

2.3.3 Radiation dose reduction

The effective dose was reported in 11 studies, and the dose value was not available in the remaining two studies (9, 23). The CTPA protocol of 80 kVp versus 100/120 kVp was reported in 11 studies, and the CTPA protocol of 70 kVp versus 100/120 kVp protocol was reported in two studies (11, 21). In one study, DECT (80/140 kVp) was compared to the standard 120 kVp with resultant increased radiation dose (17).

The effective dose was calculated using a conversion coefficient of 0.014 and 0.017 in 5 and 4 studies, respectively. A conversion coefficient of 0.016 was used in one study (22), and in another study, the conversion coefficient of 0.017 was use for the study group scanned with 120 kVp and 0.016 for the 100 kVp group (20). In the remaining two studies, the information was not available.

Effective dose reduction was reported in 12 studies (dose range: 0.4 to 23.5 mSv) with significant dose reduction between 29.6% and 87.5% using low-dose CTPA when compared to the standard CTPA ($p=0.05$). Dose increase was noted in one study comparing DECT with standard single energy 120 kVp protocol (17). Triple-rule-out CTA protocol was reported in two studies (16, 19), with highest dose reduction achieved in one study compared to other studies which were performed on routine CTPA scans (16). In that study, the low dose CTPA protocol of 100 kVp with high pitch of 3.4 resulted in effective dose of 2.7 mSv, while the effective dose from standard CTPA protocol was 21.6 mSv, thus resulting in 87.5% reduction. The lowest dose reduction was also seen in the triple-rule-out CTA protocol in another study with less than 30% dose reduction when compared to the standard CTPA protocol (19). However, the effective dose was only 5.2 mSv for the non-gated whole chest CTA (the second phase) if the first phase of coronary CTA was not included as reported in that study. Figure 2.2 is a box plot showing the mean effective dose between double low-dose and standard CTPA protocols.

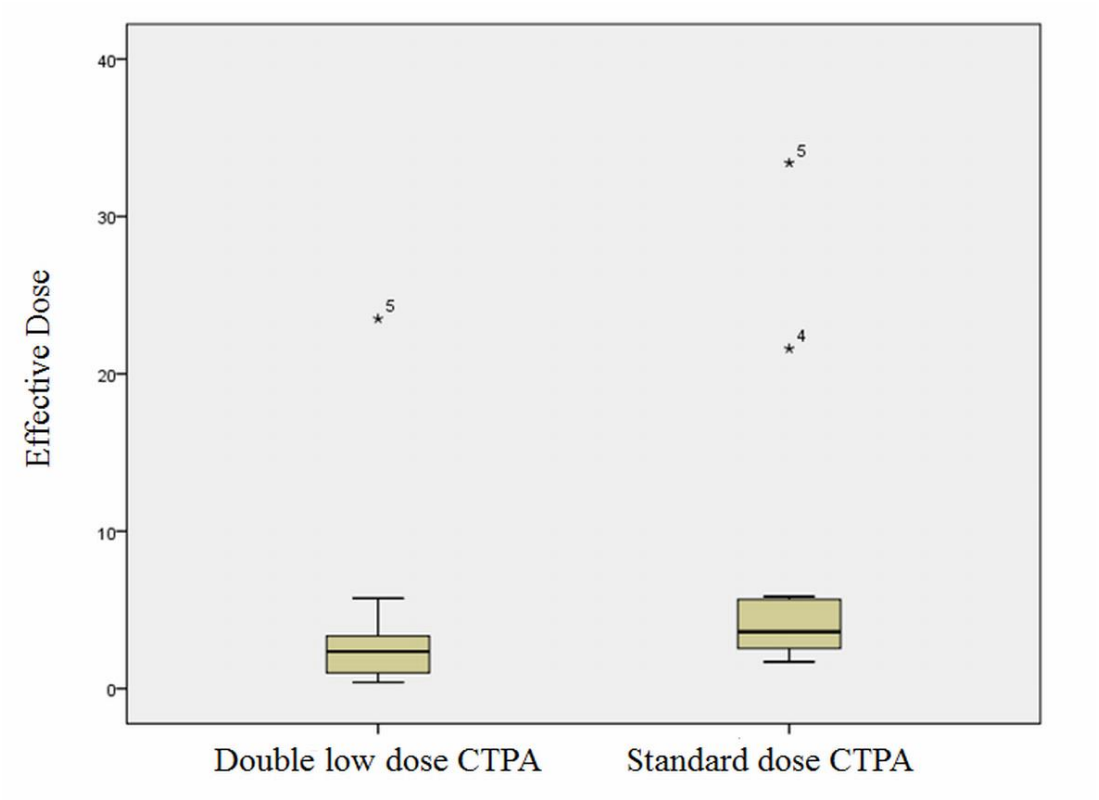

Figure 2.2 Box plot shows the mean effective dose between double low-dose CTPA and standard dose CTPA protocols in pulmonary embolism based on the review of these 13 studies. The mean effective dose of double low-dose CTPA is significantly lower than that of standard CTPA (p=0.05).

2.3.4 Contrast medium reduction

Reduction of contrast medium dose was available in all of the 13 studies, with dose reduction ranging from 25% to 67%, significantly lower in the low-dose CTPA when compared to the standard CTPA protocol ($p<0.001$). Of 13 studies, low volume contrast medium (range: 20 to 75 ml) was compared to standard volume of contrast medium (range: 50 to 101 ml) in 12 studies, while in the remaining study, low iodine concentration (270 mg I/ml) was compared to high iodine concentration (350 mg I/ml) with use of 40 ml contrast medium in both groups, but resulting in 23% reduction in contrast medium (18). In the low contrast medium group, less than 50 ml of contrast medium was reported in 8 out of 13 studies, while in contrast, this was only reported in two studies in the standard CTPA group. Figure 2.3 is a box plot showing the mean contrast medium dose between double low-dose and standard CTPA protocols.

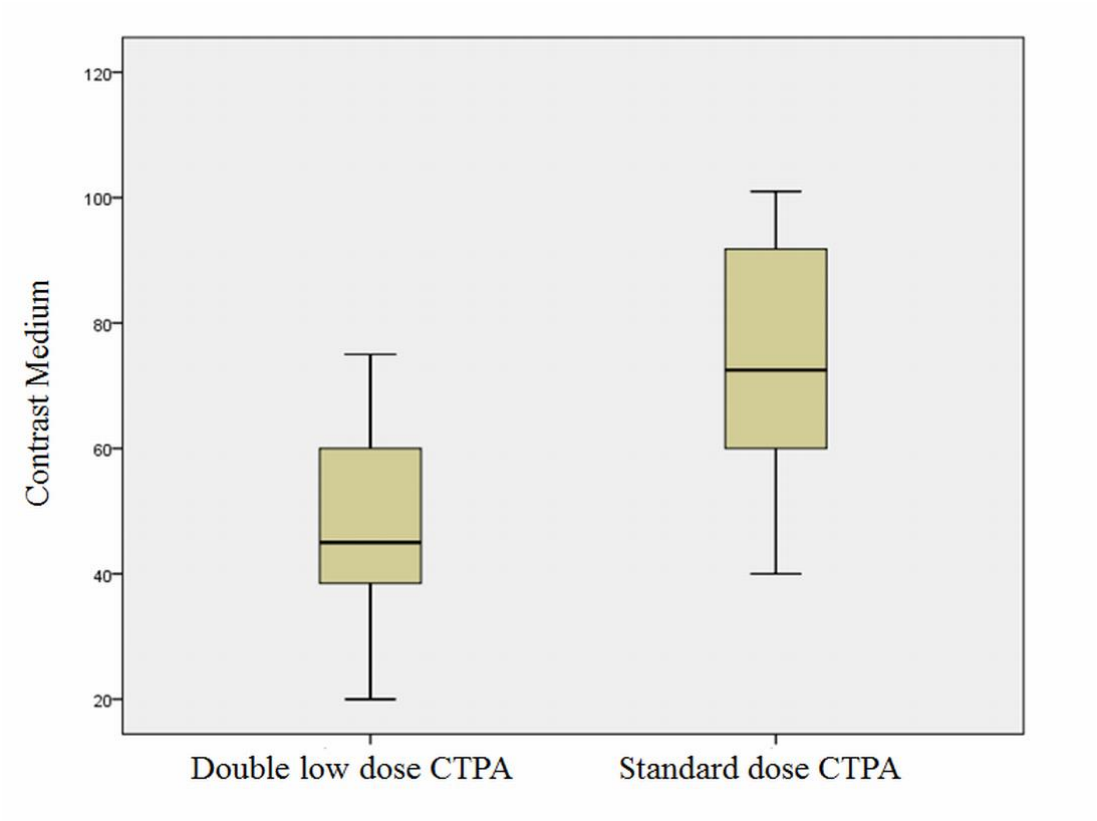

Figure 2.3 Box plot shows the mean volume of contrast medium used in double low-dose CTPA in comparison with that from standard CTPA protocol based on the review of these 14 studies. Significantly low contrast medium dose is noted in the double low-dose CTPA group ($p<0.001$).

2.3.5 Image quality assessment

Quantitative assessment of image quality in terms of signal-to-noise ratio (SNR) and contrast-to-noise ratio (CNR) was available in 11 studies, and details of quantitative assessment were not provided in 2 studies (20, 23) (Table 2.2). Both SNR and CNR were significantly higher, significantly lower and with no significant difference in 3, 3 and 4 studies, respectively in the double low-dose CTPA protocol when compared to the standard CTPA protocol. SNR was shown to be similar in 2 studies between double low-dose and standard CTPA groups (9, 23). Both SNR and CNR were not available in the remaining study (20).

Subjective assessment of image quality with use of 3-, 4- and 5-point ranking scale was reported in 3, 3 and 3 studies, respectively, with information not provided in the remaining 4 studies. Overall, subjective assessment of image quality remained the

same in both low dose and standard dose CTPA groups in 11 studies, and was improved in 1 study in the low-dose CTPA group due to significantly fewer artifacts in the low-dose protocol (20). Information was not available in the remaining study (25).

Table 2.2 Comparison of image quality between standard and double low-dose CT pulmonary angiography protocols

Author/ year of publication	Image quality of double low-dose CTPA protocol			Image quality of standard CTPA protocol		
	SNR	**CNR**	**Subjective image quality**	**SNR**	**CNR**	**Subjective image quality**
Boos et al 2016 (11)*	14.6 ± 6.0 15.1 ± 8.9*	12.4 ± 5.7 12.9 ± 8.5*	3.7 ± 0.6	13.9 ± 3.7 12.0 ± 4.5*	11.6 ± 3.3 10.0 ± 4.1*	3.7 ± 0.6
Chen et al 2015 (16)	36.7 ± 17.1	31.5 ± 16.2	2.9 ± 0.1	56.5 ± 22.0	46.2 ± 19.1	2.9 ± 0.1
Dong et al 2013 (17)	17.6 ± 5.1 21.3 ± 6.3*	14.7 ± 5.0 19.2 ± 6.3*	66.7/95.5%[#]	16.2 ± 6.5	14.4 ± 6.4	61%[#]
Hu et al 2017 (18)	24.5 ± 9.4	20.3 ± 8.9	No significant difference	29.1 ± 10.8	23.6 ± 10.2	No significant difference
Kidoh et al 2014 (19)	20.3 ± 3.3	20.7 ± 3.8	PT image contrast 4.0 ± 0.0/4.0 ± 0.0* PT image noise 3.9 ± 0.0/4.0 ± 0.2*	15.4 ± 6.1	15.9 ± 2.6	PT image contrast 4.0 ± 0.0/4.0 ± 0.0* PT image noise 4.0 ± 0.0/4.0 ± 0.0*
Kilic et al 2014 (20)	NA	NA	Vessel enhancement: 7/4/1/0 Artifact: 6/3/3/0*	NA	NA	Vessel enhancement: 9/2/3/0 Artifact: 0/6/4/2*
Li et al 2015 (21)	Between 37.3 ± 10.8 and 41.8 ± 12.5*	Between 32.4 ± 9.9 and 36.9 ± 11.7*	1.03 ± 0.16	Between 25.1 ± 13.9 and 29.1 ± 14.3*	Between 21.4 ± 12.7 and 25.4 ± 13.0 *	1.05 ± 0.22
Lu et al 2014 (13)	Between 42.0 ± 15.1 and 45.7 ± 17.1*	Between 36.5 ± 14.3 and 41.0 ± 16.3*	Score 1/2: 80/20%[#]	Between 28.0 ± 10.2 and 30.1 ± 10.5*	Between 23.5 ± 9.6 and 25.5 ± 10.0*	Score 1/2: 78/22[#]

Moynihan et al 2017 (22)	17.56 ± 6.01	15.97 ± 5.71	No significant difference	17.86 ± 5.8 15.95 ± 5.07*	15.92 ± 5.27 14.39 ± 4.98*	No significant difference
Sodickson et al 2012(23)	No significant difference	NA	No significant difference	No significant difference	NA	No significant difference
Szucs-Farkas et al 2011 (9)	10.8 ± 2.5	NA	3.73 ± 0.60	9.7 ± 2.3	NA	3.82 ± 0.50
Suntharalingam et al 2017 (24)	Between 12 ± 4.1 and 14.5 ± 6.6*	Between 10.2 ± 3.7 and 12.8 ± 6*	Score 1/2/3: 78/22/0%[#]	Between 14.7 ± 6.8 and 16.4 ± 8.5*	Between 12.7 ± 7.3 and 14.2 ± 8.5*	Score 1/2/3: 92/6/2%[#]
Viteri-Ramirez et al 2012 (25)	16.3 ± 7.5	14.8 ± 7.4	NA	13.8 ± 9.1	12.5 ± 8.6	NA

Boss et al (11): SNR and CNR were measured at pulmonary trunk and left lower segmental pulmonary artery.

Dong et al (17): * in the DECT group, SNR/CNR were reported in 70 keV and optimal keV groups; # indicates the percentage of pulmonary arteries with peripheral vascular enhancement score of 5 (no perceivable image noise).

Kidoh et al (19): * indicates readers 1 and 2 qualitative scores. PT-pulmonary trunk.

Kilic et al (20): subjective assessment of vascular enhancement using a score of 1-4: excellent, good, moderate and poor (non-diagnostic). Presence of artifact in superior vena cava 1-4: no artifact, minimum, serious and severe artifact (non-diagnostic).

Li et al (21): SNR and CNR were measured between main pulmonary artery and bilateral pulmonary arteries, upper and inferior lobe pulmonary arteries.

Lu et al (13): * indicates that SNR and CNR were measured between main pulmonary artery, bilateral pulmonary arteries, lobar, segmental and subsegmental arteries. # indicates both readers' assessment of pulmonary arteries by scoring images to 1: good to excellent quality, 2: adequate quality.

Moynihan et al (22): CTPA 120 kVp protocol using bolus tracking for Group B and using test bolus for Group C.

Suntharalingam et al (24): * indicates that SNR and CNR were measured between main pulmonary artery, bilateral pulmonary arteries, lobar and segmental arteries. # indicates consensus subjective assessment of image quality by two readers: 1: good to excellent, 2: adequate and 3 non-diagnostic quality.

2.4 Discussion

This review analyses a total of 13 studies reporting the use of double low-dose CTPA in the diagnosis of pulmonary embolism, with results confirming the feasibility of using double low-dose CTPA in clinical practice. Significant reductions in both radiation and contrast medium doses have been reported in most of these studies, with image quality increased or unchanged between the low-dose and standard CTPA groups. This is clinically significant because use of contrast medium dose is associated with potential risk of renal injury, thus, reducing contrast medium along with reduction in radiation dose during CTPA represents an effective approach in daily clinical practice.

CTPA has been widely used as a first line technique due to its high diagnostic accuracy in the detection of pulmonary embolism. However, increased use of CTPA raises concerns because of high radiation dose associated with CTPA (26, 27). Further, contrast-induced nephropathy is another concern which has attracted attention in the current literature. Low-dose CTPA has been widely studied with effective reduction in radiation dose according to some recent studies (9-13). This is confirmed in this review as the mean effective dose in low-dose CTPA group is less than 5 mSv in 9 out of 13 studies, with dose value less than 1.0 mSv in 3 studies. Of these 3 studies, CTPA with use of a high-pitch 3.2 and 70 kVp resulted in the lowest dose of 0.4 mSv (21), while in the other 2 studies, a low dose of 0.7 and 0.9 mSv was achieved in the CTPA protocol of 80 kVp and standard pitch 1.2 and 2.2 (13, 24). Therefore, use of the current dose-reduction techniques during CTPA enables significant dose reduction while still obtaining diagnostic images.

When kVp is lowered from 120 to 100, 80 or 70, contrast medium can be further reduced due to the k-edge of iodine, which improves contrast enhancement in vessels (14, 21). It has been reported that use of low kVp and low iodine in CT angiography leads to significant reductions in both radiation dose and iodine content in terms of both volume and concentration of contrast medium while maintaining image quality (14, 21, 28-40). Using low dose and low concentration of contrast medium in CTPA without affecting image quality has significant clinical value, given the adverse effects of ionisation radiation and contrast-induced renal nephropathy (41-43). This is also confirmed in this review as the double low-dose CTPA results in reductions in

effective dose and contrast medium volume, with image quality unchanged or even improved in the low-dose protocol groups. The contrast medium dose less than 50 ml was reported in more than 60% of studies in the low-dose group, with lowest doses being 20 ml in two studies and 25 ml in one study. Of these studies using the lowest contrast doses, quantitative and qualitative assessment of image quality was improved compared to the standard group in two studies, and remained unchanged in one study. Thus, this review further validates the feasibility and effectiveness of using double low-dose CTPA protocol.

Despite promising findings noted in this review, some limitations need to be acknowledged. First, due to strict selection criteria, only a small number of studies are eligible for analysis. Small sample size is another limitation as in more than half of the studies (8 out of 13), the number of patients in each group was less than 50 cases. Further, due to heterogeneity in the study design, such as use of dual-source CT, dual-energy CT, or triple-rule-out CTA protocol, only a general systematic review was conducted as we could not perform a meta-analysis. Second, not all of the studies provided the information on radiation dose. Dose values were not available in two studies (9, 23), despite dose reduction was provided in these studies. Third, for calculation of effective dose, different conversion coefficient factors were used including 0.014, 0.016 and 0.017, thus, the reported radiation dose values could be variable among these studies. Fourth, dual-energy CTPA with use of low-dose protocol was only reported in two studies. Given the advantages of virtual monoenergetic imaging and material decomposition with dual-energy CT such as iodine-based material decomposition, it is expected to improve image quality and diagnostic value of CTPA by minimising radiation dose. Recent studies have shown the significant reduction in radiation dose or contrast medium using dual-energy CT compared to single energy CT while providing excellent image quality for diagnosis of pulmonary embolism (44-46). More studies with use of double low-dose dual energy CTPA deserve to be investigated.

Finally, body mass index (BMI) for the low-dose and standard dose groups was only available in 6 out of 13 studies, and the CTPA protocols with use of low kVp and low contrast medium was compared in these patients with BMI <30 kg/m^2. Thus, further studies with inclusion of patients with BMI >30 kg/m^2 should be conducted to determine if the double low-dose CTPA is still feasible in patients with large BMI.

Further, some recent studies have shown the dose reduction using low tube voltage of 90 kVp CTA with improved image quality and similar diagnostic value when compared to the standard 120 kVp protocol (47, 48).

In conclusion, this review shows that it is feasible to achieve significant reductions in both radiation dose and contrast medium dose in the diagnosis of pulmonary embolism by CT pulmonary angiography. Double low-dose CT pulmonary angiography through lowering tube voltage and contrast medium dose (either iodine concentration or volume) allows for acquisition of diagnostic images with similar or even improved image quality compared to the standard CT pulmonary angiography protocol. Further studies based on large cohort of patients and at multi-center sites are required to confirm the clinical value of double low-dose CT pulmonary angiography.

2.5 References

1. Mayo J, Thakur Y. Pulmonary CT angiography as first-line imaging for PE: image quality and radiation dose considerations. AJR Am J Roentgenol 2013; 200(3): 522–528.
2. Wittram C. How I do it: CT pulmonary angiography. AJR Am J Roentgenol 2007;188(5): 1255–1261.
3. den Exter AL, van der Hulle T, Klok FA, Huisman MV. Advances in the diagnosis and management of acute pulmonary embolism. Thromb Res 2014;133(Suppl 2): S10-16.
4. Righini M, Le GG, Aujesky D, et al. Diagnosis of pulmonary embolism by multidetector CT alone or combined with venous ultrasonography of the leg: a randomised non-inferiority trial. Lancet 2008;371(9621): 1343-52
5. Sun Z, Lei J. Diagnostic yield of CT pulmonary angiography in the diagnosis of pulmonary embolism: a single center experience. Interv Cardiol 2017;9: 191-198.
6. Ong CW, Malipatil V, Lavercombe M, et al. Implementation of a clinical prediction tool for pulmonary embolism diagnosis in a tertiary teaching hospital reduces the number of computed tomography pulmonary angiograms performed. Intern Med J 2013;43:169-74.
7. Newman DH, Schriger DL. Rethinking testing for pulmonary embolism: less is more. Ann Emerg Med 2011; 57:622-7.e3.
8. Laqmani A, Kurfurst M, Butscheidt S, et al. CT pulmonary angiography at reduced radiation exposure and contrast material volume using iterative model reconstruction and iDose ^{4} technique in comparison to FBP. Plos One 2016;11:e0162429.
9. Szucs-Farkas Z, Schibler F, Cullmann J, et al. Diagnostic accuracy of pulmonary CT angiography at low tube voltage: intraindividual comparison of a normal-dose protocol at 120 kVp and a low-dose protocol at 80 kVp using reduced amount of contrast medium in a simulation study. AJR Am J Roentgenol 2011; 197:W852–9.
10. Szucs-Farkas Z, Schaller C, Bensler S, Patak MA, Vock P, Schindera ST. Detection of pulmonary emboli with CT angiography at reduced radiation exposure and contrast material volume: comparison of 80 kVp and 120 kVp

protocols in a matched cohort. Invest Radiol 2009;44:793–9.

11. Boos J, Kropil P, Lanzman RS, et al. CT pulmonary angiography: simultaneous low-pitch dual-source acquisition mode with 70 kVp and 40 ml of contrast medium and comparison with high-pitch spiral dual-source acquisition with automated tube potential selection. Br J Radiol 2016;89:20151059.
12. Laqmani A, Regier M, Veldhoen S, et al. Improved image quality and low radiation dose with hybrid iterative reconstruction with 80 kV CT pulmonary angiography. Eur J Radiol 2014; 83:1962–9.
13. Lu GM, Luo S, Meinel FG, et al. High-pitch computed tomography pulmonary angiography with iterative reconstruction at 80 kVp and 20 mL contrast agent volume. Eur Radiol 2014; 24:3260–8.
14. Shen Y, Hu X, Zhou X, Zhu D, Li Z, Hu D. Did low tube voltage CT combined with low contrast media burden protocols accomplish the goal of "double low" for patients? An overview of applications in vessels and abdominal parenchymal organs over the past 5 years. Int J Clin Pract 2016;70 (Suppl 9B): B5-B15.
15. Mohr D, Shamseer L, Clarke M, et al. Preferred reporting items for systematic review and meta-analysis protocols (PRISMA-P) 2015 Statement. Syst Rev 2015; 4:1.
16. Chen HL, Chen TW, Qiu LH, Diao XM, Zhang C, Chen L. Application of flash dual-source CT at low radiation dose and low contrast medium dose in triple rule-out (tro) examination. Int J Clin Exp Med 2015;8:21898-21905.
17. Dong J, Wang X, Jiang X, Gao L, Li F, Qiu J, Xu Y, Wang H. Low-contrast agent dose dual-energy CT monochromatic imaging in pulmonary angiography versus routine CT. J Comput Assist Tomogr 2013;37:618-625.
18. Hu X, Ma L, Zhang J, Li Z, Shen Y, Hu D. Use of pulmonary CT angiography with low tube voltage and low-iodine-concentration contrast agent to diagnose pulmonary embolism. Sci Rep 2017;7:12741.
19. Kidoh M, Nakaura T, Nakamura S, et al. Contrast material and radiation dose reduction strategy for triple-rule-out cardiac CT angiography: feasibility study of non-ECG-gated low kVp scan of the whole chest following coronary CT angiography. Acta Radiologica 2014;55:1186-1196.

20. Kilic K, Erbas G, Ucar M, et al. Determination of lowest possible contrast volume in computed tomography pulmonary angiography by using pulmonary transit time. Jpn J Radiol 2014;32:90-97.
21. Li X, Ni Q, Schoepf J, et al. 70-kVp high-pitch computed tomography pulmonary angiography with 40 ml contrast agent: initial experience. Acad Radiol 2015;22:1562-1570.
22. Moynihan WA, Kiely BL, O'Brien JM. A comparison of 100 kVp verusu 120 kVp CTPA acquisition with direct comparisons of test bolus and bolus tracking at same and different voltages in multidetector 64 slice CT scanner. Int J Radiol Radiat Ther 2017;4:00095.
23. Sodickson A, Weiss M. Effects of patient size on radiation dose reduction and image quality in low-kVp CT pulmonary angiography performed with reduced IV contrast dose. Emerg Radiol 2012;19:437-445.
24. Suntharalingam S, Mikat C, Stenzel E, et al. Submillisievert standard-pitch CT pulmonary angiography with ultra-low dose contrast media administration: A comparison to standard CT imaging. Plos One 2017;12:e0186694.
25. Viteri-Ramirex G, Garca-Lallana A, Simon-Yarza I, et al. Low radiation and low-contrast dose pulmonary CT angiography: comparison of 80 kVp/60 ml and 100 kVp/80 ml protocols. Clin Radiol 2012;67:833-839.
26. Mamlouk MD, vanSonnenberg E, Gosalia R, et al. Pulmonary embolism at CT angiography: implications for appropriateness, cost, and radiation exposure in 2003 patients. Radiology 2010;256(2):625-32.
27. Mitchell AM, Jones AE, Tumlin JA, Kline JA. Prospective study of the incidence of contrast-induced nephropathy among patients evaluated for pulmonary embolism by contrast-enhanced computed tomography. Acad Emerg Med 2012;19(6):618-25.
28. Shen Y, Sun Z, Xu L, Li Y, Zhang N, Yan Z, Fan Z. High-pitch, low-voltage and low-iodine-concentration CT angiography of aorta: assessment of image quality and radiation dose with iterative reconstruction. PLoS One 2015;10:e0117469.
29. Sun Z, Al Moudi M, Cao Y. CT angiography in the diagnosis of cardiovascular disease: a transformation in cardiovascular CT practice. Quant Imaging Med Surg 2014;4:376-396.
30. Cakmakci E, Ozkurt H, Tokgoz S, et al. CT-angiography protocol with low

dose radiation and low volume contrast medium for non-cardiac chest pain. Quant Imaging Med Surg 2014;4:307-312.

31. Gill MK, Vijayananthan A, Kumar G, Jayarani K, Ng KH, Sun Z. Use of 100 kV versus 120 kV in computed tomography pulmonary angiography in the detection of pulmonary embolism: effect on radiation dose and image quality. Quant Imaging Med Surg 2015;5:524-533.
32. Tan S, Yeong CH, Aman R, et al. Low tube voltage prospectively ECG-triggered coronary CT angiography: A systematic review of image quality and radiation dose. Br J Radiol 2018 Mar 29:20170874. doi: 10.1259/bjr.20170874. [Epub ahead of print].
33. Aldosari S, Almoudi M, Sun Z. Double-low dose protocol of CT pulmonary angiography in the diagnosis of pulmonary embolism: A feasible approach for reduction of both contrast medium and radiation dose. Heart Res Open J 2017;4:33-38.
34. Tan SK, Yeong CH, Ng KH, Abdul Aziz Y, Sun Z. Recent update on radiation dose assessment for the state-of-art coronary computed tomography angiography (CCTA) protocols. Plos One 2016;11:e0161543.
35. Al Shammakhi A, Sun Z. A systematic review of image quality, diagnostic value and radiation dose of coronary CT angiography using iterative reconstruction compared to filtered back projection in the diagnosis of coronary artery disease. J Med Imaging Health Inf 2015;5: 96-102.
36. Shen Y, Fan Z, Sun Z, Xu L, Li Y, Zhang N, Yan Z. High pitch dual-source whole aorta CT angiography in the detection of coronary arteries: A feasibility study of using Iodixanol 270 and 100 kVp with iterative reconstruction. J Med Imaging Health Inf 2015; 5: 117-125.
37. Sabarudin A, Mustafa Z, Nassir KM, Hamid HA, Sun Z. Radiation dose reduction in thoracic and abdomen-pelvic CT using tube current modulation: A phantom study. J Appl Clin Med Phys 2015; 16:319-328.
38. Sabarudin A, Khairuddin Md Yusof A, Tay MF, Ng KH, Sun Z. Dual-source CT coronary angiography: effectiveness of radiation dose reduction with lower tube voltage. Radiat Prot Dosim 2013; 153: 441-447.
39. Sabarudin A, Sun Z, Khairuddin Md Yusof A. Coronary CT angiography with single- source and dual-source CT: Comparison of image quality and radiation dose between prospective ECG-triggered and retrospective ECG-gated

protocols. Int J Cardiol 2013; 168: 746-753.

40. Sabarudin A, Sun Z, Ng KH. Radiation dose in coronary CT angiography associated with prospective ECG-triggered technique: comparisons with different CT generations. Radiat Prot Dosim 2013; 154: 301-307.
41. Kanematsu M, Goshima S, Miyoshi T, et al. Whole-body CT angiography with low tube voltage and low-concentration contrast material to reduce radiation dose and iodine load. AJR Am J Roentgenol 2014;202:W106-W116.
42. Rodrigues JCL, Mathias H, Negus IS, Manghat NE, Hamilton MCK. Intravenous contrast medium administration at 128 multidetector row CT pulmonary angiography: bolus tracking versus test bolus and the implications for diagnostic quality and effective dose. Clin Radiol 2012;67:1053-1060.
43. Mourits MM, Nijhof WH, van Leuken MH, Jager GJ, Rutten MJCM. Reducing contrast medium volume and tube voltage in CT angiography of the pulmonary artery. Clin Radiol 2016;71:615.e7-615.e13.
44. Petritsch B, Kosmala A, Gassenmaier T, et al. Diagnosis of pulmonary artery embolism: Comparison of single-source CT and 3rd generation dual-source CT using a dual-energy protocol regarding image quality and radiation dose. Rofo 2017;189:527-536.
45. De Zordo T, von Lutterotti K, Dejaco C, et al. Comparison of image quality and radiation dose of different pulmonary CTA protocols on a 128-slice CT: high-pitch dual source CT, dual energy CT and conventional spiral CT. Eur Radiol 2012;22:279-286.
46. Leithner D, Wichmann JL, Vogl TJ, et al. Virtual monoenergentic imaging and iodine perfusion maps improve diagnostic accuracy of dual-energy computed tomography pulmonary angiography with suboptimal contrast attenuation. Invest Radiol 2017;52:659-665.
47. Leithner D, Gruber-Rouh T, Beeres M, et al. 90-kVp low-tube-voltage CT pulmonary angiography in combination with advanced modeled iterative reconstruction algorithm: effects on radiation dose, image quality and diagnostic accuracy for the detection of pulmonary embolism. Br J Radiol Jun 5:20180269. doi: 10.1259/bjr.20180269. [Epub ahead of print]
48. Leithner D, Wichmann JL, Mahmoudi S, et al. Diagnostic yield of 90-kVp low-tube-voltage carotid and intracerebral CT-angiography: effects on radiation dose, image quality and diagnostic performance for the detection of

carotid stenosis. Br J Radiol 2018 Jun;91(1086):20170927.

Chapter 3

Patient-specific 3D printed pulmonary artery model: A preliminary study

3.1 Introduction

Three-dimensional (3D) printing is a rapidly developing technique showing increasing interest and great potential in medicine (1-5). The diagnostic application of using patient-specific 3D printed models has been reported in the diagnostic assessment of cardiovascular disease, pre-surgical planning and simulation, as well as medical education (6-13). These studies created 3D printed realistic models using either computed tomography (CT) or magnetic resonance imaging (MRI) or echocardiography data with accurate replication of anatomical structures and pathological changes. A recent systematic review of 48 studies has demonstrated the usefulness of 3D printed models in replicating complex cardiovascular anatomy with high accuracy, serving as a valuable tool for pre-surgical planning and simulation of cardiovascular disease, and medical education to healthcare professionals and medical students (14).

To the best of our knowledge, very few research studies have been conducted in the diagnostic assessment of 3D printed models in pulmonary artery diseases (15). CT pulmonary angiography (CTPA) is the preferred imaging modality in the diagnosis of pulmonary embolism (16-20). Although CTPA has high diagnostic value in detecting pulmonary embolism, it has disadvantages of the associated high radiation dose. Further, administration of contrast medium during CTPA represents another limitation with a potential risk of contrast-induced nephropathy (21, 22). Therefore, reduction of both radiation and contrast medium doses during CTPA is the current research direction with promising results achieved.

According to these studies, there is still potential for further lowering of the radiation and contrast medium doses during CTPA. To test the feasibility of different protocols, a realistic anatomic phantom is an ideal option, and a 3D printed model serves this purpose. Thus, the primary aim of this study was to use a patient-specific 3D printed pulmonary artery model to test different CTPA protocols with the aim of identifying optimal CTPA protocol. Further, potential factors including image segmentation, editing and 3D printing processes could affect the dimensional accuracy of 3D printed models (23, 24). Witowski et al in their recent systematic review indicates the lack of quantitative methods to validate liver model accuracy (25). Similarly, no studies have reported the quantitative assessment of 3D printed pulmonary model accuracy.

Therefore, the secondary aim of this study was to quantitatively assess the model accuracy of 3D printed pulmonary artery model in delineating anatomical structures.

3.2 Materials and Methods

3.2.1 Sample image selection

CTPA images from a 53-year-old female with suspected pulmonary embolism were selected in this study to generate 3D reconstructed pulmonary artery model for 3D printing. CTPA showed normal pulmonary artery without any sign of pulmonary embolism. The CT scan was performed on a 128-slice scanner (Siemens Definition Flash, Siemens Healthcare, Forchheim, Germany) with slice thickness of 1.0 mm and reconstruction interval of 0.6 mm.

3.2.2 Image post-processing and segmentation for 3D printing

Original digital imaging and communications in medicine (DICOM) of CTPA images were transferred to a separate workstation equipped with Analyze 12.0 (AnalyzeDirect, Inc., Lexana, KS, USA) for image processing and segmentation. Semi-automatic approach was used to perform image postprocessing and segmentation of 3D volume data. A CT number thresholding technique was first used to produce 3D volume rendering images with inclusion of the pulmonary trunk, left main and right main pulmonary arteries. In brief, CT attenuation in the pulmonary arteries was measured (around 150 Hounsfield unit [HU]) and applied as the lowest threshold to demonstrate only contrast-enhanced pulmonary arteries and cardiac chambers, while soft tissue, pulmonary veins and other structures with CT attenuation less than 150 HU were removed as the focus of this study was pulmonary arteries. Bony structures and cardiac chambers have high CT attenuation (>300 HU), thus, removal of these structures was conducted by the function of Object Separator that is available with Analyze 12.0. Some manual editing was applied to ensure the accuracy of 3D model in the delineation of pulmonary arterial tree. This involved further removal of some structures that were still included in the 3D volume data such as overlapping tissues and presence of artifacts, and applying a median filter to remove some image noise for better definition of pulmonary arteries with side branches. The generated model of the segmented pulmonary arteries was subsequently exported to

the Standard Tessellation Language (STL) file format which is commonly used for 3D printing. Figure 3.1 shows the steps of image post-processing and segmentation from original 2D DICOM images to generation of segmented volume data and STL file to the final step of 3D printed model.

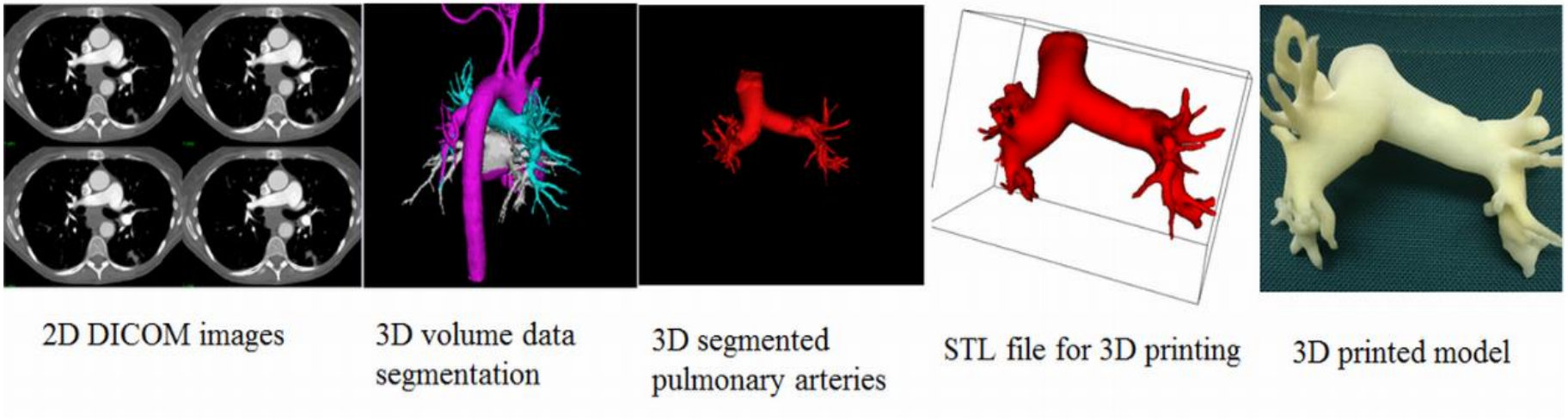
2D DICOM images
3D volume data segmentation
3D segmented pulmonary arteries
STL file for 3D printing
3D printed model

Figure 3.1 Flow diagram shows the image post-processing and segmentation steps from 2D CT images to creation of 3D printed model. Original 2D DICOM (Digital Imaging and Communications in Medicine) images were used to create 3D volume rendering image with use of CT number thresholding technique to display contrast-enhanced vessels (blue colour-pulmonary arteries, pink colour-aorta and its branches, while colour-left atrium and pulmonary veins). 3D volume rendering of pulmonary artery tree is segmented through semi-automatic segmentation and manual editing. STL (Standard Tessellation Language) file of 3D segmented volume data was generated for 3D printing of patient-specific 3D printed model.

The STL file of 3D segmented pulmonary artery was uploaded to *Shapeways*, an online 3D printing service (26). The model was printed in 'Elasto Plastic' material, which has material property closest to that of arterial wall (27).

3.2.3 CTPA scanning protocols for 3D printed model

To determine the accuracy of the 3D printed model in replicating anatomical structures, a series of CTPA scans were conducted on the 3D printed pulmonary artery model with different scanning protocols. A total of nine scans were performed, in which three tube voltages of 80, 100 and 120 kVp, three pitch values of 0.7, 0.9 and 1.2 were tested. The 3D printed model was placed in a plastic box filled with a contrast medium (Omnipaque 370) (Figure 3.2), and scans were performed on a 64-slice CT scanner (Siemens Definition AS, Siemens Healthcare, Forchheim, Germany) with slice thickness of 1.0 mm and reconstruction interval of 0.6 mm. The contrast medium was diluted to 6% resulting in CT attenuation of 150 HU which is similar to that of clinical CTPA examination. DICOM images of the scanned model were transferred to a workstation for measurements of pulmonary artery diameters and image quality.

Figure 3.2 3D printed pulmonary model is placed in a plastic box which is used to be filled with contrast medium for CT scans.

3.2.4 Measurements of pulmonary artery diameters

Diameter measurements at the pulmonary trunk, right and left main pulmonary arteries were performed on original CTPA images, STL file, 3D printed model and post-3D printing scanned CT images. Measurements were performed by two observers with more than 10 years of experience in CT imaging, with each measurement repeated three times. The two observers performed measurements separately and the results showed a very high correlation between these two observers ($r=0.99\text{-}1.0$, $p<0.001$). Figure 3.3 shows an example of measuring the pulmonary trunk using an electronic calliper.

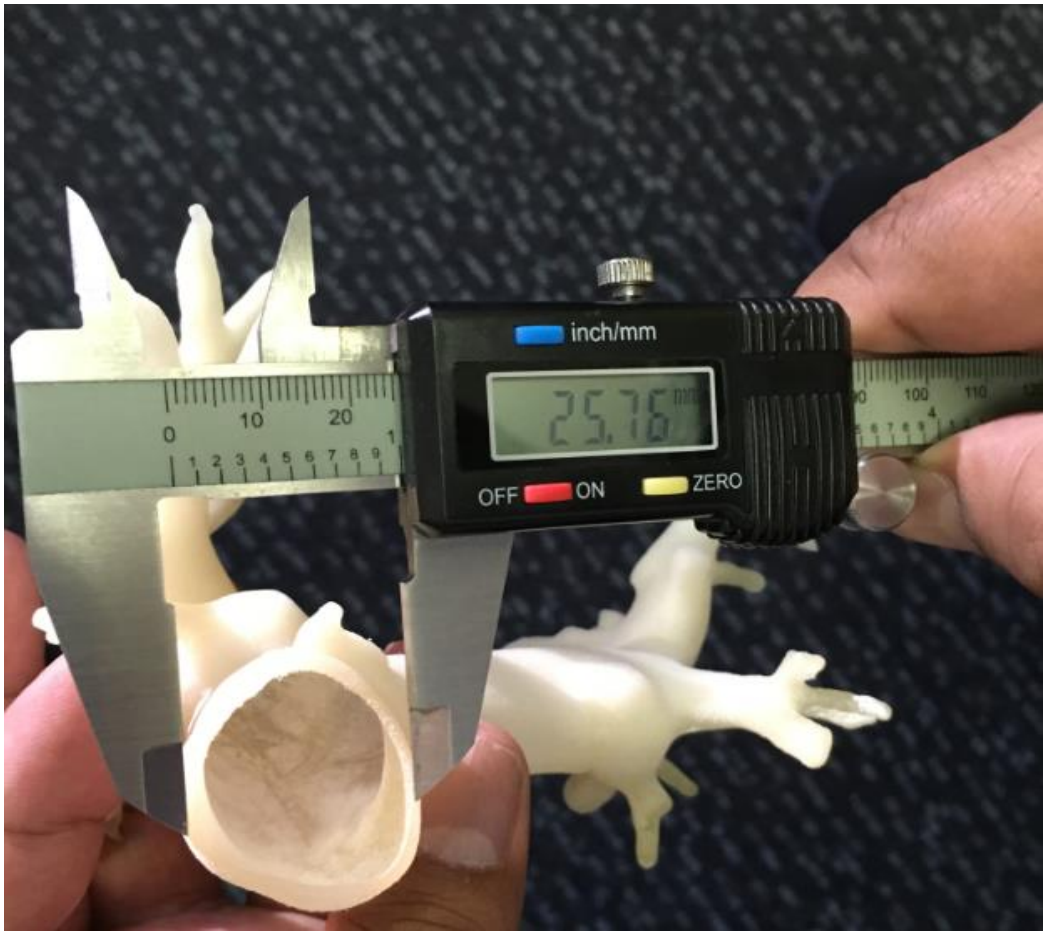

Figure 3.3 Measurement of the diameter of a pulmonary trunk using an electronic calliper.

3.2.5 Quantitative measurements of image quality

Image quality was assessed by measuring the image noise, which is defined as standard deviation (SD) of CT attenuation (HU) in the pulmonary arteries. A circular region of interest with a diameter of 50 mm^2 (containing 300 voxels within the ROI) was placed at the pulmonary trunk, left main and right main pulmonary arteries to measure the signal-to-noise ratio (SNR) which is defined as:

SNR = CT attenuation in the pulmonary artery / SD

Figure 3.4 is an example showing measurement of image quality (SNR) at the pulmonary trunk, left main and right main pulmonary arteries. Contrast-to-noise ratio (CNR) was not measured in this study due to lack of background tissue since 3D printed model was immersed into the contrast medium. The two observers performed

measurements separately and the results showed a high correlation between these two observers (r=0.99-1.0, p<0.05).

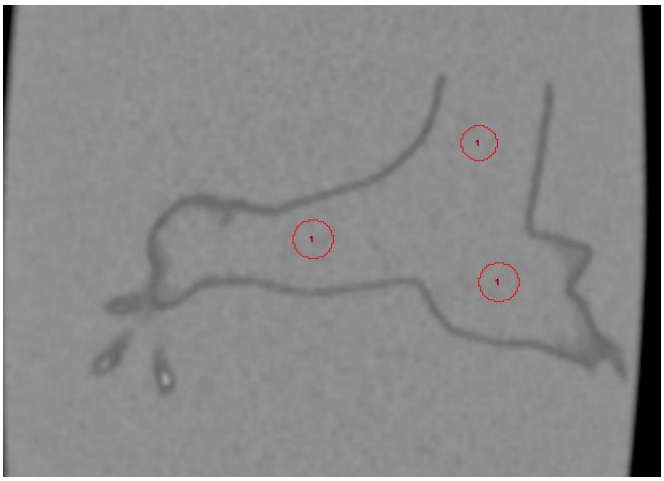

Figure 3.4 Region of interest is placed at the pulmonary trunk, right and left main pulmonary arteries for measurement of image quality.

3.2.6 Radiation dose

Radiation dose values in terms of volume CT dose index (CTDIvol) and dose length product (DLP) were available on the CT console. Effective dose (ED) was calculated by multiplying the DLP by a tissue coefficient factor, which is 0.014 mSv.mGy.cm for chest CT scan (28).

3.2.7 Statistical analysis

Data were entered into MS Excel for analysis. Continuous variables were presented as mean ± standard deviation. A paired sample Student T test was used to determine any significant differences between measurements performed at original CT, STL, 3D printed model and post-3D printing scanned images, with p value of less than 0.05 indicating statistical significance.

3.3 Results

CT scans of the 3D printed pulmonary artery model were successfully performed. Table 3.1 shows measurements of the main pulmonary arteries made with different scanning protocols when compared to the original CTPA images with differences less than 0.8 mm, indicating high accuracy of 3D printed model in replicating anatomical structures. There was also very good correlation between measurements on STL file in comparison to those on original CT images, post-3D printed CT images and 3D printed model, with the mean difference less than 0.5 mm.

Table 3.1 Diameters of pulmonary arteries measured on CT scanned 3D printed model

Measurement locations	80 kVp protocol (mean mm)			100 kVp protocol (mean mm)			120 kVp protocol (mean mm)		
	Pitch 0.7	Pitch 0.9	Pitch 1.2	Pitch 0.7	Pitch 0.9	Pitch 1.2	Pitch 0.7	Pitch 0.9	Pitch 1.2
Pulmonary trunk	25.44	25.97	25.59	25.77	25.13	25.1	25.97	25.86	25.94
Left pulmonary artery	26.57	26.11	26.88	26.25	26.72	26.31	26.22	26.79	26.86
Right pulmonary artery	21.77	21.88	21.45	21.66	21.07	21.41	21.23	21.23	21.45

LPA-left pulmonary artery, RPA-right pulmonary artery, STL-standard tessellation language

Table 3. 2 Diameters of pulmonary arteries measured on original CT images, STL images and 3D printed model

Measurements on datasets	Pulmonary trunk (mean mm)	Left main pulmonary artery (mean mm)	Right main pulmonary artery (mean mm)
Original CT images	25.93	26.20	21.63
STL images	25.98	26.03	21.90
3D printed model	25.85	26.02	21.84

3D: Three-dimensional, CT: Computed tomography, STL: Standard tessellation language

Table 3.3 shows SNR measurements at different CTPA protocols with corresponding radiation dose values. With 80 and 100 kVp protocols, SNR was slightly decreased when pitch was increased from 0.7 to 0.9 and 1.2, although this did not reach significant difference in measurements with these protocols (p=0.96-0.99). With 120 kVp protocol, SNR was slightly increased with the increase of pitch in most of the measurements, with no statistical significance difference noted (p=0.97-0.99).

Table 3.3 Quantitative measurement of image quality and radiation dose in different CT scanning protocols

Measurement locations	80 kVp protocol			100 kVp protocol			120 kVp protocol		
	Pitch 0.7	Pitch 0.9	Pitch 1.2	Pitch 0.7	Pitch 0.9	Pitch 1.2	Pitch 0.7	Pitch 0.9	Pitch 1.2
SNR at pulmonary trunk	13.28	12.79	11.41	20.29	14.68	13.36	17.18	19.46	18.99
SNR at left main pulmonary artery	13.44	12.16	10.59	14.81	14.73	10.97	14.18	16.28	16.27
SNR at right main pulmonary artery	10.25	10.84	10.08	15.11	10.97	11.19	15.21	17.35	15.72
CTDIvol (mGy)	5.81	5.73	5.62	12.96	12.84	12.64	23.12	22.90	22.61
DLP (mGy.cm)	128	128	128	286	286	286	510	511	514
ED (mSv)	1.79	1.79	1.79	4.04	4.04	4.04	7.14	7.15	7.19

SNR: Signal‑to‑noise ratio, DLP: Dose‑length product, ED: Effective dose, CTDIvol: Volume CT dose index

Table 3.3 also shows radiation dose values associated with these CTPA protocols. As shown in Table 3, CTDIvol and DLP remained almost the same despite the use of different pitch values, mainly due to the use of tube current modulation. With 80 kVp as the selected protocol, the effective dose was reduced by 55% and 75% when kVp was lowered from 100 and 120 kVp, respectively, while still maintaining diagnostic image quality. Figure 3.5 shows coronal reformatted CT images acquired with 9 different protocols with good visualisation of the pulmonary trunk and left and right main pulmonary arteries.

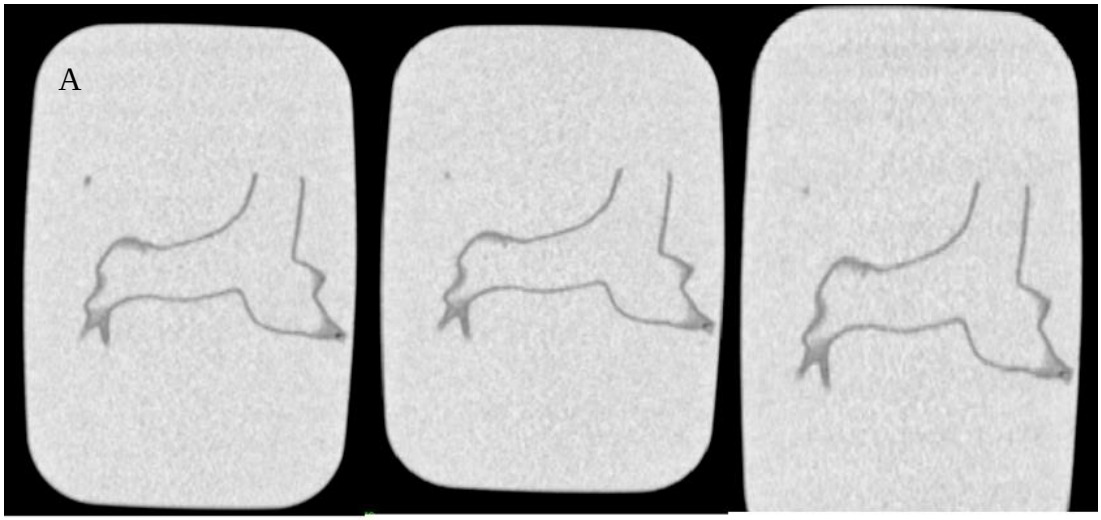

80 kVp with pitch 0.7 80 kVp with pitch 0.9 80 kVp with pitch 1.2

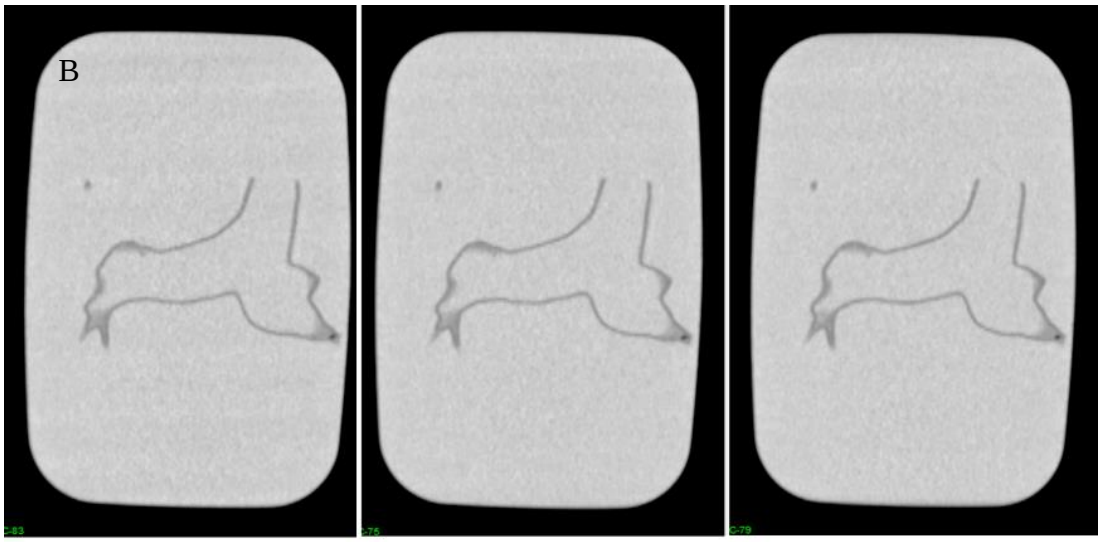

100 kVp with pitch 0.7 100 kVp with pitch 0.9 100 kVp with pitch 1.2

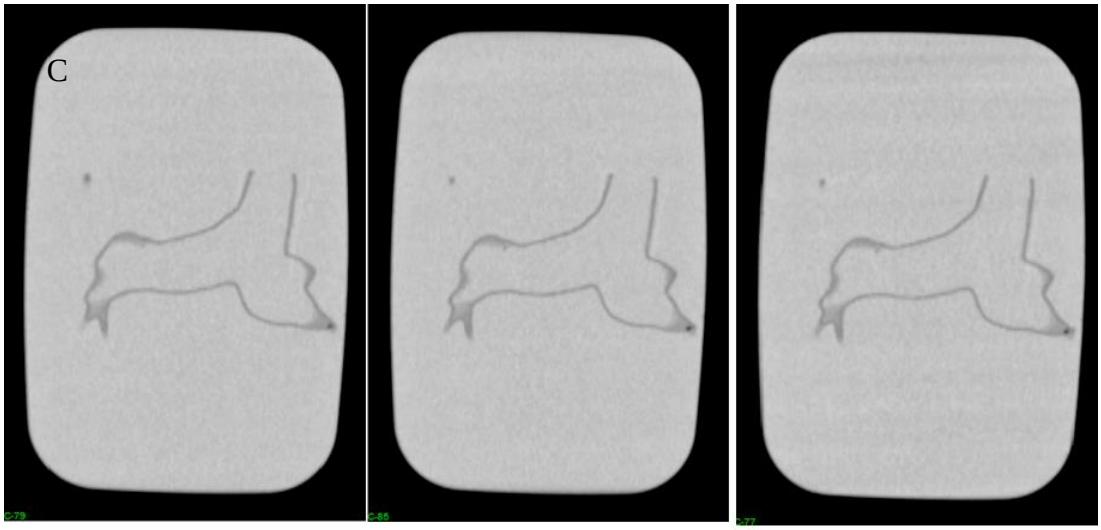

Figure 3.5 CT pulmonary angiography scanning protocols in the 3D printed model. 2D coronal reformatted images showing main pulmonary trunk, right and left main pulmonary arteries with 80 kVp, pitch 0.7, 0.9 and 1.2 (A), 100 kVp, pitch 0.7, 0.9 and 1.2 (B), 120 kVp, pitch 0.7, 0.9 and 1.2 (C).

3.4 Discussion

This preliminary study has two main findings: Firstly, 3D printed pulmonary artery model has high accuracy in replicating anatomical structures, thus it can be used as a reliable tool for testing CT scans. Secondly, an optimal CTPA protocol can be developed through testing different scanning protocols on the 3D printed model, with a protocol of 80 kVp and pitch 0.9 being the optimal one with resultant low radiation dose but maintaining diagnostic image quality.

3D printed models have been shown to enhance understanding of complexity of cardiovascular disease by demonstrating accuracy of delineating anatomical structures and pathologies, pre-operative planning and simulation, and medical education (6-15). Case reports and case series studies have proved successful applications of 3D printed models in assisting diagnosis and clinical management of congenital heart diseases including pulmonary artery abnormalities (29-33). A recent case report discussing the 3D printed model of ventricular septal defect (VSD) and pulmonary atresia showed

that 3D printing assisted the development of preoperative planning and treatment approach for managing this complex case (30). Sahayaraj et al further confirmed the clinical value of using 3D printed model in managing complex cardiovascular cases involving great vessels (31). The 3D printed model was found to have great value in improving understanding of the spatial relationship between cardiac chambers, VSD and great arteries, with biventricular physiologic repair successfully performed owing to the increased spatial perception provided by the 3D printed model.

Biglino and colleagues provided an insight into the clinical applications of 3D printed heart model based on the perspective from different stakeholders (29). The 3D printed model was considered by surgeon and cardiologist to improve understanding of the 3D relationship of different structures, such as better demonstrating the narrowed pulmonary artery and the dilated ascending aorta. Medical imaging specialist considered that 3D printed model improved communication in multidisciplinary meetings, thus allowing better decision-making in patient treatment. Further, a medical student indicated the great potential of 3D printed models in teaching anatomy and pathology (29).

Despite promising results about the clinical value of 3D printed models, reports on the dimensional accuracy of 3D printed pulmonary artery model are scarce. Most of the current studies focus on the accuracy of 3D printed heart models, in particular, congenital heart disease with good correlation between 3D printed models and original source images (5-9). However, in their recent study, Ho et al reported the mean difference of more than 1.0 mm in aortic vessel diameters between contrast-enhanced CT images before and after 3D printing (34). The variance in dimensional accuracy was also demonstrated by Lau et al who showed the mean diameter difference between 3D printed model of brain tumour and original images being 0.98%, which exceeds the recommended 0.5% deviation (35). Findings in this study showed high accuracy of the 3D printed pulmonary artery model with the mean difference less than 0.5% deviation in measurements between pre- and post-3D printing images. Thus, results of CT scans based on the 3D printed model could be used as a reliable source for determining optimal scanning protocols in terms of acquiring diagnostic images with radiation dose reduction.

Increased use of CTPA in clinical practice has raised concerns because of its associated high radiation exposure and potential risk of contrast-induced nephropathy (16, 20). Therefore, optimisation of CTPA protocol is a hot topic in the current literature with successful reductions in both radiation dose and contrast medium dose achieved. Findings of this study are in line with these previous reports on patient's data (16, 20). Low tube voltage and low pitch value such as 80 kVp and 0.9 is preferred with acquisition of acceptable diagnostic images (similar SNR values) but low radiation dose when compared to the protocol of 100 or 120 kVp and high pitch value. The current multislice CT scanners are equipped with latest dose-reduction protocols, such as automatic tube current or tube potential modulation, therefore, high pitch is not recommended. The pitch of 0.9 as recommended by this study is consistent with Boos et al who also proposed the 70 kVp and pitch of 0.9 CTPA protocol (36). We did not include 70 kVp in this study as 100 or 120 kVp is commonly used in CTPA. Further, due to 3D printed model being static instead of having hemodynamic flow features, we did not assess the effect of changing contrast medium volume on image quality. This could be addressed in further studies.

Despite promising results, this study has several limitations which need to be acknowledged. Firstly, the 3D printed model was based on a normal case without showing any sign of pulmonary embolism. Thus, no subjective assessment of image quality was conducted. Experiments on the optimal CTPA protocols in the detection of pulmonary embolism with use of 3D printed model are under investigation. Secondly, although the 3D printed model was made with elastic material, it still does not represent the real tissue properties of vascular wall. Further, the phantom was scanned in a static condition instead of representing realistic CTPA with blood circulating to the pulmonary arteries. Finally, due to including only one case, we did not perform Bland-Altman assessment of degree of agreement in measurements between pre- and post-3D printing images. Further studies should include more cases for generating 3D printed models, which would allow for more reliable detection of trends in bias.

In conclusion, we have shown the feasibility of generating patient-specific 3D printed pulmonary artery model with high accuracy in replicating normal anatomical structures. The 3D printed model is used to test different CT pulmonary angiography protocols with the protocol of 80 kVp, pitch 0.9 with 1 mm slice thickness and reconstruction interval of 0.6 mm being the optimal one. Future research based on simulation of pulmonary embolism with different CT scanning parameters is needed to determine the clinical value of 3D printed model in detection of pulmonary embolism with lower radiation dose while still maintaining diagnostic image quality.

3.5 References

1. Valverde I, Gomez G, Gonzales A, Suarez-Mejias C, Adsuar AF, et al. Three-dimensional patient-specific cardiac model for surgical planning in Nikaidoh procedure. Cardiol Young 2015;25(4):698-704.
2. Ebert J, Özkol E, Zeichner A, Uibel K, Weiss O, Koops U, et al. Direct inkjet printing of dental prostheses made of zirconia. J Dent Res 2009;88(7):673–676.
3. Ploch CC, Mansi CSSA, Jayamohan, J, Kuhl, E. Using 3D printing to create personalized brain models for neurosurgical training and preoperative planning. World Neurosurg 2016;90:668-674.
4. Martelli N, Serrano C, van den Brink H, Pineau J, Prognon P, Borget I, et al. Advantages and disadvantages of 3-dimensional printing in surgery: A systematic review. Surgery 2016;159:1485-1500.
5. Bartel T, Rivard A, Jimenez A, Mestres CA, Muller S. Medical three-dimensional printing opens up new opportunities in cardiology and cardiac surgery. Eur Heart J 2017 Feb 16. doi: 10.1093/eurheartj/ehx016. [Epub ahead of print].
6. Schmauss D, Haeberle S, Hagl C, Sodian R. Three-dimensional printing in cardiac surgery and interventional cardiology: a single-centre experience. Eur J Cardiothorac Surg 2015;47(6):1044–1052.
7. Biglino G, Koniordou D, Gasparini M, Capelli C, Leaver LK, Khambadkone S, et al. Piloting the use of patient-specific cardiac models as a novel tool to facilitate communication during clinical consultations. Pediatr Cardiol 2017;38:813-818.
8. Cantinotti M, Valverde I, Kutty S. Three-dimensional printed models in congenital heart disease. Int J Cardiovasc Imaging 2017;33:1337-144.
9. Giannopoulos AA, Mitsouras D, Yoo SJ, Liu PP, Chatzizisis YS, Rybicki FJ. Applications of 3D printing in cardiovascular diseases. Nat Rev Cardiol 2016;13:701-18.
10. Bhalta P, Tretter JT, Chikkabyrappa S, Chakravarti S, Mosca RS. Surgical planning for a complex double-outlet right ventricle using 3D printing. Echocardiography 2017;34:802-804.

11. Lim KH, Loo ZY, Goldie S, Adams J, McMenamin P. Use of 3D printed models in medical education: A randomized control trial comparing 3D prints versus cadaveric materials for learning external cardiac anatomy. Anat Sci Educ 2016;9(3):213-221.
12. Costello J, Olivieri L, Krieger A, Thabit O, Marshall MB, Yoo SJ, et al. Utilizing three-dimensional printing technology to assess the feasibility of high-fidelity synthetic ventricular septal defect models for simulation in medical education. World J Pediatr Congenit Heart Surg 2014;5(3):421-426.
13. Costello JP, Olivieri LJ, Su L, Krieger A, Alfares F, Thabit O, et al. Incorporating three-dimensional printing into a simulation-based congenital heart disease and critical care training curriculum for resident physicians. Congenit Heart Dis 2015;10(2):185–190.
14. Sun Z, Lee SY. A systematic review of 3-D printing in cardiovascular and cerebrovascular diseases. Anatol J Cardiol 2017 2017;17:423-35.
15. Giannopoulos AA, Steigner ML, George E, Barlie M, Hunssaker AR, Rybicki FJ, Mitsouras D. Cardiothoracic applications of 3-dimensional printing. J Thorac Imaging 2016:31:253-72.
16. Mayo J, Thakur Y. Pulmonary CT angiography as first-line imaging for PE: image quality and radiation dose considerations. AJR Am J Roentgenol 2013; 200(3): 522–528.
17. Wittram C. How I do it: CT pulmonary angiography. AJR Am J Roentgenol 2007;188(5): 1255–1261.
18. den Exter AL, van der Hulle T, Klok FA, Huisman MV. Advances in the diagnosis and management of acute pulmonary embolism. Thromb Res 2014;133(Suppl 2): S10-16.
19. Righini M, Le GG, Aujesky D, Roy RM, Sanchez O, Verschuren F, et al. Diagnosis of pulmonary embolism by multidetector CT alone or combined with venous ultrasonography of the leg: a randomised non-inferiority trial. Lancet 2008;371(9621): 1343-52.
20. Sun Z, Lei J. Diagnostic yield of CT pulmonary angiography in the diagnosis of pulmonary embolism: a single center experience. Interv Cardiol 2017;9: 191-198.
21. Ong CW, Malipatil V, Lavercombe M, Teo KGW, Coughlin PB, Leach D, et al. Implementation of a clinical prediction tool for pulmonary embolism

diagnosis in a tertiary teaching hospital reduces the number of computed tomography pulmonary angiograms performed. Intern Med J 2013;43:169-74.

22. Newman DH, Schriger DL. Rethinking testing for pulmonary embolism: less is more. Ann Emerg Med 2011; 57:622-7.e3.
23. Mitsouras D, Liacouras P, Imanzadeh A, Giannopolous AA, Cai T, Kumamaru KK, George E, Wake N, Caterson EJ, Pomahac B, Ho VB, Grant GT, Rybicki FJ. Medical 3D printing for the radiologist. Radiographics 2015; 35(7):1965-1988.
24. Madurska MJ, Poyade M, Eason D, Rea P, Watson AJM. Development of a patient-specific 3D-printed liver model for preoperative planning. Surg Innov 2017; 24(2):145-150.
25. Witowski JS, Coles-Black J, Zuzak TZ, Pedziwiatr M, Chuen J, Major P, Budzynki A. 3D printing in liver surgery: A systematic review. Telemed J E Health 2017; 23(12):1-5.
26. Shapeways. Frequently Asked Questions. Available from: http://www.shapeways.com/support/faq?li=footer#faq-whatisshapeways.
27. https://www.shapeways.com/materials/elasto-plastic
28. McCollough CH, Primak AN, Braun N, Kofler J, Yu L, Christner J. Strategies for reducing radiation dose in CT. Radiol Clin North Am 2009; 47: 27 –40.
29. Biglino G, Moharem-Elgamal S, Lee M, Tulloh R, Caputo M. The perception of a three-dimensional-printed heart model from the perspective of different stakeholders: A complex case of truncus ateriosus. Front Pediatr 2017;5:209.
30. Jaworski R, Haponiuk I, Chojnicki M, Olszewski H, Lulewicz P. Three-dimensional printing technology supports surgery planning in patients with complex con-genital heart defects. Kardiol Pol 2017;75:185.
31. Sahayaraj RA, Ramanan S, Subramanyan R, Cherian KM. 3D printing to model surgical repair of complex congenitally corrected transposition of the great arteries. World J Pediatr Congenit Heart Surg 2017; Jan 1:2150135117704655. doi: 10.1177/2150135117704655. [Epub ahead of print].
32. Jones TW, Seckeler MD. Use of 3D models of vascular rings and slings to improve resident education. Congenit Heart Dis 2017;12:578-582.
33. Kappanayil M, Koneti NR, Kannan RR, Kottavil BP, Kumar K. Three-dimensional-printed cardiac prototypes aid surgical decision-making and

preoperative planning in selected cases of complex congenital heart diseases: early experience and proof of concept in a resource-limited environment. Ann Pediatr Cardiol 2017:10:117–25.

34. Ho D, Squelch A, Sun Z. Modeling of aortic aneurysm and aortic dissection through 3D printing. J Med Radiat Sci 2017;64:10-17.
35. Lau I, Squelch A, Wan YL, Wong A, Ducke W, Sun Z. Patient-specific 3D printed model in delineating brain glioma and surrounding structures in a pediatric patient. Digit Med 2017;3:86-92.
36. Boos J, Kropil P, Lanzman RS, Aissa J, Schleich C, Heusch P, et al. CT pulmonary angiography: simultaneous low-pitch dual-source acquisition mode with 70 kVp and 40 ml of contrast medium and comparison with high-pitch spiral dual-source acquisition with automated tube potential selection. Br J Radiol 2016;89:20151059.

Chapter 4

Optimization of computed tomography pulmonary angiography protocols using 3D printed model with simulation of pulmonary embolism

4.1 Introduction

Computed tomography pulmonary angiography (CTPA) is currently the preferred imaging modality for diagnosis of suspected pulmonary embolism (PE). With improved spatial and temporal resolution available with modern CT scanners, CTPA has high diagnostic accuracy in the detection of segmental and subsegmental PE (1-3). However, the high radiation dose associated with CTPA is still a concern, given the high prevalence of PE and widespread use of less-invasive imaging for clinical diagnosis (1-5). Therefore, improvements in CT technique to minimize radiation dose are necessary.

A number of strategies have already been developed which include low tube voltage (kVp), use of iterative reconstruction (IR) for reducing image noise, and use of high-pitch protocols with fast speed CT scanners (6-13). Significant progress has been achieved with use of these dose-reduction strategies with radiation dose lowered to less than 2 mSv, according to some recent studies (14-16). Despite these promising results, further dose reduction by combining different parameters remains to be determined. Thus, the purpose of this study was to investigate the optimal CTPA protocols with use of different kVp and pitch values. Since it is unethical to scan patients with different CT protocols, we decided to use a patient-specific 3D printed pulmonary artery model with simulation of PE in the pulmonary arteries. In our previous paper, we described how we developed a 3D printed pulmonary artery model and confirmed its accuracy and validity in replicating normal pulmonary arteries by testing different CT scanning parameters on it (17).

In this publication we describe how we extended our previous research by inserting thrombus in the pulmonary arteries to simulate PE, and scanning the model with different CTPA protocols. Although patient-specific 3D printed models have been reported in the literature with regard to their accuracy and usefulness in preoperative planning and simulation (18-23), to the best of our knowledge, this is the first study using a 3D printed pulmonary artery model with thrombus inside the arteries for determining optimal CTPA protocols.

4.2 Materials and Methods

4.2.1 Selection of sample case and image post-processing and segmentation

CTPA images of patients with suspected PE were retrospectively reviewed and one sample case with normal CTPA findings without any sign of pulmonary embolism was selected for generation of the pulmonary artery model with details provided in our previous study (17).

The same approach was used to perform image post-processing and segmentation of CTPA images as described previously (17). Figure 4.1 shows the steps that were undertaken to generate a 3D segmented volume file for 3D printing of the pulmonary artery lumen. The 3D model was printed using an online printing service, Shapeways (24). An elastoplastic material was used to print the model since it has similar properties to that of arterial wall (25).

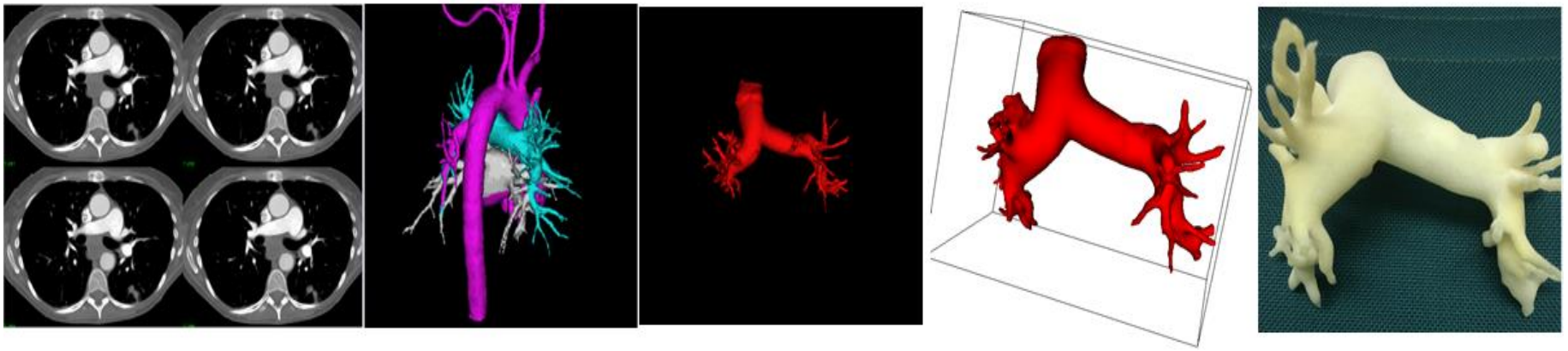

2D DICOM images | 3D volume data segmentation | 3D segmented pulmonary arteries | STL file for 3D printing | 3D printed model

Figure 4.1 Flow diagram shows the image post-processing and segmentation processes from original 2D CT images to creation of 3D printed model. Original DICOM images were used to create 3D volume rendering image for displaying contrast-enhanced vessels (blue colour-pulmonary arteries, pink colour-aorta and its branches, white colour-left atrium and pulmonary veins). 3D volume rendering of pulmonary artery tree is segmented through a semi-automatic segmentation approach with manual editing. STL (Standard Tessellation Language) file of 3D segmented volume data was generated for 3D printing of patient-specific 3D printed model. Reprinted with permission under the open access from (17).

4.2.2 3D printing of pulmonary artery model with simulation of thrombus

To simulate PE in the pulmonary arteries, animal blood clots which were obtained from a local butcher were inserted into the left and right main pulmonary arteries of the 3D printed model mimicking thrombus. To prevent the "thrombus" from moving during CT scans, the blood clots were large enough to be deployed in the main pulmonary arteries, thus remaining stable during the scans.

4.2.3 CTPA scanning protocols

The 3D printed pulmonary artery model with thrombi inside was placed in a plastic container which was filled with contrast medium to simulate contrast-enhanced CT examinations. The contrast medium Optiray^{TM} 350 (Mallinckrodt Pty Ltd, NSW, Australia) was diluted to 7% with resulting CT attenuation of 200 HU similar to that of routine CTPA. CTPA scans were performed on a dual-source 128-slice CT scanner (Siemens Definition Flash, Siemens Healthcare, Forchheim, Germany) with beam collimation of 2 x 64 x 0.6 mm and gantry rotation of 330 ms. Tube current modulation was used for all scans while different kVp and pitch values were chosen (70, 80, 100 and 120 kVp and pitch of 0.9, 2.2 and 3.2), resulting in a total of 12 datasets. A slice thickness of 1.0 mm with a 0.5 mm reconstruction interval was applied to all images, resulting in the voxel size of 0.29 x 0.29 x 0.29 mm^3 for volumetric data. All images were reconstructed with sinogram affirmed iterative reconstruction (SAFIRE, Siemens Healthcare) at a strength level of 3, and a tissue convolution kernel of I30f.

4.2.4 Image post-processing and visualization of pulmonary embolism

2D images in Digital Imaging and Communications in Medicine (DICOM) format were transferred to a workstation with Analyze V 12.0 (AnalyzeDirect, Inc., Lexana, KS, USA) for image post-processing and generation of 2D and 3D virtual intravascular endoscopy (VIE) images. VIE visualization provides intraluminal views of the arterial wall and abnormal changes such as stenosis due to calcification, plaque or thrombus, with details of generating VIE views described in our previous studies (26-30). In brief, a CT number thresholding technique was used to generate VIE views of the pulmonary artery and thrombus in these phantom images without being affected by artifact. Selection of an appropriate CT threshold is important to ensure that the VIE images are free from artifact with clear demonstration of intraluminal views of pulmonary artery wall and thrombus. Figure 4.2 is an example showing the relationship between VIE visualizations and different threshold selections.

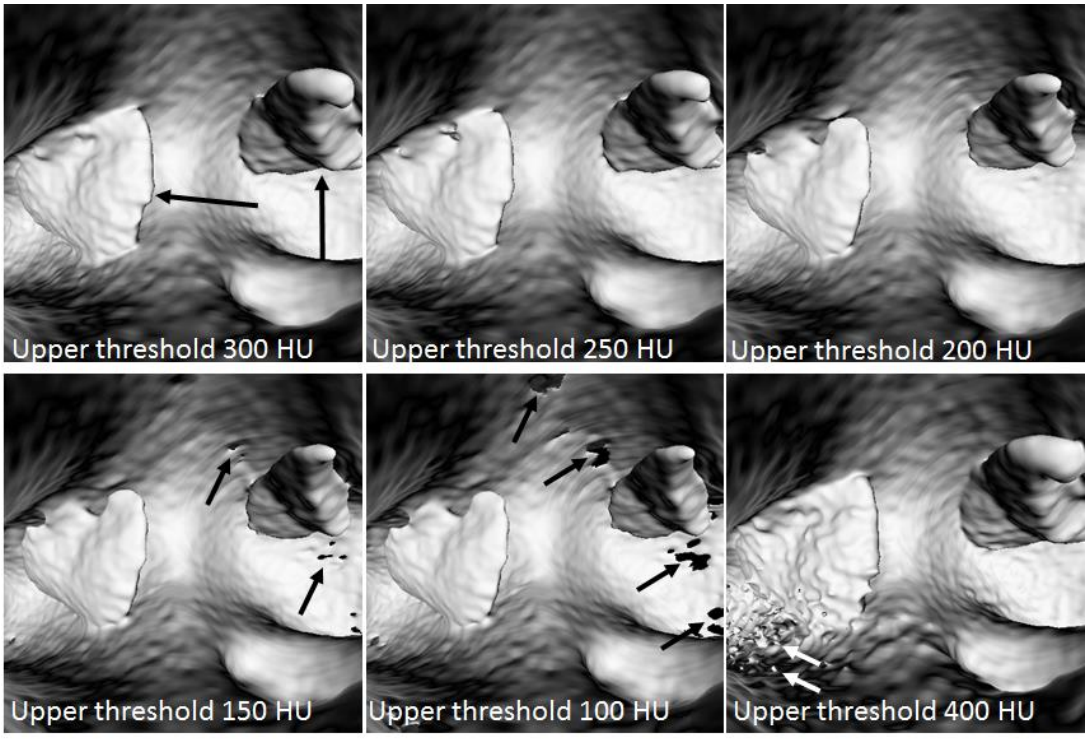

Figure 4.2 Generation of virtual intravascular endoscopy (VIE) of pulmonary embolism with selection of appropriate CT thresholds. Upper CT threshold was selected to start at 300 Hounsfield unit (HU) showing the best visualization of intraluminal thrombus (long black

arrows). When upper threshold was reduced to lower levels, pierced artifacts (short black arrows) appeared in the arterial wall resulting in disruption of the arterial lumen. When upper threshold was increased to 400 HU, floating artifacts (white arrows) appeared in the arterial lumen affecting visualization of thrombus.

4.2.5 Quantitative assessment of image quality

To determine image quality among these CTPA protocols, quantitative assessment of image quality was performed by measuring the image quality in terms of signal-to-noise ratio (SNR) in the main pulmonary arteries and within the thrombus regions. A region of interest (ROI) with an area of 25 mm^2 (containing minimum 300 voxels) was placed in the main right and left pulmonary arteries to measure the SNR. In addition, a ROI with an area of 5 mm^2 (containing 50 voxels) was placed within the thrombus region to measure SNR among these images. Figure 4.3 shows measurement of SNR in the main pulmonary arteries and within thrombus regions. Measurements were repeated three times at each location with the mean values used as the final to minimize intra-observer variability. All measurements were performed by two observers separately with excellent correlation between the observers (r=0.991, p<0.001) with mean values used as the final results.

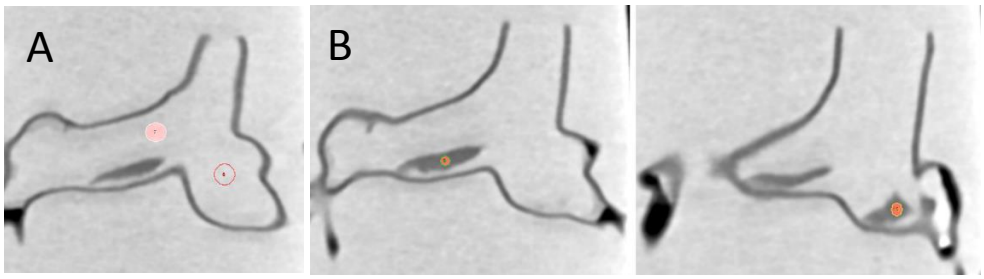

Figure 4.3 Measurement of image quality to determine signal-to-noise ratio (SNR). A: measurement of image quality at the main pulmonary arteries. B: measurement of image noise within the thrombus at both sides of pulmonary arteries.

4.2.6 Radiation dose measurement

Volume CT dose index (CTDIvol) and dose length product (DLP) were recorded and compared between these CTPA protocols. Effective dose was calculated using a tissue conversion coefficient of 0.014 mSv/mGy/cm which is commonly used for calculation of chest CT dose (31).

4.2.7 Statistical analysis

Data were entered into SPSS 24.0 (IBM Corporation, Armonk, NY, USA) for statistical analysis. Continuous variables were presented as mean and standard deviation. A paired sample t test was used to determine whether there are any significant differences in SNR measured with different CTPA protocols. A p value of less than 0.05 indicates a statistically significant difference.

4.3 Results

CTPA scans were successfully tested on the 3D printed model with use of different imaging protocols. Table 4.1 shows SNR measurements at images acquired with different CTPA protocols. Apparently SNR measured within the thrombus on both sides was significantly higher in images acquired with higher kVp such as 100 and 120 protocols than that in the low 70 and 80 kVp protocols ($p<0.001$). There were no significant differences in SNR measurements across all 100 and 120 kVp protocols ($p>0.05$), regardless of the pitch values. SNR was significantly lower in the high-pitch

protocols with 70 and 80 kVp, when compared to the protocols with use of pitch values of 0.9 and 2.2 ($p<0.01$).

Table 4.1 Measurements of SNR in images acquired with different CTPA protocols and associated radiation dose

Pitch values/ SNR and radiation dose	**70 kVp**			**80 kVp**			**100 kVp**			**120 kVp**		
	0.9	**2.2**	**3.2**	**0.9**	**2.2**	**3.2**	**0.9**	**2.2**	**3.2**	**0.9**	**2.2**	**3.2**
Right main pulmonary artery	37.06 ± 5.24	30.69 ± 1.29	27.42 ± 1.81	32.91 ± 0.60	30.53 ± 4.41	24.51 ± 1.63	29.06 ± 1.38	28.01 ± 1.23	30.89 ± 2.90	36.13 ± 0.55	39.15 ± 0.71	42.09 ± 1.19
Left main pulmonary artery	40.22 ± 3.94	29.89 ± 0.30	20.87 ± 2.03	35.27 ± 1.10	28.35 ± 1.30	25.63 ± 0.79	34.38 ± 1.46	31.31 ± 1.23	36.86 ± 2.51	58.83 ± 1.07	47.54 ± 2.32	67.30 ± 3.90
Within right thrombus	4.22 ± 0.13	4.16 ± 0.02	3.28 ± 0.16	4.84 ± 0.30	5.02 ± 0.30	4.92 ± 0.37	6.52 ± 0.27	6.44 ± 0.33	6.37 ± 0.59	10.55 ± 0.71	9.10 ± 0.65	10.07 ± 1.41
Within left thrombus	6.02 ± 0.50	4.99 ± 0.43	4.83 ± 0.49	6.48 ± 0.26	6.49 ± 0.42	4.82 ± 0.42	13.02 ± 0.51	12.36 ± 1.27	10.61 ± 1.04	13.27 ± 1.27	11.73 ± 0.73	10.89 ± 1.09
CTDIvol (mGy)	0.41	0.15	0.12	0.42	0.21	0.21	1.01	0.55	0.55	2.22	1.05	1.05
DLP (mGy/cm)	5.9	2.7	2.2	6.2	4	3.6	14.6	10.3	9.5	32.2	19.7	18.1
Effective dose (mSv)	0.08	0.04	0.03	0.09	0.06	0.05	0.20	0.14	0.13	0.45	0.28	0.25

CTPA-computed tomography pulmonary angiography, SNR-signal-to-noise ratio

SNR measured outside the thrombus in the main pulmonary arteries did not show any significant differences among these images acquired with 100 and 120 kVp protocols ($p>0.05$), except for the 120 kVp and pitch 3.2 protocol which shows significantly higher SNR than in the low pitch protocols ($p<0.05$). Similarly, SNR measured in images (both left and right main pulmonary arteries) acquired with 70 and 80 kVp and pitch of 3.2 protocol was significantly lower than that in other protocols ($p<0.05$). Figure 4.4 is an example showing coronal reformatted images of these CTPA protocols. When pitch was increased to 3.2, image noise was increased with use of low kVp protocols such as 70 and 80 kVp as shown in Figs 4.4A and 4.4B. However, the thrombi in the pulmonary arteries are clearly displayed on these images, despite the use of low-dose protocols.

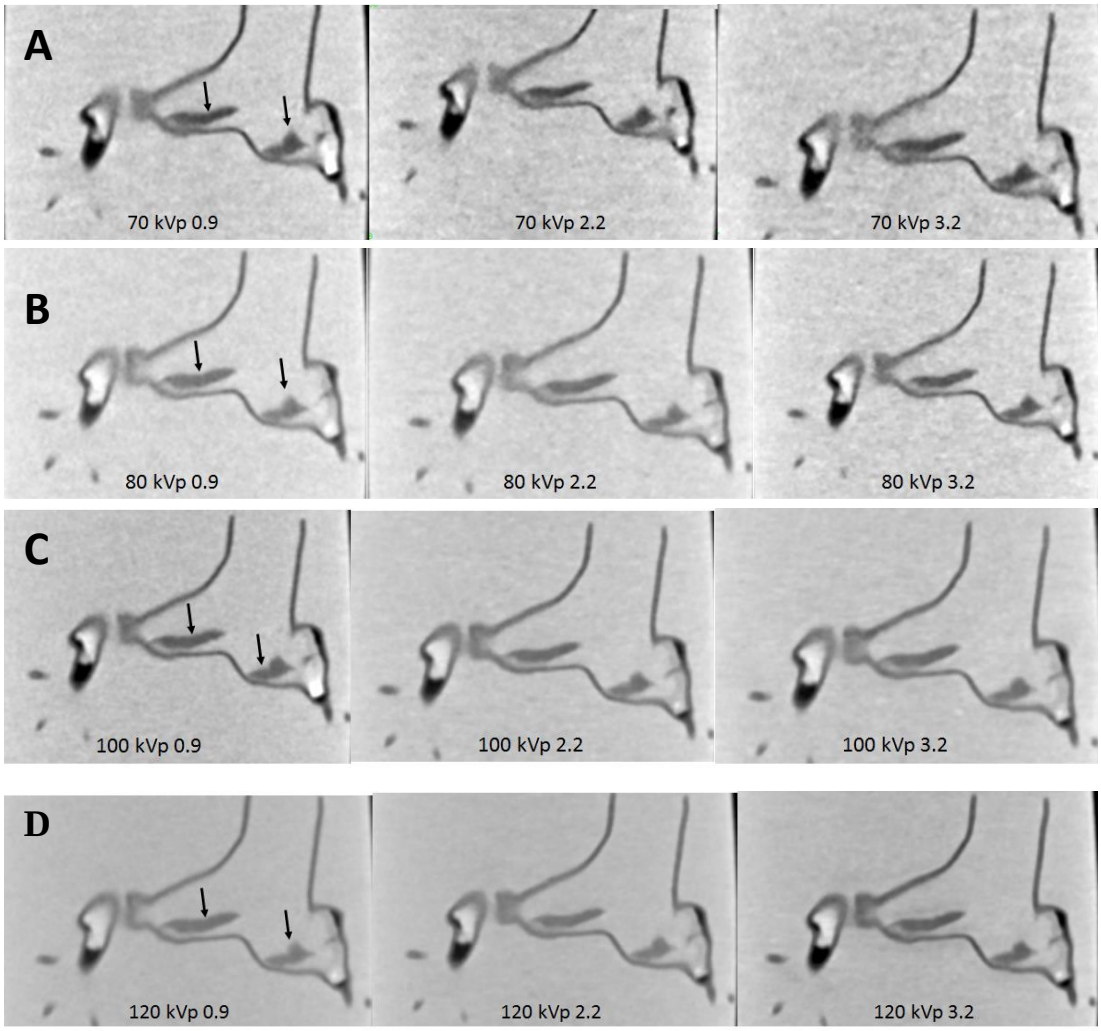

Figure 4.4 CTPA protocols with use of different kVp and pitch values. When pitch was increased to 3.2, image noise was increased with 70 and 80 kVp protocols (A and B). In contrast, no significant change of image quality was noted with 100 and 120 kVp protocols (C, D), regardless of pitch values.

3D VIE images were generated and compared across different CTPA protocols with clear visualization of intraluminal views of pulmonary artery lumen and thrombus. Figures 4.5 shows a series of VIE images generated with these CTPA protocols. As shown in the images, VIE views of the arterial wall and thrombus were not affected by changing the kVp values, although 100 and 120 protocols produced VIE images with relatively smoother intraluminal appearances (Figs 4.5A-4.5C). VIE images were not affected by changing the pitch from 0.9 to 2.2 (Figs 4.5A and 4.5B), however, when pitch was increased to the high-pitch mode of 3.2, images acquired with the 70 kVp protocol were affected, with irregular appearances of arterial wall and thrombi when compared to those protocols with use of 100 and 120 kVp (Fig 4.5C).

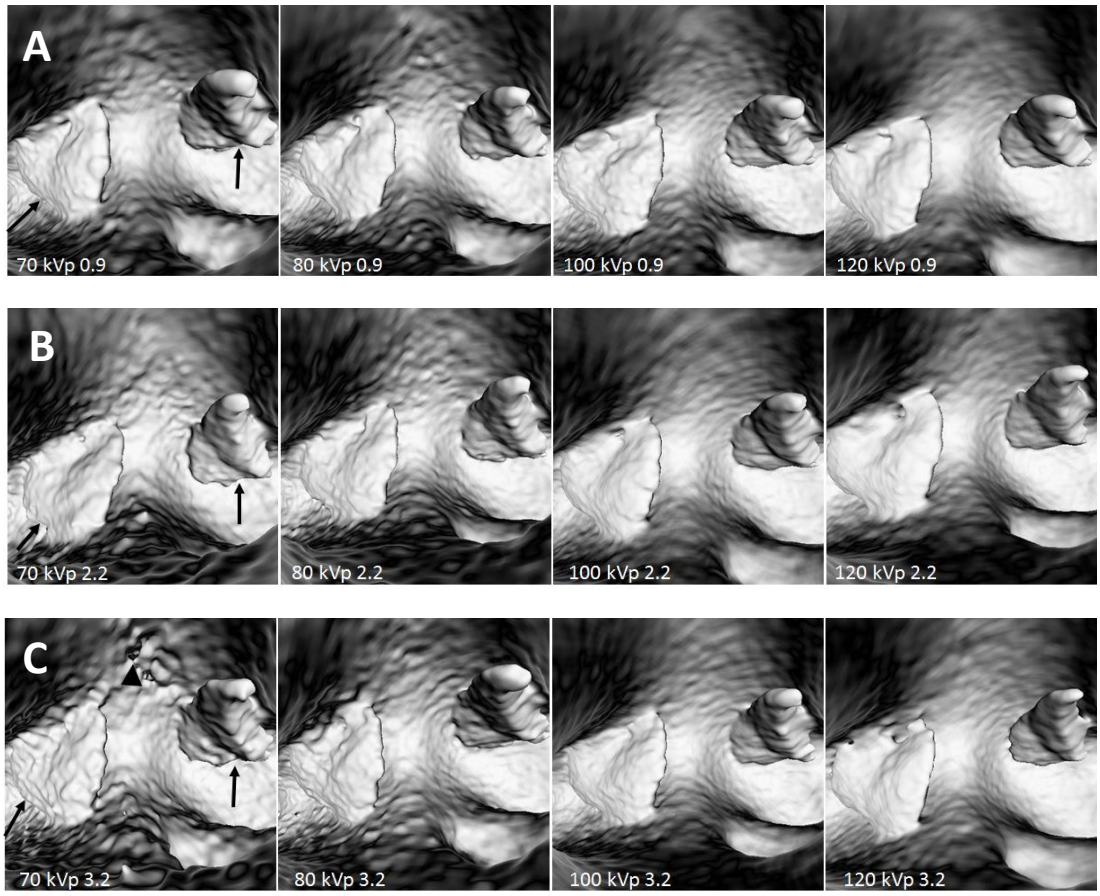

Figure 4.5 Virtual intravascular endoscopy (VIE) of thrombus in images acquired with different CTPA protocols. Intraluminal views of the thrombus are clearly demonstrated with CTPA protocols using different kVp and pitch values of 0.9 and 2.2 (4.5A and 4.5B). When high pitch of 3.2 was used, irregular appearance of the thrombus (arrows) and some artifacts (arrowhead) appeared in the low kVp 70 protocol when compared to other protocols (4.5C). VIE: virtual intravascular endoscopy; CTPA-computed tomography pulmonary angiography.

Table 4.1 shows CTDIvol and DLP as well as effective dose associated with these scanning protocols. With kVp reduced from 120 to 70 and use of high-pitch CTPA protocols, radiation dose was reduced by 33-89% when compared to the low kVp and low pitch protocols without compromising image quality.

4.4 Discussion

In this phantom study, we simulated PE in the main pulmonary arteries based on a 3D printed model and tested different CTPA protocols comprising a range of kVp and pitch values. Quantitative assessment of image quality showed no significant differences when kVp was lowered from 120 to 100 or 80 kVp, or pitch was increased from 0.9 to 3.2. This led to a significant dose reduction by more than 80% with use of low-dose CTPA protocols. 3D VIE image visualizations of pulmonary artery and thrombus demonstrated similar findings, although visualization of the thrombus was affected when the high pitch of 3.2 was used in the 70 kVp protocol. This study further confirms the feasibility of using a low-dose CTPA protocol in the detection of PE while maintaining acceptable image quality.

CTPA is currently recommended as the first line imaging modality in the diagnosis of suspected PE, given the high spatial and temporal resolution available with current CT scanners, and the high diagnostic yield (4, 13). Technical developments of CT imaging have led to significant dose reductions with use of various dose-saving strategies including low kVp, use of IR algorithms, tube current modulation, high-pitch protocol and use of dual energy CT (2, 32, 33). Low-dose CTPA using 70 or 80 kVp and high-pitch mode has been proved to achieve diagnostic image quality compared to the standard CTPA protocol, while significantly reducing radiation dose (9, 11-14). However, research on the investigation of image quality in normal pulmonary arteries and pulmonary embolism is still limited. This study adds valuable information to the current literature by exploring a variety of CTPA protocols including the lowest kVp and highest pitch value of 3.2 that is available in the literature.

A high-pitch CT protocol is available with fast speed CT scanners and decreases radiation dose significantly when pitch is increased from the standard 0.9 to 2.2 or more than 3.0. However, increasing pitch during CT scans is associated with compromising spatial resolution, which could increase image noise affecting diagnostic quality. We confirmed this in our study as image noise was increased in the 70 and 80 kVp protocols with a pitch of 3.2 (Figs 4.4A, 4.4B). This is especially apparent when visualizing the intraluminal thrombus at the images acquired with 70

kVp and the 3.2 pitch protocol (Fig 4.5C). Despite this potential limitation, clinical studies have shown the feasibility of using high-pitch CTPA protocols in the diagnosis of PE without losing image quality (12-14, 34).

Buchner et al (34) in their large single center study compared high-pitch CTPA (180 mAs with filtered back projection and pitch 1.2, and 90 mAs with IR, pitch 3.0) with standard pitch (180 mAs and pitch 1.2) and 100 kVp in 382 patients. No significant difference was noticed in image quality among these 3 groups, while significant reduction of radiation dose was found in the high-pitch and low tube current group ($p<0.001$). Their results are consistent with other reports on the use of combining low kVp with high-pitch protocols (12-15). Lowering kVp to 80 or 70 in the high-pitch CTPA protocol could be challenging due to the potential risk of compromising image quality. This was observed in our study as the SNR measured with 70 and 80 kVp protocols was significantly lower than that measured with 100 or 120 kVp protocols (Table 4.1). Further, 3D visualization of intraluminal appearances of thrombus and pulmonary artery wall is affected by artifact due to increased image noise with 70 kVp and high pitch 3.2 protocol. Previous studies focused on 2D (axial and multiplanar reformation) images for detecting PE with low-dose CTPA protocols (12-15, 34), while in this study, we assessed both 2D and 3D VIE images acquired with different CTPA protocols and corresponding image quality for visualization of PE, thus, our results provide additional information to the current literature.

With rapid developments in 3D printing techniques and increasing applications in the medical field, patient-specific 3D printed models have been shown to be highly accurate in replicating normal anatomical structures and pathologies (17, 20-23). Our recent study (17) has demonstrated the accuracy of a 3D printed pulmonary artery model with successful testing of different CT scanning protocols on the model. To our knowledge, this is the first report of using a patient-specific 3D printed pulmonary model for determining optimal CTPA protocols. Findings of this study are expected to encourage more research 3D printing techniques in other applications to develop low-dose CT protocols.

There are some limitations in this study. First, despite a realistic 3D printed model being used for studying different CTPA protocols, the model was not placed in an environment which simulated normal anatomic regions such as lungs, ribs, bones or

heart. Thus, the radiation dose associated with these protocols is much lower than the actual value as reported in other studies due to the small field of view in these CT scans. Confirmation of results with simulation of normal thoracic structures are required. Second, only SNR was measured to determine image quality while no contrast-to-noise ratio (CNR) was measured. This is due to the reason that the 3D printed model was immersed in the diluted contrast medium instead of only filling the pulmonary arteries with contrast medium. Quantitative assessment of image quality using both SNR and CNR would allow us to draw robust conclusions. Third, pulmonary embolism was simulated in the main pulmonary arteries, while no blood clot was used in the peripheral arteries to simulate embolism. Although CTPA has high diagnostic value, accurate detection of peripheral (segmental or subsegmental) or small thrombus in the peripheral pulmonary artery branches with a low-dose protocol would be required. This is currently being investigated with the aim of simulating small emboli in the peripheral arterial branches. Finally, no subjective assessment of image quality was included due to the fact that the pulmonary emboli were large. This could be assessed in the ongoing study with simulation of peripheral pulmonary embolism with different CTPA protocols.

In conclusion, we have demonstrated the feasibility of simulating pulmonary embolism in a 3D printed pulmonary model with different CT scanning protocols tested. Low-dose CTPA protocol is achievable with use of low kVp such as 70 or 80 with acceptable image quality. When high-pitch of 3.2 is used for CTPA, kVp can be lowered to 80 or 100 without compromising image quality in most of the protocols. Use of a low-dose CTPA protocol by combining 70 kVp with high-pitch 3.2 should be avoided due to its negative impact on the image quality of both pulmonary arteries and thrombus, as well as on intraluminal visualization of thrombus and pulmonary artery wall. Further studies on a low-dose CTPA protocols for detection of peripheral pulmonary embolism are underway.

4.5 References

1. Sherk WM, Stojanovska J. Role of clinical decision tools in the diagnosis of pulmonary embolism. AJR Am J Roentgenol 2017;208:W60-W70.
2. Albrecht MH, Bickford MW, Nance JW Jr, Zhang L, De Cecco CN, Wichmann JL, Vogl TJ, Schoepf UJ. State-of-the-Art pulmonary CT angiography for acute pulmonary embolism. AJR Am J Roentgenol 2017;208:495-504.
3. Kligerman SJ, Mitchell JW, Sechrist JW, Meeks AK, Galvin JR, White CS. Radiologist performance in the detection of pulmonary embolism: Features that favor correct interpretation and risk factors for errors. J Thorac Imaging 2018 Aug 23. doi: 10.1097/RTI.0000000000000361. [Epub ahead of print].
4. Sun Z, Lei J. Diagnostic yield of CT pulmonary angiography in the diagnosis of pulmonary embolism: a single center experience. Interv Cardiol 2017;9: 191-198.
5. Ong CW, Malipatil V, Lavercombe M, Teo MG, Coughlin PB, Leach D, Spanger MC, Thien F. Implementation of a clinical prediction tool for pulmonary embolism diagnosis in a tertiary teaching hospital reduces the number of computed tomography pulmonary angiograms performed. Intern Med J 2013;43:169-74.
6. Chen EL, Ross JA, Grant C, Wilbur A, Mehta N, Hart E, Mar WA. Improved image quality of low-dose CT pulmonary angiograms. J Am Coll Radiol 2017;14:648-653.
7. Wichmann JL, Hu X, Kerl JM, Schulz B, Frellesen C, Bodelle B, Kaup M, Scholtz JE, Lehnert T, Vogl TJ, Bauer RW. 70 kVp computed tomography pulmonary angiography: potential for reduction of iodine load and radiation dose. J Thorac Imaging 2015;30:69-76.
8. Martini K, Meier A, Higashhigaito K, Saltybaeva N, Alkadhi H, Frauenfelder T. Prospective randomized comparison of high-pitch CT at 80 kVp under free breathing with standard-pitch CT at 100 kVp under breath-hold for detection of pulmonary embolism. Acad Radiol 2016;23:1335-1341.
9. Li X, Ni QQ, Schoepf UJ, Wichmann JL, Felmly LM, Qi L, Kong X, Zhou CS, Luo S, Zhang LJ, Lu GM. 70-kVp high-pitch computed tomography

pulmonary angiography with 40 mL contrast agent: initial experience. Acad Radiol 2015; 22:1562–1570.

10. Kligerman S, Lahiji K, Weihe E, Lin CT, Terpenning S, Jeudy J, Frazier A, Pugatch R, Galvin JR, Mittal D, Kothari K, White CS. Detection of pulmonary embolism on computed tomography: improvement using a model-based iterative reconstruction algorithm compared with filtered back projection and iterative reconstruction algorithms. J Thorac Imaging 2015;30:60-68.
11. Bolen MA, Renapurkar RD, Popovic ZB, Popovic ZB, Heresi GA, Flamm SD, Lau CT, Lau CT, Halliburton SS. High-pitch ECG synchronized pulmonary CT angiography versus standard CT pulmonary angiography: a prospective randomized study. Am J Roentgenol 2013; 201:971–976.
12. Lu GM, Luo S, Meinel FG, McQuiston AD, Zhou CS, Kong X, Zhao YE, Zheng L, Schoepf UJ, Zhang LJ. High-pitch computed tomography pulmonary angiography with iterative reconstruction at 80 kVp and 20 mL contrast agent volume. Eur Radiol 2014; 24:3260–3268.
13. Sabel BO, Buric K, Karara N, Thierfelder KM, Dinkel J, Sommer WH, Meinel FG. High-pitch CT pulmonary angiography in third generation dual-source CT: image quality in an unselected patient population. PLoS ONE 2016; 11:e0146949.
14. Boos J, Kropil P, Lanzman RS, Aissa J, Schleich C, Heusch P, Sawichi LM, Antoch G, Thomas C. CT pulmonary angiography: simultaneous low-pitch dual-source acquisition mode with 70 kVp and 40 ml of contrast medium and comparison with high-pitch spiral dual-source acquisition with automated tube potential selection. Br J Radiol 2016;89:20151059.
15. Laqmani A, Regier M, Veldhoen S, Backhaus A, Wassenberg F, Sehner S, Groth M, Nagel HD, Adam G, Henes FO. Improved image quality and low radiation dose with hybrid iterative reconstruction with 80 kV CT pulmonary angiography. Eur J Radiol 2014; 83:1962–9.
16. Hu X, Ma L, Zhang J, Li Z, Shen Y, Hu D. Use of pulmonary CT angiography with low tube voltage and low-iodine-concentration contrast agent to diagnose pulmonary embolism. Sci Rep 2017;7:12741.
17. Aldosari S, Squelch A, Sun Z. Patient-specific 3D printed pulmonary artery model: A preliminary study. Digit Med 2017;3:170-177.

18. Olivieri LJ, Krieger A, Loke YH, Nath DS, Kim PC, Sable CA. Three-dimensional printing of intracardiac defects from three-dimensional echocardiographic images: feasibility and relative accuracy. J Am Sco Echocardiogr. 2015;28: 392-97.
19. Cantinotti M, Valverde I, Kutty S. Three-dimensional printed models in congenital heart disease. Int J Cardiovasc Imaging. 2017;33(1):137-144.
20. Lau I, Liu D, Xu L, Fan Z, Sun Z. Clinical value of patient-specific three-dimensional printing of congenital heart disease: Quantitative and qualitative Assessments. PLoS One 2018;13:e0194333.
21. Liu D, Sun Z, Chaichana T, Ducke W, Fan Z. Patient-specific 3D printed models of renal tumours using home-made 3D printer in comparison with commercial 3D printer. J Med Imaging Health Inf 2018;8:303-308.
22. Sun Z, Liu D. A systematic review of clinical value of three-dimensional printing in renal disease. Quant Imaging Med Surg 2018;8:311-325.
23. Lau I, Sun Z. Three-dimensional printing in congenital heart disease: A systematic review. J Med Radiat Sci 2018;65:226-236.
24. Shapeways. Frequently Asked Questions. Available from: http:// www.shapeways.com/support/faq?li=footer#faq-whatisshapeways.
25. Available from: https://www.shapeways.com/materials/ elasto-plastic.
26. Xu L, Sun Z. Virtual intravascular endoscopy visualization of calcified coronary plaques: a novel approach of identifying plaque features for more accurate assessment of coronary lumen stenosis. Medicine 2015;94:e805.
27. Sun Z, Dosari SA, Ng C, al-Muntashari A, Almaliky S. Multislice CT virtual intravascular endoscopy for assessing pulmonary embolisms: a pictorial review. Korean J Radiol 2010;11:222-230.
28. Sun Z, Dimpudus FJ, Nugroho J, Adipranoto JD. CT virtual intravascular endoscopy assessment of coronary artery plaques: a preliminary study. Eur J Radiol 2010;75:e112-e119.
29. Sun Z, Winder JR, Kelly BE, Ellis PK, Kennedy PT, Hirst DG. Assessment of VIE image quality using helical CT angiography: in vitro phantom study. Comput Med Imaging Graph. 2004; 28:3-12.
30. Sun Z, Gallagher E. Multislice CT virtual intravascular endoscopy for abdominal aortic aneurysm stent grafts. J Vasc Intervent Radiol. 2004; 15:961-970.

31. McCollough CH, Primak AN, Braun N, Kofler J, Yu L, Christner J. Strategies for reducing radiation dose in CT. Radiol Clin North Am 2009;47:27-40.
32. Henzler T, Barraza JM, Nance JW, Jr, Costello P, Krissak R, Fink C, Schoepf UJ. CT imaging of acute pulmonary embolism. J Cardiovasc Comput Tomogr 2011;5:3–11.
33. Zhang LJ, Lu GM, Meinel FG, McQuiston AD, Ravenel JG, Schoepf UJ. Computed tomography of acute pulmonary embolism: state-of-the-art. Eur Radiol 2015;25:2547–2557.
34. Bucher AM, Kerl MJ, Albrecht MH, Beeres M, Ackermann H, Wichmann JL, Vogl TJ, Bauer RW, Lehnert T. Systematic comparison of reduced tube current protocols for high-pitch and standard-pitch pulmonary CT angiography in a large single-center population. Acad Radiol 2016;23:619-627.

Chapter 5

Patient-specific 3D printed pulmonary artery model with simulation of peripheral pulmonary embolism for developing optimal computed tomography pulmonary angiography protocols

5.1 Introduction

Computed tomography pulmonary angiography (CTPA) is increasingly used in the diagnosis of patients with suspected pulmonary embolism (PE) due to its high sensitivity and specificity for detecting segmental and subsegmental PE (1-5). However, the high radiation dose associated with the increased use of CTPA examinations has raised concerns leading to the paradigm shift of developing optimal CTPA protocols to lower radiation dose while still achieving diagnostic images. Low-dose CTPA protocols have been reported in some studies showing the feasibility of reducing tube voltage to 80 and 70 kVp with use of high pitch values with resultant effective dose of less than 2 mSv (6-13). The main disadvantage of lowering tube voltage during CTPA is associated with increased image noise, with noise further increased when a high pitch protocol is used. Use of iterative reconstruction (IR) algorithms have been shown to compensate for increased image noise arising from low kVp protocols, thus improving image quality for diagnosis of PE (14-17). This has created potential opportunities for developing low-dose CT protocols through combining low kVp and high pitch protocols with IR.

Testing different CT protocols on a 3D printed realistic anatomy model represents a new research direction for investigation of optimal CT angiography protocols as 3D printed models accurately replicate both normal anatomical structures and pathologies (18-23). In our previous papers, we reported how we developed a patient-specific 3D printed pulmonary artery model with high accuracy, and tested different CTPA protocols on the model with simulation of thrombus in the main pulmonary arteries (24, 25). Through quantitative assessment of image quality, we concluded that low-dose CTPA is achievable with tube voltage lowering to 100 and 80 kVp and use of high pitch 3.2 with more than 80% radiation dose reduction without compromising image quality. In this study we extended our previous research by simulating thrombus in the peripheral pulmonary arteries and scanning the model with different parameters using the latest CT scanner, the 3rd generation dual-source CT, Siemens Force. Further, advanced modelled iterative reconstruction (ADMIRE) available with the Siemens Force system is the latest IR algorithm which offers higher radiation dose reduction while reducing image noise and minimizing artifacts. The purpose of this study was

to determine optimal CTPA protocols for detection of small and peripheral thrombus in the pulmonary arteries with resulting low radiation dose and acceptable diagnostic images.

5.2 Materials and Methods

5.2.1 3D printed pulmonary artery model

This study used the same 3D printed pulmonary artery model as reported in our previous papers (24, 25). The model was confirmed to be highly accurate in delineating anatomical structures of pulmonary arteries with successful simulation of pulmonary embolism in the main pulmonary arteries.

5.2.2 Simulation of thrombus in the peripheral pulmonary arteries

Animal blood clots were obtained from a local butcher with small amounts inserted into the peripheral pulmonary arteries to mimic pulmonary embolism. Figure 5.1 shows selection of small thrombus for insertion into the distal pulmonary artery branches prior to CT scans.

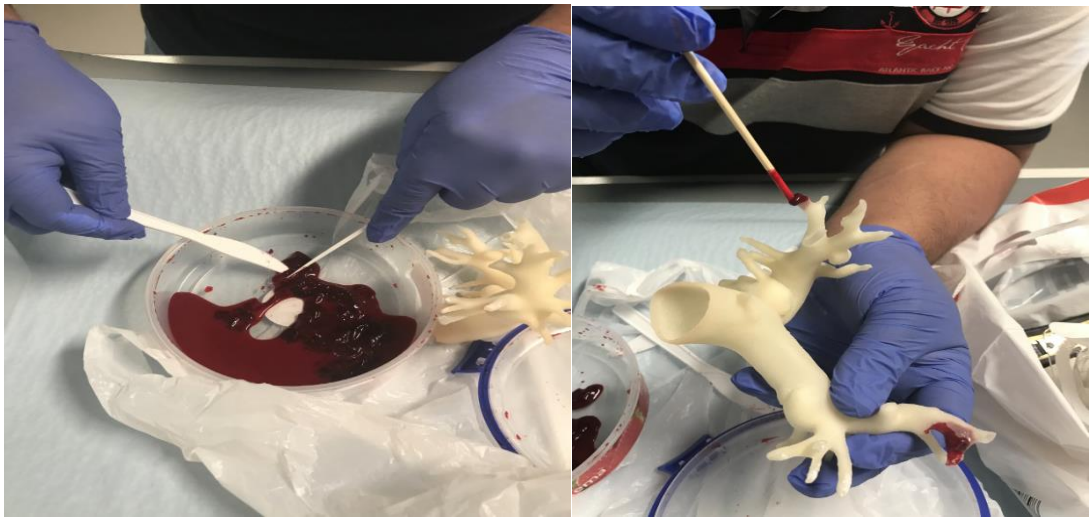

A B

Figure 5.1 Procedure to insert blood clots in the 3D printed pulmonary artery model. A: Blood clots which were obtained from a local butcher were broken into small pieces. B: Insertion of small blood clots in the peripheral segments of pulmonary arteries in the 3D printed model.

5.2.3 CTPA scanning protocols

Similar to our previous papers, the 3D printed model with peripheral thrombus in the pulmonary arteries was immersed in a plastic container which was filled with diluted contrast medium to create a CT attenuation of 200 HU which is similar to that of CTPA examinations (Fig 5.2). CTPA scans were performed on a 3rd generation dual-source 192-slice CT scanner (Siemens Force, Siemens Healthcare, Forchheim, Germany) with beam collimation of 192 x 0.6 mm and gantry rotation of 250 ms. The CTPA scanning protocols were as follows: 70, 80, 100 and 120 kVp, pitch of 0.9, 2.2 and 3.2, resulting in a total of 12 datasets. The tube current was adjusted for CTPA protocols with pitch of 0.9 based on the kVp, with mAs of 121, 35, 42 and 52 corresponding to 70, 80, 100 and 120 kVp, respectively. For higher pitch values of 2.2 and 3.2, 80 mAs was used for the remaining protocols, regardless of the kVp values. All images were acquired with a slice thickness of 1.0 mm and 0.5 mm reconstruction interval, resulting in the voxel size of 0.31 x 0.31 x 0.31 mm^3 for volumetric data. All images were reconstructed with ADMIRE (Siemens Medical Solutions, Forchheim, Germany) at a strength level of 3, and a tissue convolution kernel of Br40d.

Figure 5.2 3D visualization of 3D printed pulmonary artery model which was placed inside the container filled with contrast medium. Since the model was immersed into the water with diluted contrast medium with similar CT attenuation to that of routine CT pulmonary angiography, surface voxel projection was used to create 3D view of the model.

5.2.4 Qualitative assessment of image quality

Images were presented to two experienced thoracic radiologists (each with more than 5 years of experience in interpreting chest CT images) in a random order without showing any information about the scanning parameters. The two assessors were blinded to the scanning protocols and they assessed image quality independently using a 5-point Likert scale with a score of 3 or above indicating that image quality is diagnostic:

- 5: excellent visualization of thrombus with high confidence,
- 4: good visualization of thrombus with good confidence,
- 3: average visualization of thrombus with moderate confidence,
- 2: suboptimal visualization of thrombus with low confidence, and
- 1 poor visualization of thrombus with no confidence.

5.2.5 Quantitative assessment of image quality

Quantitative assessment of image quality was determined by measuring the image noise in the main pulmonary arteries in terms of signal-to-noise ratio (SNR). A region of interest (ROI) with an area of >0.5 cm^2 (containing minimum 500 voxels) was placed in both main pulmonary arteries to measure the SNR. Due to the presence of air bubbles in the pulmonary arteries, ROI was placed in the central part of the main pulmonary arteries to avoid inclusion of any air bubbles which could affect the measurements. Figure 5.3 shows SNR measurements in the main pulmonary arteries. Measurements at each location were repeated three times with the mean values used to reduce intra-observer variability. Two observers performed the measurements separately with excellent correlation between them (r=0.918, p<0.001). Mean values of measurements from these two observers were used as the final results.

A B

Figure 5.3 Measurement of signal-to-noise ratio (SNR) in the main pulmonary arteries. A and B: SNR measurements at the right and left main pulmonary arteries.

5.2.6 Radiation dose calculation

Volume CT dose index (CTDIvol) and dose length product (DLP) were available on CT console after scans. These values were used to calculate effective dose based on a tissue conversion coefficient of 0.014 mSv/mGy/cm for chest CT dose calculation (26).

5.2.7 Statistical analysis

Data were analysed using SPSS 24.0 (IBM Corporation, Armonk, NY, USA). Mean and standard deviation were used to represent continuous variables. A paired sample Student T test was used to determine any significant differences in SNR measurements among different CTPA protocols. Inter-observer agreement for image quality assessment was assessed by kappa statistics: poor: k<0.20; fair: k=0.21-0.40; moderate: k=0.41-0.60; good: k=0.61-0.80, and excellent agreement k=0.81-1.00. A statistically significant difference was reached at a p value of less than 0.05.

5.3 Results

Insertion of small blood clots into the side or peripheral pulmonary was found to be challenging due to softness of the blood clots which were easily broken into small pieces during the insertion procedure (Fig 5.1). We managed to insert two small blood clots in the pulmonary arteries with one in the left segmental pulmonary arterial branch and another one in the distal segment of right main pulmonary artery simulating thrombus. CTPA scans with different protocols were successfully performed on the 3D printed model with simulation of PE.

Table 5.1 shows SNR measurements at the main pulmonary arteries corresponding to different CTPA protocols. Although low kVp 70 and 80 protocols were associated with increased image noise when compared to 100 and 120 kVp protocols, a high CT attenuation was found in these low kVp protocols in comparison with the high kVp

protocols (340-440 HU vs 210-260 HU). Thus, SNR measured with the 70 kVp protocols was found to be even higher than that with 80 or 100 kVp protocols as shown in the Table. There were no significant differences in SNR measurements across all CTPA protocols ($p>0.05$), regardless of the pitch or kVp values. SNR was slightly higher in the 120 kVp with pitch 0.9 and 2.2 protocols, however, this did not reach statistical significance compared to other protocols ($p>0.05$).

Table 5.1 Measurements of SNR in images acquired with different CTPA protocols and associated radiation dose

Pitch values/ SNR and radiation dose	**70 kVp**			**80 kVp**			**100 kVp**			**120 kVp**		
	0.9	2.2	3.2	0.9	2.2	3.2	0.9	2.2	3.2	0.9	2.2	3.2
Right main pulmonary artery	39.69 ± 4.39	29.75 ± 0.10	31.66 ± 1.49	31.33 ± 0.50	37.84 ± 2.57	35.83 ± 1.04	26.48 ± 2.12	37.44 ± 1.72	39.17± 1.85	40.17 ± 0.61	43.35 ± 1.55	38.92 ± 2.00
Left main pulmonary artery	31.05 ± 0.92	30.81 ± 1.43	26.11 ± 0.69	28.24 ± 1.10	30.31 ± 0.60	28.27 ± 1.85	31.60 ± 0.45	29.90 ± 1.11	24.30 ± 0.47	40.43 ± 1.94	33.72 ± 0.49	27.68 ± 1.07
CTDIvol (mGy)	1.42	0.72	0.72	0.68	1.17	1.17	1.72	2.53	2.53	3.53	4.26	4.26
DLP (mGy/cm)	30.4	14.7	15.6	14.6	24	25.5	36.7	51.6	55	75.4	87.2	92.7
Effective dose (mSv)	0.42	0.20	0.21	0.20	0.33	0.35	0.51	0.72	0.77	1.05	1.22	1.29

CTPA-computed tomography pulmonary angiography, SNR-signal-to-noise ratio, CTDIvol-volume computed tomography dose index, DLP-dose length product.

Figures 5.4-5.7 show coronal reformatted images acquired with different CTPA protocols demonstrating pulmonary emboli in the pulmonary artery branches. Despite low kVp or high pitch protocols, thrombi are still visible in all images, although 100 and 120 kVp protocols allowed for better visualization of the small thrombus, especially at the left side. Inter-observer agreement was fair (k=0.333, p=0.118). The protocol of 70 kVp and pitch 3.2 was scored 3, the lowest score by these two assessors, indicating that images are still acceptable with the low-dose protocol. All of the remaining images were scored 4 or 5 by the two assessors.

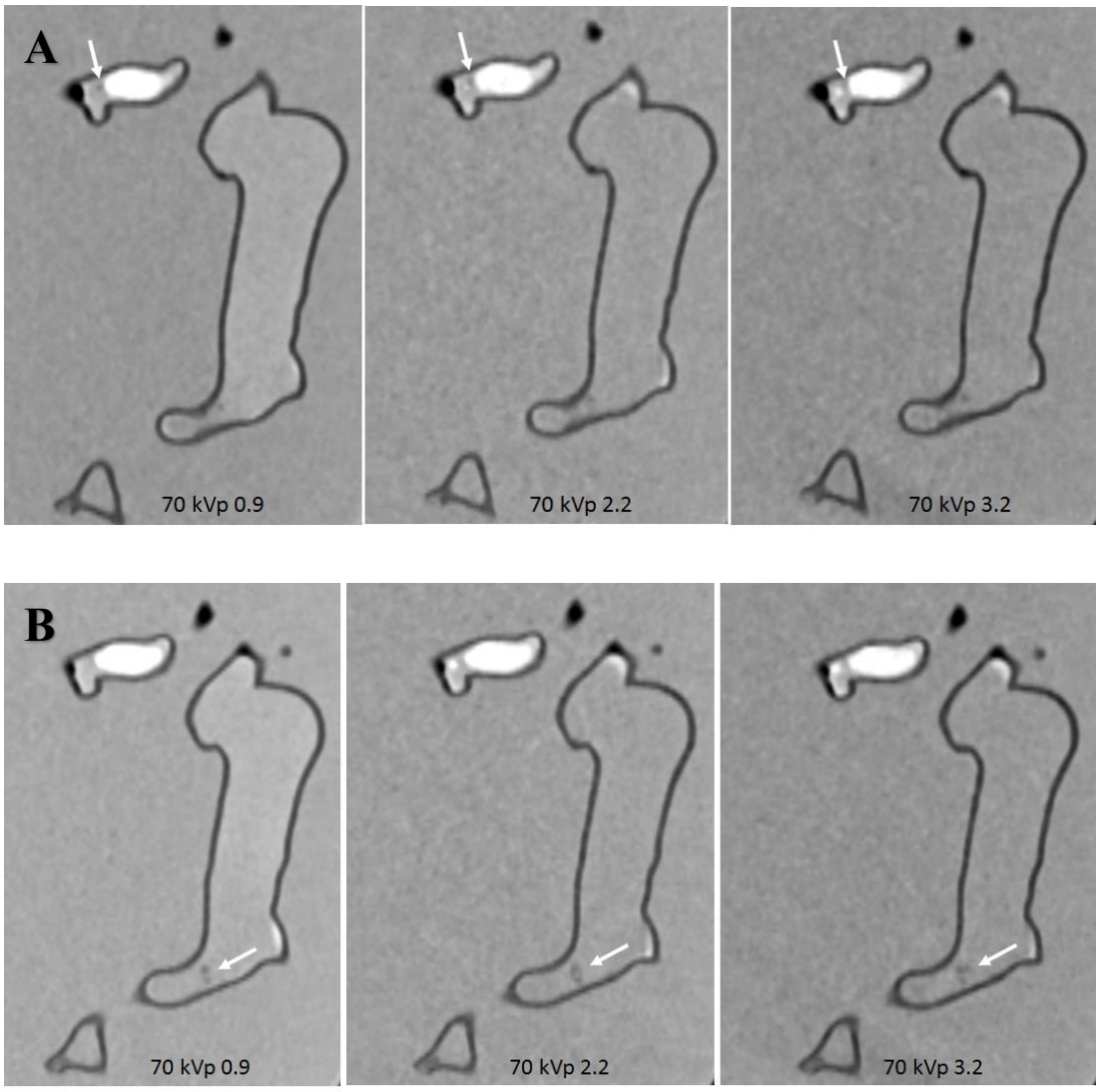

Figure 5.4 CTPA protocols with use of 70 kVp and different pitch values. A: Visualization of small thrombus in the left segmental pulmonary artery with low-attenuation filling defect (arrows). Thrombus was more clearly visualized in pitch 0.9 and 2.2 protocols when

compared to the high pitch 3.2 protocol. B: Visualization of small thrombus in the distal part of right main pulmonary artery with filling defect (arrows) detected in all of the protocols.

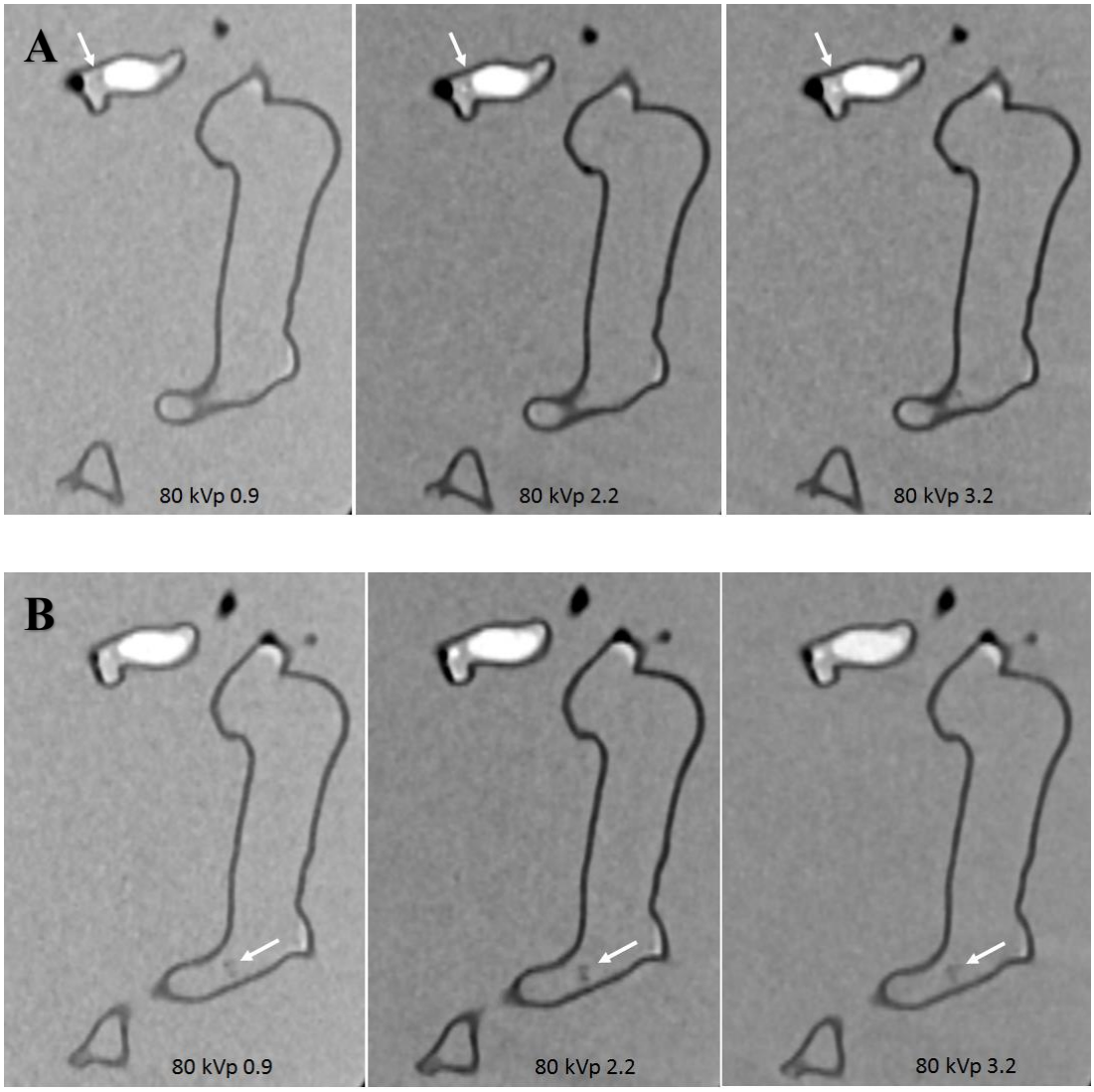

Figure 5.5 CTPA protocols with use of 80 kVp and different pitch values. A and B: The small thrombus is viewed as low-attenuation filling defect in the left segmental pulmonary artery (arrows in A) and right pulmonary artery (arrows in B) and thrombi are visible in all protocols, regardless of pitch values used.

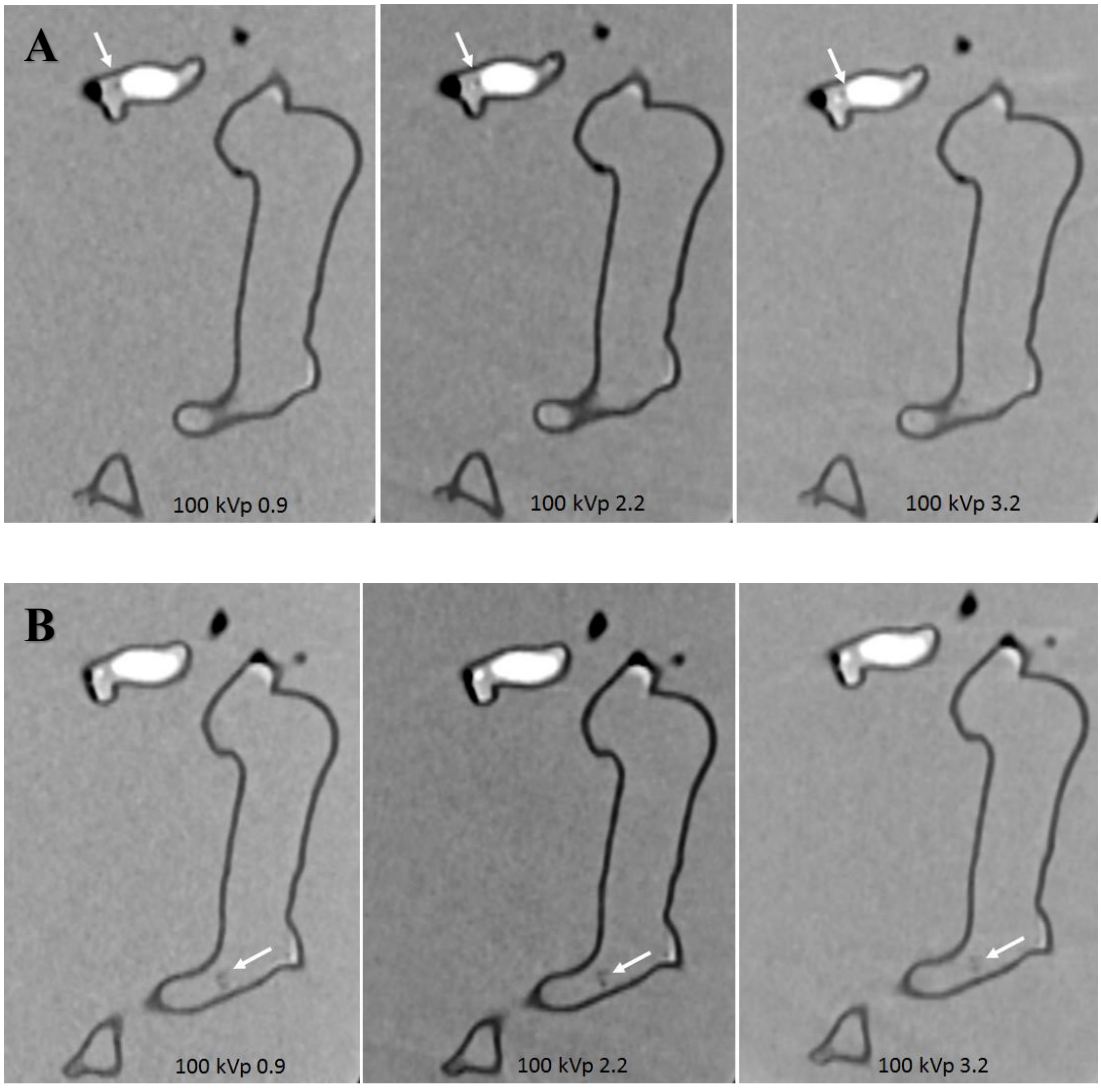

Figure 5.6 CTPA protocols with use of 100 kVp and different pitch values. A and B: The small thrombus is viewed as low-attenuation filling defect in the left segmental pulmonary artery (arrows in A) and right pulmonary artery (arrows in B) and they are visible in all protocols, regardless of pitch values used.

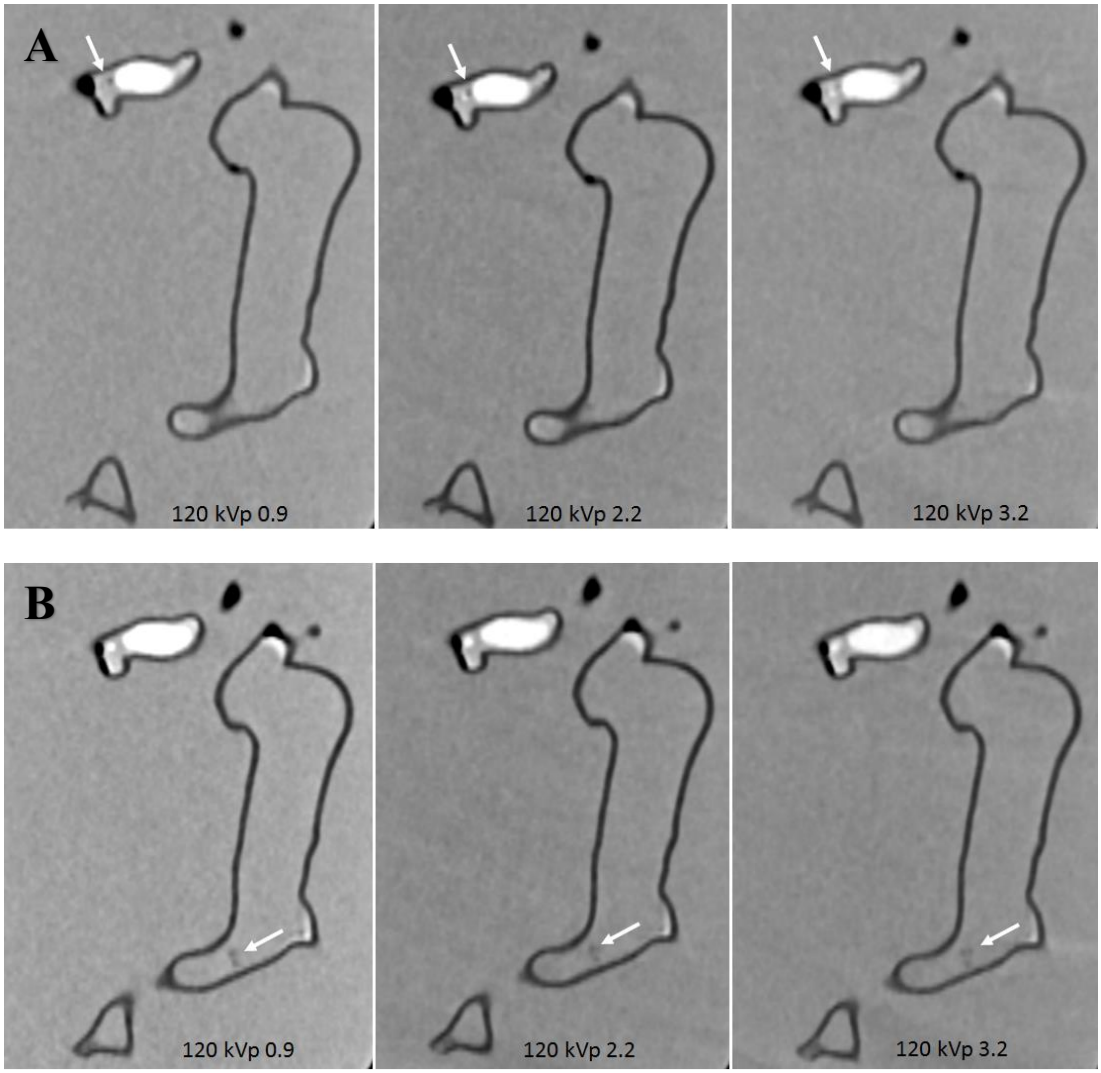

Figure 5.7 CTPA protocols with use of 120 kVp and different pitch values. A and B: The small thrombus is viewed as low-attenuation filling defect in the left segmental pulmonary artery (arrows in A) and right pulmonary artery (arrows in B) and are visible in all protocols, regardless of pitch values used.

Table 5.1 shows radiation dose values associated with these CTPA protocols. When kVp was reduced from 120 to 70 and pitch was increased from 0.9 to 2.2 or 3.2, radiation dose was reduced by up to 84% without compromising diagnostic image quality as evaluated by qualitative and quantitative assessments. It should be noted that CTDIvol remains the same for pitch of 2.2 and 3.2 protocols and this is due to the use of same mAs of 80 for these high pitch protocols. Therefore, as shown in the Table

5.1, the effective dose of these high pitch protocols remains unchanged or even slightly increased. Further, due to selection of different mAs corresponding to kVp values in the low pitch 0.9 protocols, the CTPA protocol of 80 kVp and 0.9 pitch resulted in the lowest dose compared to other protocols. This needs to be interpreted with caution.

5.4 Discussion

In this phantom study, we further confirmed the feasibility of low-dose CTPA protocols with simulation of thrombus in peripheral pulmonary arteries. Quantitative assessment of image quality did not show any significant differences among these CTPA protocols with 70 kVp protocols even producing higher SNR than that of 80 or 100 kVp protocols. Qualitative analysis of image quality by experienced observers showed that all of the images are acceptable for detection of small thrombus, despite lowering kVp to 70 or increasing pitch to 3.2. Radiation dose reduction by more than 80% could be achieved with use of low-dose CTPA protocol while maintaining diagnostic image quality.

Low-dose CTPA has been reported in the literature with radiation dose down to 2 mSv or even less than 1.0 mSv (7-12). Lu et al compared 80 kVp and 2.2 pitch protocol with 100 kVp and pitch 1.2 in 100 patients with suspected PE with 50 cases in each group (8). No significant difference was found in subjective scoring of image quality between the two groups, while quantitative measurements of image quality were significantly higher in the low-dose protocol than the standard group, with significant dose reduction achieved in the low kVp and high pitch protocol (0.9 vs 1.7 mSv). Li and colleagues reported similar findings by using 70 kVp and high pitch 3.2 CTPA protocol in 80 patients with 40 in each group (9). Their results showed no significant difference in the subjective image quality but with significantly higher quantitative assessments in the low-dose group. Up to 80% dose reduction was noted in the 70 kVp and 3.2 protocol (0.4 vs 2.0 mSv). Our results are consistent with these findings. Low-dose CTPA protocol comprising 70 kVp and 3.2 pitch was scored to be acceptable for detection of small thrombus in the pulmonary arteries, with more than 80% dose reduction. The effective dose of the low-dose protocol in our study is 0.21 mSv, almost

half of what has been reported by Li's study. Thus, our study validates the feasibility of using lower kVp and high pitch CTPA protocol with further dose reduction.

Despite the great benefit of reducing radiation dose with a high-pitch CT protocol, the disadvantage of increasing pitch is associated with increased image noise which could affect diagnostic quality. This was noticed in our recent paper with increased image noise in the 70 kVp protocol with a pitch of 3.2 affecting visualization of thrombus and pulmonary arterial wall (25). With the latest CT scanners, advanced IR algorithms are developed to improve image quality by reducing image noise associated with the use of low-dose CT protocols (27, 28). This is confirmed by findings in our study as the IR available with the Siemens Force scanner represents the latest algorithm used in image reconstruction for reducing image noise. A combination of low-dose protocol with advanced IR resulted in increased quantitative image quality, with low kVp 70 and high pitch 2.2 and 3.2 protocols still producing diagnostic images, but with much lower radiation dose.

3D printed models derived from patient's imaging data are increasingly used in medical applications, with most of the studies focusing on the clinical value of patient-specific 3D printed models such as pre-surgical planning and simulation, medical education and patient-doctor communication (18-23, 29, 30). A new research direction of clinical application of 3D printed models is to develop optimal CT scanning protocols for radiation dose reduction. Abdullah et al created a 3D printed cardiac phantom based on CT images of anthropomorphic chest phantom and inserted filling materials into the phantom to simulate different anatomical structures (31). CT scans of the 3D printed model showed that CT attenuations of these filling materials were similar to those from patient's CT images (contrast medium, air, oil/fat and jelly/muscle). Despite the novel design of this cardiac insert phantom, testing different scanning protocols on the 3D printed model remains to be investigated.

Our recent papers have addressed this limitation by developing a realistic pulmonary artery model with different CTPA protocols tested on the model with simulation of pulmonary embolism (24, 25). With model's accuracy validated in the first paper, we

scanned the model with a combination of different kVp and pitch values on a 128-slice dual-source CT scanner by inserting thrombus in the main pulmonary arteries. A dose reduction of 80% was achieved with use of low kVp 80 and high pitch 3.2 protocol when compared to the standard 100 or 120 kVp protocols, while low-dose 70 kVp and high pitch 3.2 was not recommended due to high image noise (25). In the current study, we simulated small thrombus in peripheral pulmonary arteries and scanned the 3D printed model using the same CTPA protocols as in our previous paper, but on a latest CT scanner with use of advanced IR algorithm for image reconstruction. No significant differences were found in SNR measurements among all the protocols, with all images scored as diagnostic by two observers. Therefore, low-dose CTPA with 70 kVp and high pitch 2.2 or 3.2 is acceptable for detection of small pulmonary embolism with dose reduction up to 80%. Findings of this study further advanced our previous research and others, thus contributing to the current literature by recommending low-dose CTPA protocols with significant dose reduction.

Some limitations in this study should be acknowledged. Limitations that have been addressed in our previous papers still apply to the current study, such as the necessity of simulating a realistic anatomical environment with lungs, ribs, heart and other thoracic structures. Although small thrombus was inserted into in the left peripheral pulmonary artery branch, we failed to insert the thrombus in other small branches of the right pulmonary artery due to difficulty with handling the soft blood clots during the procedure. This could be addressed in future studies by simulating peripheral pulmonary embolism which is made of materials with similar attenuation to that of blood but with solid properties which can be easily deployed in the 3D printed models. Finally, air bubbles which are present in the pulmonary artery branches could affect the visualization and assessment of image quality to some extent (Fig 5.8). This needs to be considered in further experiments with approaches undertaken to reduce the negative impact of air bubbles.

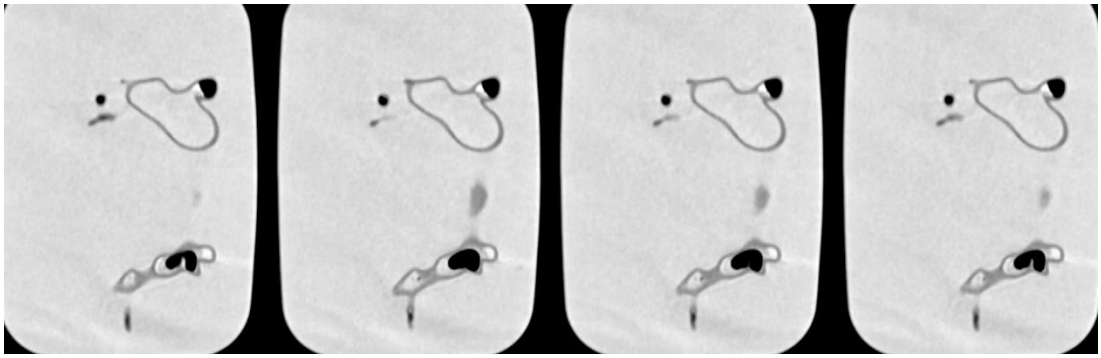

Figure 5.8 Air bubbles in the pulmonary arteries. Multiple air bubbles with different sizes are present in main and side branches of both pulmonary arteries which could affect assessment of image quality.

In conclusion, we have simulated the small pulmonary embolism in the 3D printed pulmonary model and scanned the model with different CT pulmonary angiography protocols using the latest 3rd generation dual-source CT scanner with images reconstructed using the advanced IR algorithm. Low-dose CTPA protocols comprising low kVp 70 and high pitch of 2.2 or 3.2 result in more than 80% dose reduction, but still producing acceptable image quality as determined by quantitative and qualitative assessments. The small pulmonary embolism can still be detected on this low-dose CTPA protocol, further validating the feasibility of lowering kVp to 70 and increasing pitch up to 3.2 for diagnosis of patients with suspected pulmonary embolism. Findings of this study could stimulate further similar research to develop optimal CT scanning protocols in other areas based on realistic 3D printed models.

5.5 References

1. Albrecht MH, Bickford MW, Nance JW Jr, Zhang L, De Cecco CN, Wichmann JL, Vogl TJ, Schoepf UJ. State-of-the-Art pulmonary CT angiography for acute pulmonary embolism. AJR Am J Roentgenol 2017;208:495-504.
2. Sun Z, Lei J. Diagnostic yield of CT pulmonary angiography in the diagnosis of pulmonary embolism: a single center experience. Interv Cardiol 2017;9: 191-198.
3. Chen EL, Ross JA, Grant C, Wilbur A, Mehta N, Hart E, Mar WA. Improved image quality of low-dose CT pulmonary angiograms. J Am Coll Radiol 2017;14:648-653.
4. Devaraj A, Sayer C, Sheard S, Grubnic S, Nair A, Vlahos I. Diagnosing acute pulmonary embolism with computed tomography: imaging update. J Thorac Imaging 2015;30:176-192.
5. Henzler T, Barraza JM, Nance JW, Jr, Costello P, Krissak R, Fink C, Schoepf UJ. CT imaging of acute pulmonary embolism. J Cardiovasc Comput Tomogr 2011;5:3–11.
6. Wichmann JL, Hu X, Kerl JM, Schulz B, Frellesen C, Bodelle B, Kaup M, Scholtz JE, Lehnert T, Vogl TJ, Bauer RW. 70 kVp computed tomography pulmonary angiography: potential for reduction of iodine load and radiation dose. J Thorac Imaging 2015;30:69-76.
7. Martini K, Meier A, Higashhigaito K, Saltybaeva N, Alkadhi H, Frauenfelder T. Prospective randomized comparison of high-pitch CT at 80 kVp under free breathing with standard-pitch CT at 100 kVp under breath-hold for detection of pulmonary embolism. Acad Radiol 2016;23:1335-1341.
8. Lu GM, Luo S, Meinel FG, McQuiston AD, Zhou CS, Kong X, Zhao YE, Zheng L, Schoepf UJ, Zhang LJ. High-pitch computed tomography pulmonary angiography with iterative reconstruction at 80 kVp and 20 mL contrast agent volume. Eur Radiol 2014; 24:3260–3268.
9. Li X, Ni QQ, Schoepf UJ, Wichmann JL, Felmly LM, Qi L, Kong X, Zhou CS, Luo S, Zhang LJ, Lu GM. 70-kVp high-pitch computed tomography pulmonary angiography with 40 mL contrast agent: initial experience. Acad Radiol 2015; 22:1562–1570.

10. Bolen MA, Renapurkar RD, Popovic ZB, Popovic ZB, Heresi GA, Flamm SD, Lau CT, Lau CT, Halliburton SS. High-pitch ECG synchronized pulmonary CT angiography versus standard CT pulmonary angiography: a prospective randomized study. AJR Am J Roentgenol 2013; 201:971–976.
11. Sabel BO, Buric K, Karara N, Thierfelder KM, Dinkel J, Sommer WH, Meinel FG. High-pitch CT pulmonary angiography in third generation dual-source CT: image quality in an unselected patient population. PLoS ONE 2016; 11:e0146949.
12. Boos J, Kropil P, Lanzman RS, Aissa J, Schleich C, Heusch P, Sawichi LM, Antoch G, Thomas C. CT pulmonary angiography: simultaneous low-pitch dual-source acquisition mode with 70 kVp and 40 ml of contrast medium and comparison with high-pitch spiral dual-source acquisition with automated tube potential selection. Br J Radiol 2016;89:20151059.
13. Bucher AM, Kerl MJ, Albrecht MH, Beeres M, Ackermann H, Wichmann JL, Vogl TJ, Bauer RW, Lehnert T. Systematic comparison of reduced tube current protocols for high-pitch and standard-pitch pulmonary CT angiography in a large single-center population. Acad Radiol 2016;23:619-627.
14. Kligerman S, Lahiji K, Weihe E, Lin CT, Terpenning S, Jeudy J, Frazier A, Pugatch R, Galvin JR, Mittal D, Kothari K, White CS. Detection of pulmonary embolism on computed tomography: improvement using a model-based iterative reconstruction algorithm compared with filtered back projection and iterative reconstruction algorithms. J Thorac Imaging 2015;30:60-68.
15. Laqmani A, Regier M, Veldhoen S, Backhaus A, Wassenberg F, Sehner S, Groth M, Nagel HD, Adam G, Henes FO. Improved image quality and low radiation dose with hybrid iterative reconstruction with 80 kV CT pulmonary angiography. Eur J Radiol 2014; 83:1962–9.
16. McLaughlin PD, Liang T, Homiedan M, Louis LJ, O'Connell TW, Krzymyk K, Nicolaou S, Mayo JR. High pitch, low voltage dual source CT pulmonary angiography: assessment of image quality and diagnostic acceptability with hybrid iterative reconstruction. Emerg Radiol 2015;22:117-123.
17. Wortman JR, Adduci AJ, Sodickson AD. Synergistic radiation dose reduction by combining automatic tube voltage selection and iterative reconstruction. J Thorac Imaging 2016;31:111-118.

18. Olivieri LJ, Krieger A, Loke YH, Nath DS, Kim PC, Sable CA. Three-dimensional printing of intracardiac defects from three-dimensional echocardiographic images: feasibility and relative accuracy. J Am Sco Echocardiogr 2015;28: 392-97.
19. Cantinotti M, Valverde I, Kutty S. Three-dimensional printed models in congenital heart disease. Int J Cardiovasc Imaging 2017;33(1):137-144.
20. Lau I, Liu D, Xu L, Fan Z, Sun Z. Clinical value of patient-specific three-dimensional printing of congenital heart disease: Quantitative and qualitative Assessments. PLoS One 2018;13:e0194333.
21. Liu D, Sun Z, Chaichana T, Ducke W, Fan Z. Patient-specific 3D printed models of renal tumours using home-made 3D printer in comparison with commercial 3D printer. J Med Imaging Health Inf 2018;8:303-308.
22. Sun Z, Liu D. A systematic review of clinical value of three-dimensional printing in renal disease. Quant Imaging Med Surg 2018;8:311-325.
23. Lau I, Sun Z. Three-dimensional printing in congenital heart disease: A systematic review. J Med Radiat Sci 2018;65:226-236.
24. Aldosari S, Squelch A, Sun Z. Patient-specific 3D printed pulmonary artery model: A preliminary study. Digit Med 2017;3:170-177.
25. Aldosari S, Jansen S, Sun Z. Optimization of computed tomography pulmonary angiography using 3D printed model with simulation of pulmonary embolism. Quant Imaging Med Surg 2018 (Epub ahead of print). doi: 10.21037/qims.2018.09.15.
26. McCollough CH, Primak AN, Braun N, Kofler J, Yu L, Christner J. Strategies for reducing radiation dose in CT. Radiol Clin North Am 2009;47:27-40.
27. Leithner D, Gruber-Rouh T, Beeres M, Wichmann JL, Mahmoudi S, Martin SS, Lenga L, Albrecht MH, Booz C, Vogl TJ, Scholtz JE. 90-kVp low-tube-voltage CT pulmonary angiography in combination with advanced modeled iterative reconstruction algorithm: effects on radiation dose, image quality and diagnostic accuracy for the detection of pulmonary embolism. Br J Radiol 2018;91:20180269.
28. Leithner D, Wichmann JL, Mahmoudi S, Martin SS, Albrecht MH, Vogl TJ, Scholtz JE. Diagnostic yield of 90-kVp low-tube-voltage carotid and intracerebral CT-angiography: effects on radiation dose, image quality and diagnostic performance for the detection of carotid stenosis. Br J Radiol

2018;91:20170927.

29. White SC, Sedler J, Jones TW, Seckeler M. Utility of three-dimensional models in resident education on simple and complex intracardiac congenital heart defects. Congenit Heart Dis 2018 Sep 19. doi: 10.1111/chd.12673. [Epub ahead of print].
30. Loke YH, Harahsheh AS, Krieger A, Olivieri LJ. Usage of 3D models of tetralogy of Fallot for medical education: impact on learning congenital heart disease. BMC Med Educ 2017;17:54.
31. Abdullah KA, McEntee MF, Reed W, Kench PL. Development of an organ-specific insert phantom generated using a 3D printer for investigations of cardiac computed tomography protocols. J Med Radiat Sci 2018;65:175-183.

Chapter 6

Double low-dose computed tomography pulmonary angiography in the diagnosis of pulmonary embolism

6.1 Introduction

Computed tomography pulmonary angiography (CTPA) is the first line imaging modality in the diagnosis of patients with suspected pulmonary embolism (PE) owing to its high sensitivity and specificity (1, 2). Despite high diagnostic yield of CTPA in PE, appropriate use of CTPA needs to be medically justified due to its associated high radiation dose and widespread use of CTPA in clinical practice (3-5). Technological developments in CT scanners have allowed the CTPA to be performed widely in many clinical centres with significant reduction of radiation dose which used to be a major concern of CT imaging. Currently, low-dose CTPA is available with use of various dose-reduction strategies including low kVp, tube current modulation, high pitch protocol and use of iterative reconstruction algorithms with resultant effective dose of less than 2.0 mSv or even less than 1.0 mSv, according to some recent studies (6-10). Thus, significant progress has been achieved in reducing radiation dose associated with CTPA.

Another concern related to CTPA is the risk of using contrast medium during contrast-enhanced CT scans since contrast medium has potential risk of contrast-induced nephropathy (CIN). Characteristics of a contrast medium, including volume and osmolality may influence the risk of CIN. In patients with cardiovascular disease such as coronary artery disease and pulmonary embolism, reducing the risk of CIN is necessary since these patients are often associated with chronic kidney disease or with diabetes mellitus. This has drawn increasing attention in recent years with an attempt to reduce contrast volume or lower concentration of contrast medium during CT scans. Studies have shown the feasibility of reducing radiation dose and contrast medium dose or concentration in coronary CT angiography examinations (11-15). Similar trend has seen in CTPA protocols with regard to the recommendation of double low-dose protocols aiming to reduce both radiation and contrast medium doses.

Low-dose CTPA has been shown to be feasible with significant dose reductions while still maintaining diagnostic images (6-10, 16-20). We performed a systematic review of double low-dose CTPA through analysis of 13 studies reporting the use of low radiation and low contrast medium doses as reported in Chapter 2 (21). The review shows that radiation dose was reduced to up to 88% and contrast medium dose reduced up to 67% with acceptable image quality as evaluated by quantitative and qualitative

assessments. Although promising results are available in the literature, studies on the use of double low-dose CTPA protocols are still limited to certain clinical centres and not yet widely recommended. Thus, the purpose of this study was to further investigate the clinical application of CTPA in the diagnosis of pulmonary embolism with regard to the use of double low-dose protocol in routine practice without compromising diagnostic image quality. The study design is also based on our previous phantom experiments of testing various CTPA protocols on a patient-specific 3D printed pulmonary artery model with simulation of pulmonary embolism in the main pulmonary arteries and peripheral branches as reported in Chapters 3-5 (22-24). The phantom study confirms that kVp can be lowered to 80 or even 70 with use of high pitch mode of 2.2 or 3.2, with acquisition of acceptable CTPA images, with up to 80% dose reduction. According to these previous findings, a high-pitch CTPA protocol of 3.2 was applied to some patients, making this study to be both retrospective and prospective in nature.

6.2 Materials and Methods

6.2.1 Participant recruitment

A retrospective review of patients with suspected PE who underwent CTPA examinations during January 2017 and February 2018 was performed in a tertiary clinical center. Inclusion criteria included: confirmed presence of PE in at least one of the pulmonary artery branches and CTPA was successfully performed without any complications. The rationale of including only patients with confirmed PE in the study is to determine the clinical value of CTPA in the detection of PE as CTPA for diagnostic assessment of normal pulmonary arteries has been well studied in the literature. Patients younger than 18 years or allergic to contrast medium were excluded. Ethics approval was obtained from the local ethics committee and Curtin University Human Research Ethics.

Participants were divided into three groups: Group 1 consisted of 23 patients who underwent CTPA using the 100 kVp and a pitch of 0.9 protocol as a low-dose protocol. Group 2 included 30 patients who underwent CTPA using the standard 120 kVp and

a pitch of 0.9 protocol, while Group 3 comprised 6 patients who received a CTPA protocol with 120 kVp and a high pitch 3.2. Participants in groups 1 and 2 were retrospectively included in the study, while participants in group 3 were prospectively recruited with use of high-pitch CTPA protocol with the aim of using low radiation dose and low contrast medium volume. Tube current modulation was applied to all patients.

6.2.2 CTPA scanning protocols

CT scans were performed on 64- and 128-slice CT scanners with details as follows: 52 patients were scanned on a 128-slice dual-source CT (Siemens Definition Flash, Siemens Healthcare, Forchheim, Germany), 4 patients were on a 64-slice scanner (GE VCT, GE Healthcare, USA) and 3 cases were on a 64-slice GE Revolution (GE Medical Systems, Waukesha, USA), respectively. Contrast medium Iohexol (Omnipague 350, GE Healthcare, USA) was injected using a power injector with a flow rate of 5 ml/s, followed by a saline flush of 40 ml at the same injection rate. The volume of contrast medium was determined by each group's scanning protocol, ranging from 20-30 ml to 35 to 45 ml. A testing bolus technique was used in all of the patients except in one patient which bolus tracking was used with a threshold of 150 HU in the pulmonary trunk used as the triggering threshold to initiate scans.

6.2.3 Image reconstruction

All images were reconstructed with a soft tissue kernel using the standard filtered back projection. The slice thickness was 1 mm with 0.5 mm reconstruction interval. In addition to axial images, multiplanar reformations including coronal and sagittal views and maximum intensity projections were reconstructed to demonstrate the location of thrombus in the pulmonary arteries.

6.2.4 Quantitative image quality assessment

Original images in digital imaging and communications in medicine (DICOM) format were transferred to a workstation with Analyze 12.0 (AnalyzeDirect, Inc., Lexana, KS, USA) of image post-processing and measurement. Quantitative assessment of image quality was determined by measuring signal-to-noise ratio (SNR) and contrast-to-noise ratio (CNR) in the main pulmonary arteries. CT attenuation in the background was measured in the paravertebral muscle. A region of interest (ROI) (containing minimum 150 voxels) was placed in the pulmonary trunk with SNR and CNR calculated as follows:

SNR=CT attenuation in pulmonary trunk/SD (image noise)

CNR=(CT attenuation in pulmonary trunk-background CT attenuation)/SD (image noise)

The standard deviation (SD) refers to the image noise measured in the pulmonary trunk.

6.2.5 Qualitative image quality assessment

Qualitative assessment of image quality was performed by two independent experienced radiologists (each with more than 5 years' experience in reporting CTPA) using a 5-point scale:

- 5: excellent image quality
- 4: good image quality
- 3: moderate image quality
- 2: suboptimal image quality and
- 1: poor image quality

Criteria for determining image quality was based on pulmonary arterial attenuation, image noise, presence of artifacts and diagnostic confidence in detecting PE. Both

observers were blinded to CTPA scanning protocols and clinical information and they scored the images separately. Inter-observer agreement was assessed by Cohen's kappa statistics. A score of 3 or more indicates acceptable image quality.

6.2.6 Radiation dose

Volumetric dose index (CTDIvol) and dose length product (DLP) were available in CT console from each scanning protocol. Effective dose was calculated by multiplying the DLP with a tissue conversion factor of 0.014 mSv/mGy/cm (25).

6.2.7 Statistical analysis

Data were analysed using SPSS 24.0 (IBM Corporation, Armonk, NY, USA). Continuous variables were presented as mean ± standard deviation. One way analysis of variance (ANOVA) was used to determine if there is any significant difference in SNR and CNR between groups and within groups using different CTPA protocols. Kruskal-Wallis test was used to determine any significant difference in CTPA protocols with respect to image quality as assessed by two radiologists. A *k* value was calculated to determine inter-observer agreement $k \leq 0.20$ as poor, k =0.21-0.40 fair, k =0.41-0.60 moderate, k =0.61-0.8 good and $k > 0.81$ excellent. A p value less than 0.05 was considered statistically significant.

6.3 Results

6.3.1 Patient demographics

There were no significant differences in patient's age and gender among these three CTPA protocols (all $p>0.05$) (Table 6.1). The patient's body weight in the 100 kVp protocol was significantly smaller than that in the 120 kVp protocols ($p<0.001$), while there was no significant difference in the body weight between 120 kVp standard pitch and high pitch protocols ($p=0.27$). Pulmonary embolism was presented in all cases

with both sides of pulmonary arteries having emboli in more than half of the patients (54%). Inter-observer agreement was good (k=0.78) for the diagnosis of pulmonary embolism.

6.3.2 Image quality assessment

All images were scored as diagnostic with a score of 3 given by one assessor and a score of 4 by another assessor in two cases. In the remaining cases, a score of 4 or 5 was given in 13 and 44 cases by these two assessors, respectively. No significant difference was found in the qualitative assessment of image quality among the three groups (4.61 ± 0.45 vs 4.76 ± 0.48 vs 4.58 ± 0.49, respectively, p>0.05) (Table 6.1). Kruskal-Wallis test indicates that neither radiologist (observer) 'sees' any significant difference in CTPA protocols with respect to image quality scores (p=0.135 and 0.621 for Radiologist 1 and 2, respectively).

Similarly, there were no significant differences in SNR and CNR among these CTPA protocols, although the SNR and CNR measured with the 120 kVp and high pitch 3.2 protocol were lower than those with the 100 and 120 kVp with standard pitch protocols (p=0.181 and 0.186 for SNR and CNR, respectively) (Table 6.1). Figure 6.1 shows the ANOVA analysis of SNR and CNR between and within groups.

ANOVA

		Sum of Squares	df	Mean Square	F	Sig.
CNR Contrast to Noise Ratio	Between Groups	153.825	2	76.912	1.734	.186
	Within Groups	2483.295	56	44.345		
	Total	2637.120	58			
SNR Signal to Noise Ratio	Between Groups	187.867	2	93.933	1.763	.181
	Within Groups	2984.490	56	53.294		
	Total	3172.357	58			

Figure 6.1. ANOVA analysis of SNR and CNR between and within these three different groups

Table 6.1 Measurements of SNR and CNR associated with different CTPA protocols.

Clinical and imaging characteristics	**Group 1 100 kVp pitch 0.9 (n=23)**	**Group 2 120 kVp pitch 0.9 (n=30)**	**Group 3 120 kVp pitch 3.2 (n=6)**	***P* values**
Age (years)	52.77 ± 21.28	47.53 ± 16.78	48 ± 13.17	0.31-0.94
Gender (M/F)	8/15	14/16	2/4	-
Body weight (kg)	76.34 ± 4.38	95.6 ± 11.09	90.5 ± 3.61	<0.001/0.27*
SNR	21.56 ± 6.40	22.06 ± 8.21	15.99 ± 4.99	0.09-0.96
CNR	19.82 ± 5.88	19.71 ± 7.44	14.42 ± 4.75	0.06-0.77
Qualitative assessment of image quality	4.61 ± 0.45	4.76 ± 0.48	4.58 ± 0.49	0.23-0.90
Contrast medium (ml)	35-45	35-45	20-30	-
CTDIvol (mGy)	6.09 ± 1.14	10.06 ± 3.20	7.46 ± 0.69	<0.05
DLP (mGy.cm)	173.83 ± 29.18	332.73 ± 126.24	238.08 ± 42.88	<0.001*/0.06-0.08[#]
Effective dose (mSv)	2.43 ± 0.41	4.66 ± 1.76	3.33 ± 0.60	<0.001/0.08*

* significant differences in CTDIvol and effective dose between 100 kVp and 120 kVp protocols, [#] but no significant difference between 120 kVp low pitch and high pitch protocols.

6.3.3 Contrast medium volume

The contrast medium ranged from 35 to 45 ml in the 100 and 120 kVp with standard pitch protocols, 20 to 30 ml in the 120 kVp with high pitch protocol, as shown in Table 6.1. Figures 6.2- 6.4 are examples of image quality for Groups A-C with use of different CTPA protocols for demonstration of pulmonary embolism in 2D axial and coronal reformatted images. Despite the use of low contrast volume in the high-pitch protocol, image quality is still acceptable for detection of pulmonary embolism as shown in Figure 6.4.

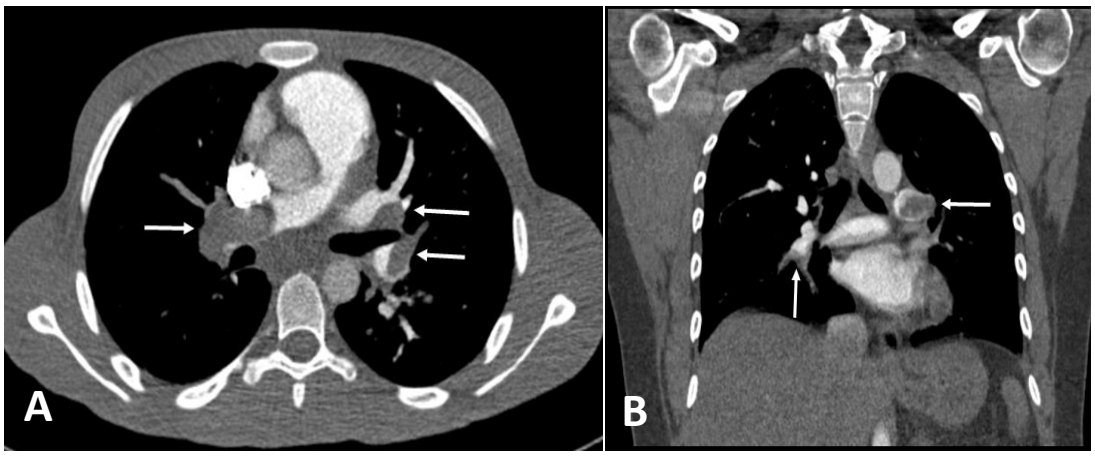

Figure 6.2 Computed tomography pulmonary angiography with use of 100 kVp, pitch 0.9 and contrast medium of 40 ml in a 26-year-old male with diagnosed pulmonary embolism. Multiple emboli are seen at both sides of pulmonary arteries as shown on 2D axial and coronal reformatted images (arrows in A and B).

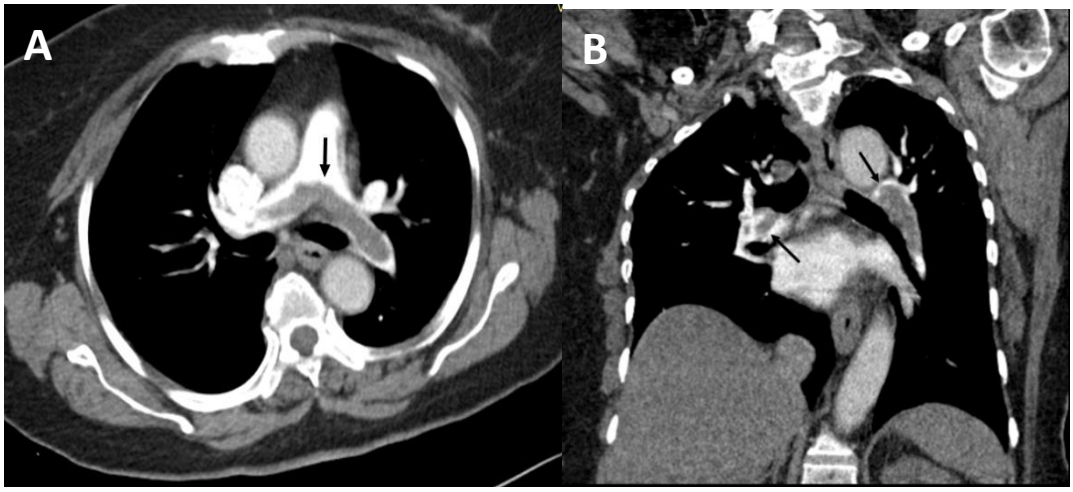

Figure 6.3 Computed tomography pulmonary angiography with use of 120 kVp, pitch 0.9 and contrast medium of 45 ml in a 71-year-old female with diagnosed pulmonary embolism. A large thrombus is seen in the pulmonary trunk extending to both sides of pulmonary arteries shown as filling defect on 2D axial and coronal reformatted images (arrows in A and B).

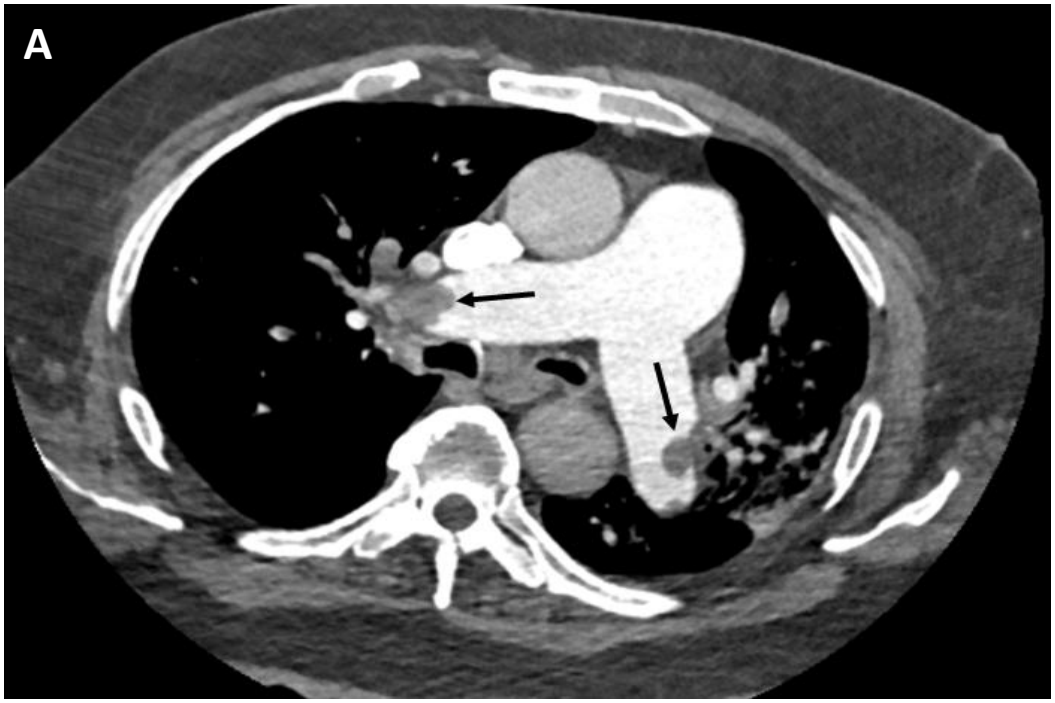
A

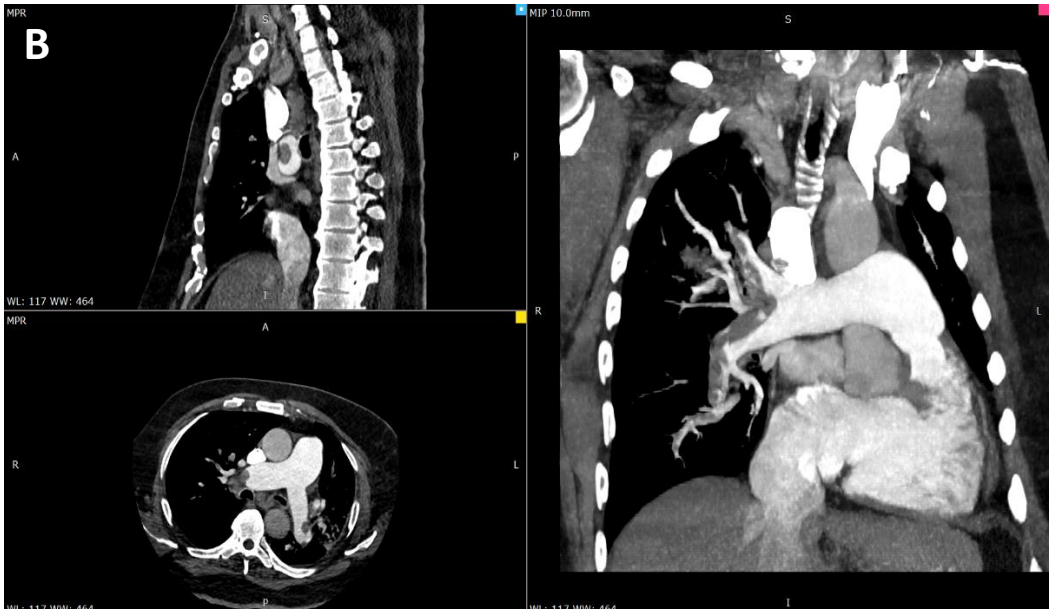
B
MPR
MIP 10.0mm
WL: 117 WW: 464

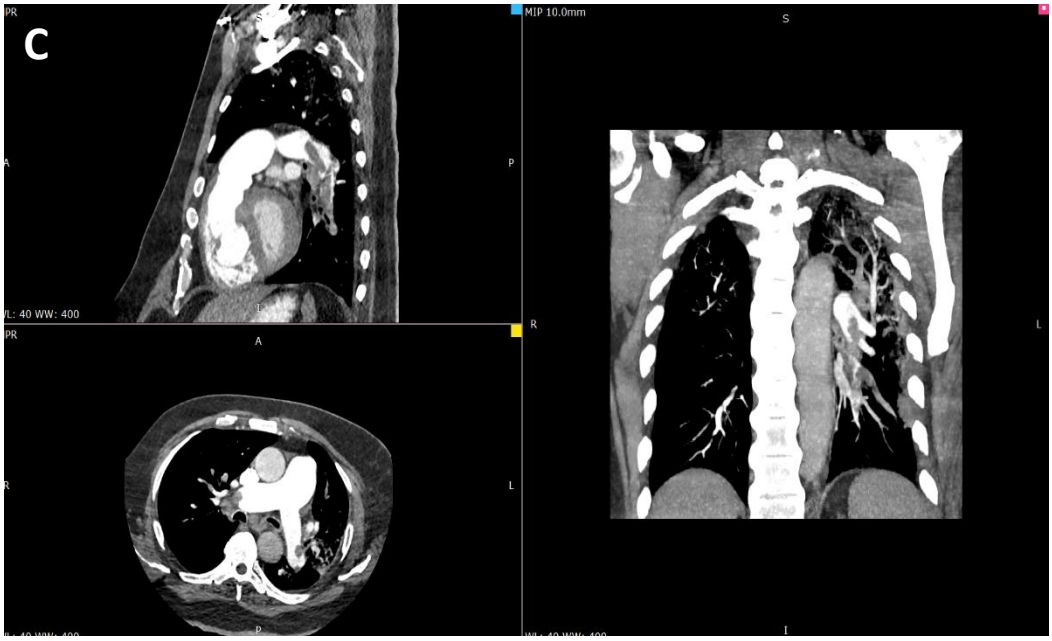

Figure 6.4 Computed tomography pulmonary angiography with use of 120 kVp, pitch 3.2 and 25 ml contrast medium in a 59-year-old male with diagnosed pulmonary embolism. A: Multiple emboli are observed in both sides of pulmonary arteries shown as filling defect on 2D axial images (arrows). B and C: Maximum-intensity projection (MIP) images demonstrate emboli involving multiple pulmonary artery branches on both sides.

6.3.4 Radiation dose

There are highly significant differences in dose values between different CTPA protocols. CTDIvol, DLP and effective dose were significantly lower in the 100 kVp and standard pitch protocol than those in the 120 kVp with standard and high pitch protocols ($p<0.05$) (Table 6.1). In addition to the comparison of mean dose values among these groups, we further analysed the dose value differences in relation to each age group as shown in Table 6.2. ANOVA analysis shows there were no significant differences in these dose values among the four age groups ($p>0.05$). With use of 100 kVp and standard pitch protocol in Group 1, a dose reduction of 48% was achieved when compared to Group 2.

Table 6.2. Radiation dose based on different age groups.

Dose/Ages	<30 yrs	31-40 yrs	41-50 yrs	>50 yrs	*P* values
CTDIvol (mGy)	7.13 ± 3.44	8.24 ± 2.23	9.2 ± 3.46	7.92 ± 2.90	0.054
DLP (mGy.cm)	262.23 ± 204.80	282.89 ± 99.10	326.02 ± 122.96	246.59 ± 88.68	0.491
Effective dose (mSv)	3.67 ± 2.86	3.67 ± 1.39	4.08 ± 1.72	3.45 ± 1.24	0.20

6.4 Discussion

This study further confirms the usefulness of low kVp for radiation dose reduction in CTPA examinations. A significant dose reduction of 48% was achieved in the 100 kVp and standard pitch protocol with use of less than 45 ml of contrast medium. Further, low contrast medium of less than 30 ml was found to be feasible in the 120 kVp and high pitch CTPA protocol with acquisition of diagnostic images.

CTPA is the first line imaging modality in the diagnosis of patients with suspected PE and it is widely used in many clinical centres. Previous concerns about high radiation associated with CTPA have been well addressed by applying various dose-reduction strategies with significant dose reduction achieved (6-10). Lowering kVp from traditional 120 to 100 and 80, or even 70 kVp is the common approach that has been shown to be effective in dose reduction (7, 8, 10). CTPA with use of 100 kVp offers high contrast concentrations in patients with normal body weight with reported effective dose of 3.6 mSv according to a study by Takahasi et al (26). The effective dose associated with 100 kVp group in our study is 2.43 mSv, while the CNR is the highest among all of the three groups (Table 6.1). This is consistent with the literature highlighting the reduction of radiation dose by reducing kVp to a lower level.

Recent studies with use of latest CT scanners further confirms the feasibility of lowering kVp in combination with iterative reconstruction (IR) algorithms during CT angiographic examinations (9-13, 16, 17). With use of these combined dose saving

methods, low-dose or ultra low-dose CTPA is available with effective dose less than 2 or lower than 1 mSv reported in some recent studies, mainly due to the use of high-pitch in 70 or 80 kVp protocol (6, 7, 9, 27, 28). Use of high pitch 2.2 or 3.2 in the 120 kVp CTPA does not lead to dose reduction as opposed to the use of low kVp and high pitch CTPA protocol. This has been confirmed in our previous phantom experiments and other studies. Schafer et al compared CTPA protocol of 120 kVp and pitch 3 with 70 kVp and pitch 3 in patients scanned with 2nd and 3rd generation dual-source CT, respectively (29). The overall effective dose was 4.40 and 2.06 mSv for the 120 kVp and 70 kVp with high pitch protocols, indicating the important role of kVp in dose reduction. Our phantom experiments are consistent with their findings (23, 24). The highest radiation dose was noted in the 120 kVp with pitch of 2.2 or 3.2 protocols, while the lowest dose was seen in the 80 or 70 kVp with pitch of 2.2 or 3.2 protocols (up to 80% dose reduction) without compromising diagnostic image quality. The current study shows that up to 27% dose reduction was achieved when comparing 120 kVp with pitch 3.2 to 100 kVp and pitch 0.9 protocols.

The effective dose in this study is within the reported dose range, however, it is still higher than some reported low dose CTPA studies. This is due to the fact that no IR algorithms were applied in our data, mainly because of the use of 64- and 128-slice CT scanners in this cohort with image reconstructed using traditional filtered back projection (FBP). IR is a widely available image reconstruction algorithm due to improved image quality by suppressing image noise, thus significantly reducing radiation dose (30-32). Dose reduction up to 60% has been reported previously with use of IR when compared to FBP (33, 34). With implementation of high-pitch protocol combined with IR algorithms, further dose reduction of up to 75% can be achieved while maintaining diagnostic images (35). This is also confirmed in our previous studies with dose reduction of up to 80% in the high-pitch and low kVp (70 or 80) CTPA protocols (23, 24). Therefore, use of combined different dose-reduction strategies should be recommended in CTPA protocols.

In addition to reduction in radiation dose, lowering contrast medium volume during CT angiographic examinations is another area that has attracted increasing attention in recent years because of the risk of CIN. Double low-dose CTPA represents the current research direction in CTPA and this has been confirmed by our recent

systematic review (21). The traditional approach of using 80-100 ml contrast medium has been replaced by low contrast medium such as 40-60 ml, followed by 30-60 ml saline flush (36). Some studies have reported that contrast medium can be even lowered to 20 ml with high-pitch CTPA protocol with acquisition of similar image quality when compared to the standard pitch CTPA, but with significant radiation and contrast medium dose reduction (37, 38). Our findings are in align with these reports as 20-30 ml contrast medium was used in the high-pitch CTPA protocol with resulting similar image quality as opposed to the 35-45 ml contrast medium used in the standard pitch protocols. This confirms the double low-dose CTPA protocol in routine diagnosis, although more cases are needed to validate these findings.

This study has some limitations. First, this is a single centre experience with limited number of participants. Prospective studies with inclusion of large cohorts comprising different CTPA protocols should be conducted to confirm our findings. Second, CTPA scans were done on 64- and 128-slice scanners, without implementing IR in image reconstruction, which leads to relatively high radiation dose. Use of IR has been a common approach in many CT applications, thus further studies should include data analysis of images reconstructed with IR algorithms for more dose reduction. Third, low kVp such as 70 or 80 was not used in our cohort due to relatively large body mass. Furthermore, body mass index (BMI) was not available in most of the patients due to the retrospective nature of the study without recording BMI, although body weight was available in these patients. Using BMI to adjust kVp is a routine protocol and this should be followed in daily practice. Finally, we only included patients with confirmed pulmonary embolism, which could introduce bias in image analysis. Inclusion of patients with small or peripheral embolism is desirable for determining low-dose CT protocol, and this needs to be addressed in future studies.

In conclusion, despite small sample size and retrospective nature, this study further confirms the feasibility of double low-dose CT pulmonary angiography in the diagnosis of pulmonary embolism. Low radiation dose can be achieved with use of 100 kVp and standard pitch when compared to 120 kVp and standard or high pitch protocol, with dose reduction of nearly 50% while maintaining diagnostic image quality. Contrast medium can be reduced to 20-30 ml in the high-pitch CTPA protocol

producing similar image quality. Further research should focus on including more patients with testing different CTPA protocols.

6.5 References

1. Albrecht MH, Bickford MW, Nance JW Jr, Zhang L, De Cecco CN, Wichmann JL, et al. State-of-the-Art pulmonary CT angiography for acute pulmonary embolism. AJR Am J Roentgenol 2017;208:495-504.
2. Yan Z, Ip IK, Raja AS, Gupta A, Kosowsky JM, Khorasani R. Yield of CT pulmonary angiography in the emergency department when providers override evidence-based clinical decision support. Radiology 2017;282:717-725.
3. Sherk WM, Stojanovska J. Role of clinical decision tools in the diagnosis of pulmonary embolism. AJR Am J Roentgenol 2017;208:W60-W70.
4. Dunne RM, IpIK, Albbett S, Gershanik EF, Raja AS, Hunsaker A, et al. Effect of evidence-based clinical decision support on the use and yield of CT pulmonary angiographic imaging in hospitalized patients. Radiology 2015;276:167-174.
5. Raja AS, Ip IK, Prevedello LM, Sodickson AD, Farkas C, Zane RD, et al. Effect of computerized clinical decision support on the use and yield of CT pulmonary angiography in the emergency department. Radiology 2012;262:468-474.
6. Bolen MA, Renapurkar RD, Popovic ZB, Popovic ZB, Heresi GA, Flamm SD, Lau CT, Lau CT, Halliburton SS. High-pitch ECG synchronized pulmonary CT angiography versus standard CT pulmonary angiography: a prospective randomized study. AJR Am J Roentgenol 2013; 201:971–976.
7. Wichmann JL, Hu X, Kerl JM, Schulz B, Frellesen C, Bodelle B, Kaup M, Scholtz JE, Lehnert T, Vogl TJ, Bauer RW. 70 kVp computed tomography pulmonary angiography: potential for reduction of iodine load and radiation dose. J Thorac Imaging 2015;30:69-76.
8. Martini K, Meier A, Higashhigaito K, Saltybaeva N, Alkadhi H, Frauenfelder T. Prospective randomized comparison of high-pitch CT at 80 kVp under free breathing with standard-pitch CT at 100 kVp under breath-hold for detection of pulmonary embolism. Acad Radiol 2016;23:1335-1341.

9. Sauter A, Koehler T, Brendel B, Aichele J, Neumann J, Noel PB, et al. CT pulmonary angiography: dose reduction via a next generation iterative reconstruction algorithm. Acta Radiol 2018 Jan 1:284185118784976. doi: 10.1177/0284185118784976. [Epub ahead of print].
10. Sauter A, Koehler T, Fingerle AA, Brendel B, Richter V, Rasper M, et al. Ultra low dose CT pulmonary angiography with iterative reconstruction. PloS One 2016;11:e0162716.
11. Shen Y, Sun Z, Xu L, Zhang N, Yan Z, Fan Z. High-pitch, low-voltage and low-iodine-concentration CT angiography of aorta: assessment of image quality and radiation dose with iterative reconstruction. PloS One 2015;10:e01174689.
12. Yin WH, Lu B, Gao JB, Li PL, Sun K, Yang WL, et al. Effect of reduced x-ray tube voltage, low iodine concentration contrast medium, and sinogram-affirmed iterative reconstruction on image quality and radiation dose at coronary CT angiography: results of the prospective multicenter REALISE trial. J Cardiovasc Comput Tomogr 2015;9:215-224.
13. Zheng M, Liu Y, Wei M, Wu Y, Zhao H, Li J. Low concentration contrast medium for dual-source computed tomography coronary angiography by a combination of iterative reconstruction and low-tube-voltage technique: feasibility study. Eur J Radiol 2014;83:e92-e99.
14. Zheng M, Wu Y, Wei M, Liu Y, Zhao H, Li J. Low-concentration contrast medium for 128-slice dual-source CT coronary angiography at a very low radiation dose using prospectively ECG-triggered high-pitch spiral acquisition. Acad Radiol 2015;22:195-202.
15. Wang H, Xu L, Zhang N, Fan Z, Zhang Z, Sun Z. Coronary computed tomographic angiography in coronary artery bypass grafts: Comparison between low-concentration Iodixanol 270 and Iohexol 350. J Comput Assist Tomogr 2015;39:112-118.
16. Zhao Y, Zuo Z, Cheng S, Wu Y. CT pulmonary angiography using organ dose modulation with an iterative reconstruction algorithm and 3D Smart mA in different body mass indices: image quality and radiation dose. Radiol Med 2018;123:676-685.
17. Zhao YX, Zuo ZW, Sui HN, Wang JN, Chang J. CT pulmonary angiography using automatic tube current modulation combination with different noise

index with iterative reconstruction algorithm in different body mass index: Image quality and radiation dose. Acad Radiol 2016;23:1513-1520.

18. Schafer JC, Haubenreisser H, Meyer M, Gruttner J, Walter T, Borggrefe M, et al. Feasibility of a single contrast bolus high-pitch pulmonary CT angiography protocol followed by low-dose retrospectively ECG-gated cardiac CT in patients with suspected pulmonary embolism. Rofo 2018;190:542-550.
19. McLaughlin PD[1], Liang T, Homiedan M, Louis LJ, O'Connell TW, Krzymyk K, et al. High pitch, low voltage dual source CT pulmonary angiography: assessment of image quality and diagnostic acceptability with hybrid iterative reconstruction. Emerg Radiol 2015;22:117-123.
20. Co SJ, Mayo J, Liang T, Krzymyk K, Yousefi M, Nicolaou S. Iterative reconstructed ultra high pitch CT pulmonary angiography with cardiac bowtie-shaped filter in the acute setting: effect on dose and image quality. Eur J Radiol 2013;82:1571-1576.
21. Aldosari S, Sun Z. A systematic review of double low-dose CT pulmonary angiography in pulmonary embolism. Curr Med Imaging Rev 2018 (Epub ahead of print). Doi: 10.2174/1573405614666180813120619.
22. Aldosari S, Squelch A, Sun Z. Patient-specific 3D printed pulmonary artery model: A preliminary study. Digit Med 2017;3:170-177.
23. Aldosari S, Jansen S, Sun Z. Optimization of computed tomography pulmonary angiography protocols using 3D printing model with simulation of pulmonary embolism. Quant Imaging Med Surg 2018 (Epub ahead of print). doi: 10.21037/qims.2018.09.15.
24. Aldosari S, Jansen S, Sun Z. Patient-specific 3D printed pulmonary artery model with simulation of peripheral pulmonary embolism for developing optimal computed tomography pulmonary angiography protocols. Quant Imaging Med Surg 20198 (Epub ahead of print). doi: 10.21037/qims.2018.10.13.
25. McCollough CH, Primak AN, Braun N, Kofler J, Yu L, Christner J. Strategies for reducing radiation dose in CT. Radiol Clin North Am 2009;47:27-40.
26. Takahashi EA, Yoon H-C. Four-Year Cumulative radiation exposure in patients undergoing computed tomography angiography for suspected pulmonary embolism. Radiol Res Pract 2013; 2013:482403.
27. Leithner D, Gruber-Rouh T, Beeres M, Wichmann JL, Mahmoudi S, Martin

SS, Lenga L, Albrecht MH, Booz C, Vogl TJ, Scholtz JE. 90-kVp low-tube-voltage CT pulmonary angiography in combination with advanced modeled iterative reconstruction algorithm: effects on radiation dose, image quality and diagnostic accuracy for the detection of pulmonary embolism. Br J Radiol 2018;91:20180269.

28. Leithner D, Wichmann JL, Mahmoudi S, Martin SS, Albrecht MH, Vogl TJ, Scholtz JE. Diagnostic yield of 90-kVp low-tube-voltage carotid and intracerebral CT-angiography: effects on radiation dose, image quality and diagnostic performance for the detection of carotid stenosis. Br J Radiol 2018;91:20170927.
29. Schäfer JC, Haubenreisser H, Meyer M, Grüttner J, Walter T, Borggrefe M, et al. Feasibility of a sing**l**e contrast bolus high-pitch pulmonary CT angiography protocol followed by low-dose retrospectively ECG-gated cardiac CT in patients with suspected pulmonary embolism. Rofo 2018;190:542-550.
30. Kordolaimi SD, Argentos S, Pantos I, Kelekis NL, Efstathopoulos EP. A new era in computed tomographic dose optimization: the impact of iterative reconstruction on image quality and radiation dose. J Comput Assist Tomogr 2013;37:924-931.
31. Nelson RC, Feuerlein S, Boll DT. New iterative reconstruction techniques for cardiovascular computed tomography: how do they work, and what are the advantages and disadvantages? J Cardiovasc Comput Tomogr 2011;5:286-292.
32. Beister M, Kolditz D, Kalender WA. Iterative reconstruction methods in x-ray CT. Phys Med 2012;28:94-108.
33. den Harder AM, Willemink MJ, de Ruiter QM, Schilham AM, Krestin GP, Leiner T, et al. Achievable dose reduction using iterative reconstruction for chest computed tomography: a systematic review. Eur J Radiol 2015; 84: 2307–13.
34. Morimoto LN, Kamaya A, Boulay-Coletta I, Fleischmann D, Molvin L, Tian L, et al. Reduced dose CT with model-based iterative reconstruction compared to standard dose CT of the chest, abdomen, and pelvis in oncology patients: intra-individual comparison study on image quality and lesion conspicuity. Abdom Radiol 2017;42: 2279–88.

35. Gariani J, Martin SP, Botsikas D, Becker CD, Montet X. Evaluating the effect of increased pitch, iterative reconstruction and dual source CT on dose reduction and image quality. Br J Radiol 2018;91:20170443.
36. Aldosari S, Al Moudi M, Sun Z. Double-low dose protocol of computed tomography pulmonary angiography (CTPA) in the diagnosis of pulmonary embolism: A feasible approach for reduction of both contrast medium and radiation doses. Heart Res Open J 2017;4:33-38.
37. Lu G, Luo S, Meinel FG, et al. High-pitch computed tomography pulmonary angiography with iterative reconstruction at 80 kVp and 20 ml contrast agent volume. Eur Radiol 2014; 24(12):3260-3268.
38. Saade C, Mayat A, El-Merhi F. Exponentially decelerated contrast media injection rate combined with a novel patient-specific contrast formula reduces contrast volume administration and radiation dose during computed tomography pulmonary angiography. J Comput Assist Tomogr 2016; 40(3): 370-374.

Chapter 7

Conclusion and Future directions

7.1 Conclusion

In this thesis, the research has investigated the feasibility of using low-dose CT pulmonary angiography for diagnosis of pulmonary embolism with the aim of reducing both radiation dose and contrast volume. This research has developed a novel patient-specific 3D printed model and tested different CT pulmonary angiography protocols for dose reduction strategies.

A series of CT pulmonary angiography protocols comprising different kVp and pitch values were tested on the 3D printed pulmonary artery model with simulation of thrombus in the main and peripheral pulmonary arteries. Both quantitative and qualitative assessments of image quality indicated that low-dose CT pulmonary angiography allows for significant dose reductions of more than 80% when kVp was reduced from 120 to 80 or 70, and pitch increased from 0.9 to 2.2 or 3.2, without compromising diagnostic image quality.

Patient data analysis has further confirmed that low-dose CT pulmonary angiography allows for detection of pulmonary embolism by comparing three different CT scanning protocols which involved low radiation dose and low contrast volume. Both radiation dose and contrast volume can be reduced with use of low-dose protocols while still acquiring diagnostic images. The research outcomes of this study are summarised as follows:

- Low-dose CT pulmonary angiography can be achieved with use of low kVp such as 70 or 80, and high pitch mode of 2.2 or 3.2, with significant reductions in radiation dose while maintaining diagnostic images of detecting pulmonary embolism. When images are acquired with 64 or 128-slice CT, use of high pitch 3.2 in 70 kVp protocol is cautious due to high image noise which could negatively affect image quality.

- Low-dose CT pulmonary angiography can be achieved with use of low kVp down to 70 and high pitch 2.2 or 3.2 when images are acquired with latest CT scanners, such as 3rd generation dual-source Siemens Force scanner along with

image reconstruction with use of advanced iterative reconstruction algorithms. No significant differences were found in image quality assessments, regardless of CT pulmonary angiography protocols, while more than 80% dose reduction was achieved.

- Traditionally, anthropomorphic phantoms are used for dose reduction studies, however, they only represent average adult or paediatric patient sizes. 3D printed patient-specific models based on patient's imaging data are highly accurate, thus offering unique opportunities for optimising CT protocols. This study has demonstrated its usefulness through developing a realistic pulmonary artery model with simulation of pulmonary embolism in the arteries and successfully tested different scanning protocols on the model.

- Double low-dose CT pulmonary angiography is also feasible according to patient's data analysis with use of low kVp or low contrast medium volume protocol. The contrast medium can be lowered to 20 or 30 ml without affecting image quality.

Low-dose CT protocols represent the current research direction in CT angiographic imaging and this study has further confirmed its clinical value by significantly reducing radiation dose based on phantom experiments and patient's study. Furthermore, double low-dose CT pulmonary angiography is feasible from a clinical perspective, highlighting the paradigm shift in the current CT practice which involves reductions in both radiation dose and contrast medium dose.

7.2 Future research directions

This study improves our understanding of the clinical value of low-dose CT angiography with regard to reductions in radiation dose/contrast medium volume and image quality. Research findings highlight the feasibility of using 3D printed pulmonary artery model for development of optimal CT protocols. This encourages more research on use of 3D printed realistic models in other applications to optimise CT protocols. However, there are some suggestions for the future research:

- Studies involving multi-centre sites with inclusion of a large population and diagnostic accuracy are necessary to allow robust conclusions to be drawn;

- Despite usefulness of the 3D printed pulmonary model in this study, simulation of normal thoracic region with inclusion of lungs, ribs, heart and bones is preferable to create an environment similar to normal body tissues;

- Iterative reconstruction algorithms are commonly used in modern CT scanners, however, judicious use of them is recommended due to potential negative impact on image quality. Further studies on the investigation of effect of different strengths of iterative reconstruction algorithms on image quality and radiation dose of CT pulmonary angiography are recommended;

- Dual-energy CT is another promising technique showing potential value in the diagnosis of pulmonary embolism with low radiation dose and contrast medium, thus further studies could focus on comparing low-dose single energy CT with dual-energy pulmonary angiography.

- Artificial intelligence (AI) is increasingly used in diagnostic radiology with rapid automated detection and characterization of lesions with high accuracy when compared to human performance. Future research may consider using integrating AI or machine learning tools into the clinical workflow for automated detection of pulmonary embolism (in particular, the small and peripheral thrombus) to assist clinical diagnosis and patient management.

Appendix I: Statements of contributions of others

Statement of Contribution of Others to (Optimization of computed tomography pulmonary angiography protocols using 3D printed model with simulation of pulmonary embolism).

Aldosari S, Jansen S, Sun Z. Optimization of computed tomography pulmonary angiography protocols using 3D printed model with simulation of pulmonary embolism. Quant Imaging Med Surg 2018 (Epub ahead of print). doi: 10.21037/qims.2018.09.15 (IF=2.231)

To Whom It May Concern

I, Sultan Al-Dosari contributed (I designed the study and conducted image post-processing and segmentation of the CT imaging data; I performed measurements of dimensional accuracy of anatomical structures and image quality, and finally I wrote the manuscript) to the paper (Optimization of computed tomography pulmonary angiography protocols using 3D printed model with simulation of pulmonary embolism).

Sultan Al-Dosari

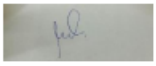

I, as a Co-Author, endorse that this level of contribution by the candidate indicated above is appropriate.

Jansen S (Signature of Co-Author 1)

Zhonghua Sun (Signature of Co-Author 2) 

Original Article

Optimization of computed tomography pulmonary angiography protocols using 3D printed model with simulation of pulmonary embolism

Sultan Aldosari[1], Shirley Jansen[2,3,4,5], Zhonghua Sun[1]

[1]Discipline of Medical Radiation Sciences, School of Molecular and Life Sciences, Curtin University, Perth, Western Australia, Australia; [2]Department of Vascular and Endovascular Surgery, Sir Charles Gairdner Hospital, Perth, Western Australia, Australia; [3]School of Public Health, Curtin University, Perth, Western Australia, Australia; [4]Faculty of Health and Medical Sciences, University of Western Australia, Crawley, Western Australia, Australia; [5]Heart and Vascular Research Institute, Harry Perkins Medical Research Institute, Perth, Western Australia, Australia

Correspondence to: Professor Zhonghua Sun. Discipline of Medical Radiation Sciences, School of Molecular and Life Sciences, Curtin University, GPO Box U1987, Perth, Western Australia 6845, Australia. Email: z.sun@curtin.edu.au.

Background: Three-dimensional (3D) printing has been shown to accurately replicate anatomical structures and pathologies in complex cardiovascular disease. Application of 3D printed models to simulate pulmonary arteries and pulmonary embolism (PE) could assist development of computed tomography pulmonary angiography (CTPA) protocols with low radiation dose, however, this has not been studied in the literature. The aim of this study was to investigate optimal CTPA protocols for detection of PE based on a 3D printed pulmonary model.

Methods: A patient-specific 3D printed pulmonary artery model was generated with thrombus placed in both main pulmonary arteries to represent PE. The model was scanned with 128-slice dual-source CT with slice thickness of 1 and 0.5 mm reconstruction interval. The tube voltage was selected to range from 70, 80, 100 to 120 kVp, and pitch value from 0.9 to 2.2 and 3.2. Quantitative assessment of image quality in terms of signal-to-noise ratio (SNR) was measured in the main pulmonary arteries and within the thrombus regions to determine the relationship between image quality and scanning protocols. Both two-dimensional (2D) and 3D virtual intravascular endoscopy (VIE) images were generated to demonstrate pulmonary artery and thrombus appearances.

Results: PE was successfully simulated in the 3D printed pulmonary artery model. There were no significant differences in SNR measured in the main pulmonary arteries with 100 and 120 kVp CTPA protocols ($P>0.05$), regardless of pitch value used. SNR was significantly lower in the high-pitch 3.2 protocols when compared to other protocols using 70 and 80 kVp ($P<0.05$). There were no significant differences in SNR measured within the thrombus among the 100 and 120 kVp protocols ($P>0.05$). For low dose 70 and 80 kVp protocols, SNR was significantly lower in the high-pitch of 3.2 protocols than that in other protocols with different pitch values ($P<0.01$). 2D images showed the pulmonary arteries and thrombus clearly, while 3D VIE demonstrated intraluminal appearances of pulmonary wall and thrombus in all protocols, except for the 70 kVp and pitch 3.2 protocol, with visualization of thrombus and pulmonary artery wall affected by artifact associated with high image noise. Radiation dose was reduced by up to 80% when lowering kVp from 120 to 100 and 80 kVp with use of 3.2 high-pitch protocol, without significantly affecting image quality.

Conclusions: Low-dose CT pulmonary angiography can be achieved with use of low kVp (80 and 100) and high-pitch protocol with significant reduction in radiation dose while maintaining diagnostic images of PE. Use of high pitch, 3.2 in 70 kVp protocol should be avoided due to high image noise and poorer quality.

Keywords: Computed tomography pulmonary angiography (CTPA); diagnosis; dose; image quality; model; three-dimensional printing

Submitted Sep 14, 2018. Accepted for publication Sep 24, 2018.
doi: 10.21037/qims.2018.09.15
View this article at: http://dx.doi.org/10.21037/qims.2018.09.15

Introduction

Computed tomography pulmonary angiography (CTPA) is currently the preferred imaging modality for diagnosis of suspected pulmonary embolism (PE). With improved spatial and temporal resolution available with modern CT scanners, CTPA has high diagnostic accuracy in the detection of segmental and subsegmental PE (1-3). However, the high radiation dose associated with CTPA is still a concern, given the high prevalence of PE and widespread use of less-invasive imaging for clinical diagnosis (1-5). Therefore, improvements in CT technique to minimize radiation dose are necessary.

A number of strategies have already been developed which include low tube voltage (kVp), use of iterative reconstruction (IR) for reducing image noise, and use of high-pitch protocols with fast speed CT scanners (6-13). Significant progress has been achieved with use of these dose-reduction strategies with radiation dose lowered to less than 2 mSv, according to some recent studies (14-16). Despite these promising results, further dose reduction by combining different parameters remains to be determined. Thus, the purpose of this study was to investigate the optimal CTPA protocols with use of different kVp and pitch values. Since it is unethical to scan patients with different CT protocols, we decided to use a patient-specific three-dimensional (3D) printed pulmonary artery model with simulation of PE in the pulmonary arteries. In our previous paper, we described how we developed a 3D printed pulmonary artery model and confirmed its accuracy and validity in replicating normal pulmonary arteries by testing different CT scanning parameters on it (17).

In this publication we describe how we extended our previous research by inserting thrombus in the pulmonary arteries to simulate PE, and scanning the model with different CTPA protocols. Although patient-specific 3D printed models have been reported in the literature with regard to their accuracy and usefulness in preoperative planning and simulation (18-23), to the best of our knowledge, this is the first study using a 3D printed pulmonary artery model with thrombus inside the arteries for determining optimal CTPA protocols.

Methods

Selection of sample case and image post-processing and segmentation

CTPA images of patients with suspected PE were retrospectively reviewed and one sample case with normal CTPA findings without any sign of PE was selected for generation of the pulmonary artery model with details provided in our previous study (17).

The same approach was used to perform image post-processing and segmentation of CTPA images as described previously (17). *Figure 1* shows the steps that were undertaken to generate a 3D segmented volume file for 3D printing of the pulmonary artery lumen. The 3D model was printed using an online printing service, Shapeways (24). An elastoplastic material was used to print the model since it has similar properties to that of arterial wall (25).

3D printing of pulmonary artery model with simulation of thrombus

To simulate PE in the pulmonary arteries, animal blood clots which were obtained from a local butcher were inserted into the left and right main pulmonary arteries of the 3D printed model mimicking thrombus. To prevent the "thrombus" from moving during CT scans, the blood clots were large enough to be deployed in the main pulmonary arteries, thus remaining stable during the scans.

CTPA scanning protocols

The 3D printed pulmonary artery model with thrombi inside was placed in a plastic container which was filled with contrast medium to simulate contrast-enhanced CT examinations. The contrast medium OptirayTM 350 (Mallinckrodt Pty Ltd, NSW, Australia) was diluted to 7% with resulting CT attenuation of 200 HU similar to that of routine CTPA. CTPA scans were performed on a dual-source 128-slice CT scanner (Siemens Definition Flash, Siemens Healthcare, Forchheim, Germany) with beam collimation of 2×64×0.6 mm and gantry rotation of 330 ms. Tube current modulation was used for all scans while different

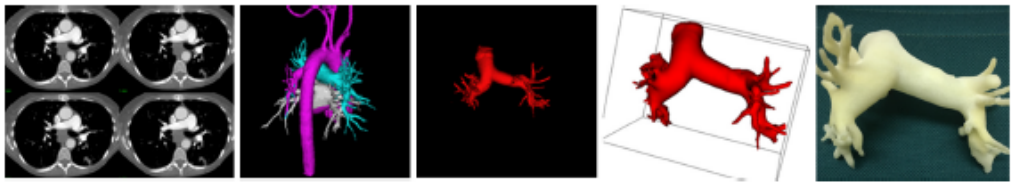

Figure 1 Flow diagram shows the image post-processing and segmentation processes from original 2D CT images to creation of 3D printed model. Original DICOM images were used to create 3D volume rendering image for displaying contrast-enhanced vessels (blue colour-pulmonary arteries, pink colour-aorta and its branches, white colour-left atrium and pulmonary veins). 3D volume rendering of pulmonary artery tree is segmented through a semi-automatic segmentation approach with manual editing. STL file of 3D segmented volume data was generated for 3D printing of patient-specific 3D printed model. Reprinted with permission under the open access from (17). CT, computed tomography; DICOM, digital imaging and communications in medicine; 2D, two-dimensional; 3D, three-dimensional; STL, standard tessellation language.

kVp and pitch values were chosen (70, 80, 100 and 120 kVp and pitch of 0.9, 2.2 and 3.2), resulting in a total of 12 datasets. A slice thickness of 1.0 mm with a 0.5 mm reconstruction interval was applied to all images, resulting in the voxel size of 0.29×0.29×0.29 mm^3 for volumetric data. All images were reconstructed with sinogram affirmed iterative reconstruction (SAFIRE, Siemens Healthcare) at a strength level of 3, and a tissue convolution kernel of I30f.

Image post-processing and visualization of PE

Two-dimensional (2D) images in digital imaging and communications in medicine (DICOM) format were transferred to a workstation with Analyze V 12.0 (AnalyzeDirect, Inc., Lexana, KS, USA) for image post-processing and generation of 2D and 3D virtual intravascular endoscopy (VIE) images. VIE visualization provides intraluminal views of the arterial wall and abnormal changes such as stenosis due to calcification, plaque or thrombus, with details of generating VIE views described in our previous studies (26-30). In brief, a CT number thresholding technique was used to generate VIE views of the pulmonary artery and thrombus in these phantom images without being affected by artifact. Selection of an appropriate CT threshold is important to ensure that the VIE images are free from artifact with clear demonstration of intraluminal views of pulmonary artery wall and thrombus. *Figure 2* is an example showing the relationship between VIE visualizations and different threshold selections.

Quantitative assessment of image quality

To determine image quality among these CTPA protocols, quantitative assessment of image quality was performed by measuring the image quality in terms of signal-to-noise ratio (SNR) in the main pulmonary arteries and within the thrombus regions. A region of interest (ROI) with an area of 25 mm^2 (containing minimum 300 voxels) was placed in the main right and left pulmonary arteries to measure the SNR. In addition, a ROI with an area of 5 mm^2 (containing 50 voxels) was placed within the thrombus region to measure SNR among these images. *Figure 3* shows measurement of SNR in the main pulmonary arteries and within thrombus regions. Measurements were repeated three times at each location with the mean values used as the final ones to minimize intra-observer variability. All measurements were performed by two observers separately with excellent correlation between the observers ($r=0.991$, $P<0.001$) with the mean values used as the final results.

Radiation dose measurement

Volume CT dose index (CTDIvol) and dose length product (DLP) were recorded and compared between these CTPA protocols. Effective dose was calculated using a tissue conversion coefficient of 0.014 mSv/mGy/cm which is commonly used for calculation of chest CT dose (31).

Statistical analysis

Data were entered into SPSS 24.0 (IBM Corporation,

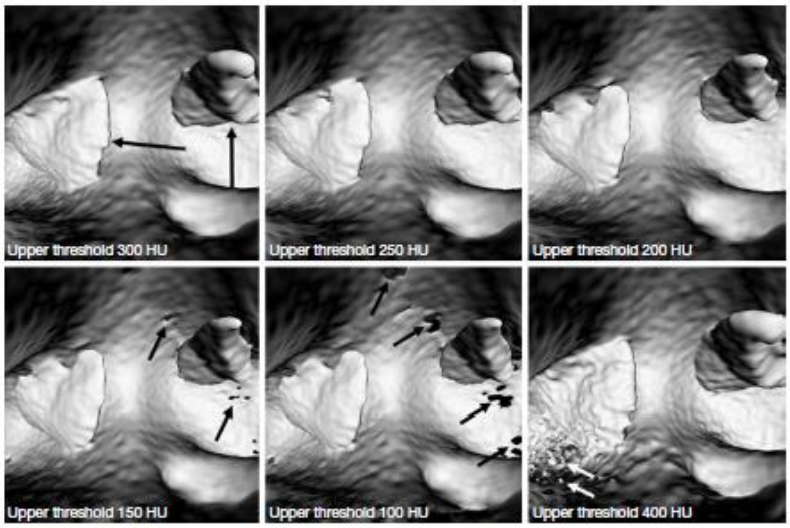

Figure 2 Generation of VIE of pulmonary embolism with selection of appropriate CT thresholds. Upper CT threshold was selected to start at 300 HU showing the best visualization of intraluminal thrombus (long black arrows). When upper threshold was reduced to lower levels, pierced artifacts (short black arrows) appeared in the arterial wall resulting in disruption of the arterial lumen. When upper threshold was increased to 400 HU, floating artifacts (white arrows) appeared in the arterial lumen affecting visualization of thrombus. VIE, virtual intravascular endoscopy; CT, computed tomography; HU, Hounsfield unit.

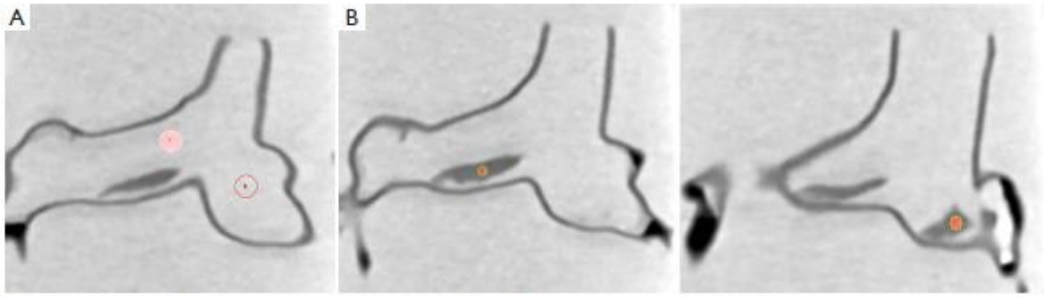

Figure 3 Measurement of image quality to determine SNR. (A) Measurement of image quality at the main pulmonary arteries; (B) measurement of image noise within the thrombus at both sides of pulmonary arteries. SNR, signal-to-noise ratio.

Armonk, NY, USA) for statistical analysis. Continuous variables were presented as mean and standard deviation. A paired sample *t* test was used to determine whether there are any significant differences in SNR measured with different CTPA protocols. A P value of less than 0.05 indicates a statistically significant difference.

Results

CTPA scans were successfully tested on the 3D printed model with use of different imaging protocols. *Table 1* shows SNR measurements at images acquired with different CTPA protocols. Apparently, SNR measured within the thrombus

Table 1 Measurements of SNR in images acquired with different CTPA protocols and associated radiation dose

Pitch values/SNR and radiation dose	70 kVp			80 kVp			100 kVp			120 kVp		
	0.9	2.2	3.2	0.9	2.2	3.2	0.9	2.2	3.2	0.9	2.2	3.2
Right main pulmonary artery	37.06±5.24	30.69±1.29	27.42±1.81	32.91±0.60	30.53±4.41	24.51±1.63	29.06±1.38	28.01±1.23	30.89±2.90	36.13±0.55	39.15±0.71	42.09±1.19
Left main pulmonary artery	40.22±3.94	29.89±0.30	20.87±2.03	35.27±1.10	28.35±1.30	25.63±0.79	34.38±1.46	31.31±1.23	36.86±2.51	58.83±1.07	47.54±2.32	67.30±3.90
Within right thrombus	4.22±0.13	4.16±0.02	3.28±0.16	4.84±0.30	5.02±0.30	4.92±0.37	6.52±0.27	6.44±0.33	6.37±0.59	10.55±0.71	9.10±0.65	10.07±1.41
Within left thrombus	6.02±0.50	4.99±0.43	4.83±0.49	6.48±0.26	6.49±0.42	4.92±0.42	13.02±0.51	12.96±1.27	10.61±1.04	13.27±1.27	11.73±0.73	10.89±1.09
CTDIvol (mGy)	0.41	0.15	0.12	0.42	0.21	0.21	1.01	0.55	0.55	2.22	1.05	1.05
DLP (mGy/cm)	5.90	2.70	2.20	6.20	4.00	3.60	14.60	10.30	9.50	32.20	19.70	18.10
Effective dose (mSv)	0.08	0.04	0.03	0.09	0.06	0.05	0.20	0.14	0.13	0.45	0.28	0.25

SNR, signal-to-noise ratio; CTPA, computed tomography pulmonary angiography; CTDIvol, volume CT dose index; DLP, dose length product.

on both sides was significantly higher in images acquired with higher kVp such as 100 and 120 protocols than that in the low 70 and 80 kVp protocols ($P<0.001$). There were no significant differences in SNR measurements across all 100 and 120 kVP protocols ($P>0.05$), regardless of the pitch values. SNR was significantly lower in the high-pitch protocols with 70 and 80 kVp, when compared to the protocols with use of pitch values of 0.9 and 2.2 ($P<0.01$).

SNR measured outside the thrombus in the main pulmonary arteries did not show any significant differences among these images acquired with 100 and 120 kVp protocols ($P>0.05$), except for the 120 kVp and pitch 3.2 protocol which shows significantly higher SNR than in the low pitch protocols ($P<0.05$). Similarly, SNR measured in images (both left and right main pulmonary arteries) acquired with 70 and 80 kVp and pitch of 3.2 protocol was significantly lower than that in other protocols ($P<0.05$). *Figure 4* is an example showing coronal reformatted images of these CTPA protocols. When pitch was increased to 3.2, image noise was increased with use of low kVp protocols such as 70 and 80 kVp as shown in *Figure 4A,B*. However, the thrombi in the pulmonary arteries are clearly displayed on these images, despite the use of low-dose protocols.

3D VIE images were generated and compared across different CTPA protocols with clear visualization of intraluminal views of pulmonary artery lumen and thrombus. *Figure 5* shows a series of VIE images generated with these CTPA protocols. As shown in the images, VIE views of the arterial wall and thrombus were not affected by changing the kVp values, although 100 and 120 protocols produced VIE images with relatively smoother intraluminal appearances (*Figure 5A,B,C*). VIE images were not affected by changing the pitch from 0.9 to 2.2 (*Figure 5A,B*), however, when pitch was increased to the high-pitch mode of 3.2, images acquired with the 70 kVp protocol were affected, with irregular appearances of arterial wall and thrombi when compared to those protocols with use of 100 and 120 kVp (*Figure 5C*).

Table 1 shows CTDIvol and DLP as well as effective dose associated with these scanning protocols. With kVp reduced from 120 to 80 and use of high-pitch CTPA protocols, radiation dose was reduced by 33–80% when compared to the low kVp and low pitch protocols without compromising image quality.

Discussion

In this phantom study, we simulated PE in the main pulmonary arteries based on a 3D printed model and tested

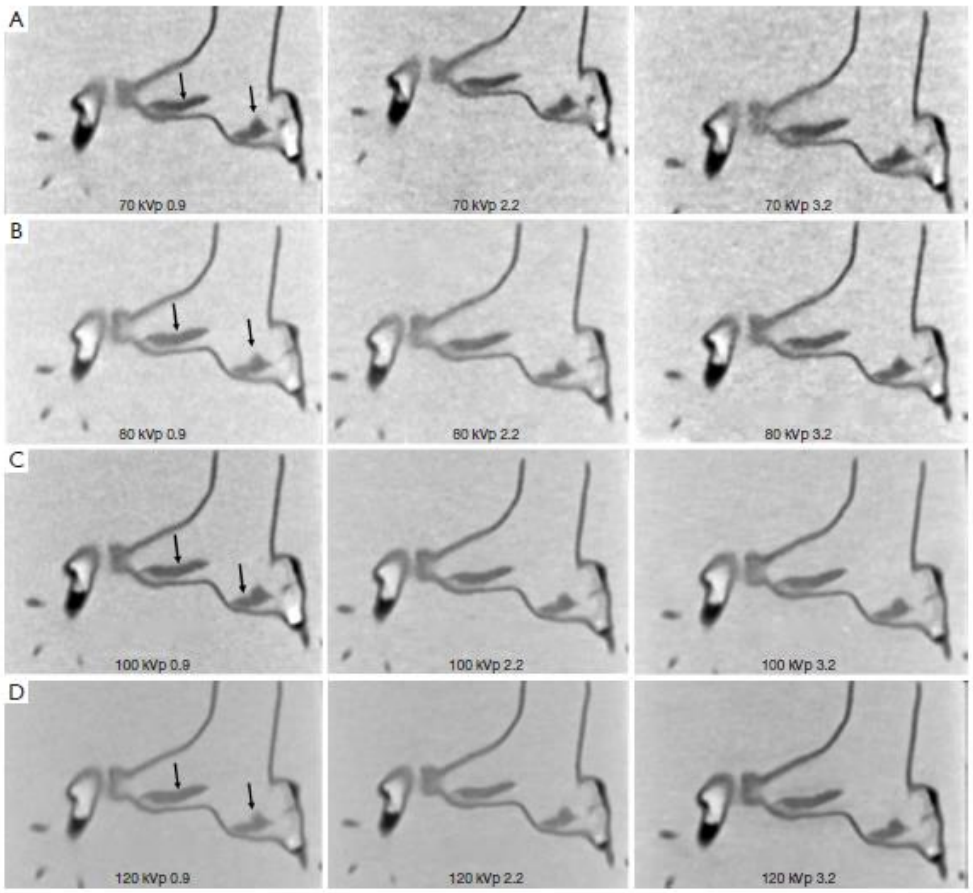

Figure 4 CTPA protocols with use of different kVp and pitch values. (A,B) When pitch was increased to 3.2, image noise was increased with 70 and 80 kVp protocols; (C,D) in contrast, no significant change of image quality was noted with 100 and 120 kVp protocols, regardless of pitch values. CTPA, computed tomography pulmonary angiography.

different CTPA protocols comprising a range of kVp and pitch values. Quantitative assessment of image quality showed no significant differences when kVp was lowered from 120 to 100 or 80 kVp, or pitch was increased from 0.9 to 3.2. This led to a significant dose reduction by more than 80% with use of low-dose CTPA protocols. 3D VIE image visualizations of pulmonary artery and thrombus demonstrated similar findings, although visualization of the thrombus was affected when the high pitch of 3.2 was used in the 70 kVp protocol. This study further confirms the feasibility of using a low-dose CTPA protocol in the detection of PE while maintaining acceptable image quality.

CTPA is currently recommended as the first line imaging modality in the diagnosis of suspected PE, given the high spatial and temporal resolution available with current CT scanners, and the high diagnostic yield (4,13). Technical developments of CT imaging have led to significant dose reductions with use of various dose-saving strategies

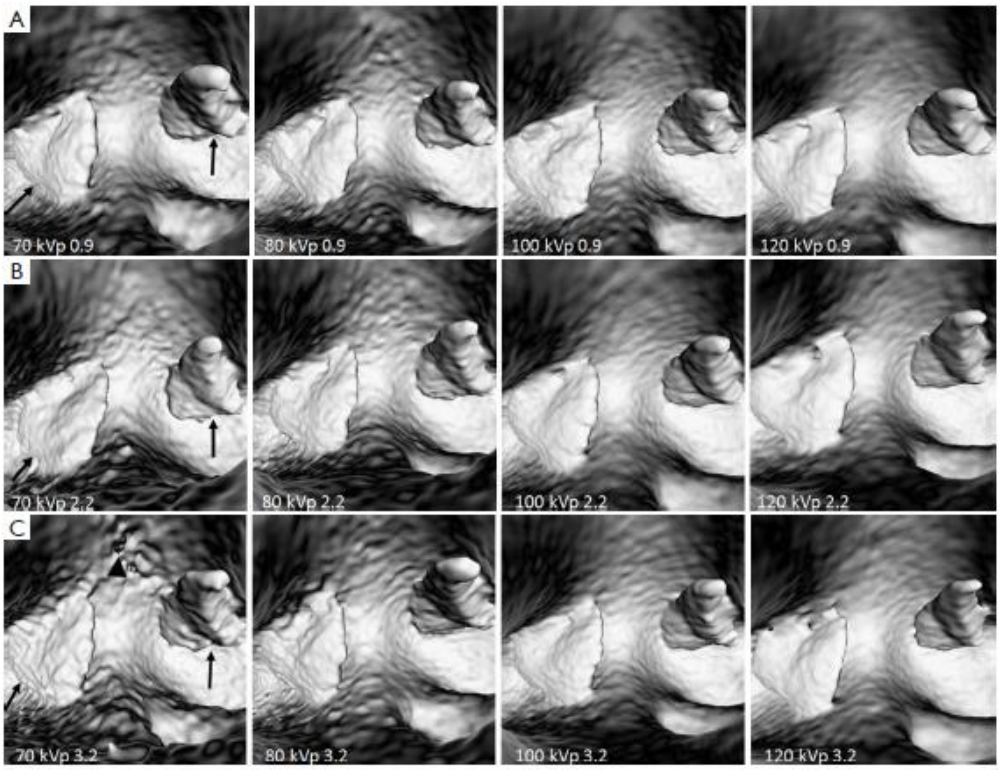

Figure 5 VIE of thrombus in images acquired with different CTPA protocols. (A,B) Intraluminal views of the thrombus are clearly demonstrated with CTPA protocols using different kVp and pitch values of 0.9 and 2.2. (C) when high pitch of 3.2 was used, irregular appearance of the thrombus (arrows) and some artifacts (arrowhead) appeared in the low kVp 70 protocol when compared to other protocols. VIE, virtual intravascular endoscopy; CTPA, computed tomography pulmonary angiography.

including low kVp, use of IR algorithms, tube current modulation, high-pitch protocol and use of dual energy CT (2,32,33). Low-dose CTPA using 70 or 80 kVp and high-pitch mode has been proved to achieve diagnostic image quality compared to the standard CTPA protocol, while significantly reducing radiation dose (9,11-14). However, research on the investigation of image quality in normal pulmonary arteries and PE is still limited. This study adds valuable information to the current literature by exploring a variety of CTPA protocols including the lowest kVp and highest pitch value of 3.2 that is available in the literature.

A high-pitch CT protocol is available with fast speed CT scanners and decreases radiation dose significantly when pitch is increased from the standard 0.9 to 2.2 or more than 3.0. However, increasing pitch during CT scans is associated with compromising spatial resolution, which could increase image noise affecting diagnostic quality. We confirmed this in our study as image noise was increased in the 70 and 80 kVp protocols with a pitch of 3.2 (*Figure 4A,B*). This is especially apparent when visualizing the intraluminal thrombus at the images acquired with 70 kVp and the 3.2 pitch protocol (*Figure 5C*). Despite this potential limitation, clinical studies have shown the feasibility of using high-pitch CTPA protocols in the diagnosis of PE without losing image quality (12-14,34).

Buchner *et al.* (34) in their large single center study compared high-pitch CTPA (180 mAs with filtered back projection and pitch 1.2, and 90 mAs with IR, pitch 3.0) with standard pitch (180 mAs and pitch 1.2) and 100 kVp in 382 patients. No significant difference was noticed in image quality among these 3 groups, while significant reduction of radiation dose was found in the high-pitch and low tube current group (P<0.001). Their results are consistent with other reports on the use of combining low kVp with high-pitch protocols (12-15). Lowering kVp to 80 or 70 in the high-pitch CTPA protocol could be challenging due to the potential risk of compromising image quality. This was observed in our study as the SNR measured with 70 and 80 kVp protocols was significantly lower than that measured with 100 or 120 kVp protocols (*Table 1*). Further, 3D visualization of intraluminal appearances of thrombus and pulmonary artery wall is affected by artifact due to increased image noise with 70 kVp and high pitch 3.2 protocol. Previous studies focused on 2D (axial and multiplanar reformation) images of low-dose CTPA protocols for detection of PE (12-15,34), while in this study, we assessed both 2D and 3D VIE images acquired with different CTPA protocols and corresponding image quality for visualization of PE. Thus, our results provide additional information to the current literature.

With rapid developments in 3D printing techniques and increasing applications in the medical field, patient-specific 3D printed models have been shown to be highly accurate in replicating normal anatomical structures and pathologies (17,20-23). Our recent study (17) has demonstrated the accuracy of a 3D printed pulmonary artery model with successful testing of different CT scanning protocols on the model. To our knowledge, this is the first report of using a patient-specific 3D printed pulmonary model for determining optimal CTPA protocols. Findings of this study are expected to encourage more research 3D printing techniques in other applications to develop low-dose CT protocols.

There are some limitations in this study. First, despite a realistic 3D printed model being used for studying different CTPA protocols, the model was not placed in an environment which simulated normal anatomic regions such as lungs, ribs, bones or heart. Thus, the radiation dose associated with these protocols is much lower than the actual value as reported in other studies due to the small field of view in these CT scans. Confirmation of results with simulation of normal thoracic structures are required. Second, only SNR was measured to determine image quality while no contrast-to-noise ratio (CNR) was measured. This is due to the reason that the 3D printed model was immersed in the diluted contrast medium instead of only filling the pulmonary arteries with contrast medium. Quantitative assessment of image quality by using both SNR and CNR would allow us to draw robust conclusions. Third, PE was simulated in the main pulmonary arteries, while no blood clot was used in the peripheral arteries to simulate embolism. Although CTPA has high diagnostic value, accurate detection of peripheral (segmental or subsegmental) or small thrombus in the peripheral pulmonary artery branches with a low-dose protocol would be required. This is currently being investigated with the aim of simulating small emboli in the peripheral arterial branches. Finally, no subjective assessment of image quality was included due to the fact that the pulmonary emboli were large. This could be assessed in the ongoing study with simulation of peripheral PE with different CTPA protocols.

In conclusion, we have demonstrated the feasibility of simulating PE in a 3D printed pulmonary model with different CT scanning protocols tested. Low-dose CTPA protocol is achievable with use of low kVp such as 70 or 80 with acceptable image quality. When high-pitch of 3.2 is used for CTPA, kVp can be lowered to 80 or 100 without compromising image quality in most of the protocols. Use of a low-dose CTPA protocol by combining 70 kVp with high-pitch 3.2 should be avoided due to its negative impact on the image quality of both pulmonary arteries and thrombus, as well as on intraluminal visualization of thrombus and pulmonary artery wall. Further studies on a low-dose CTPA protocols for detection of peripheral PE are underway.

Aoknowledgments

Authors would like to thank Mr Tom Tiang from Perth Children's Hospital for his assistance in CT scanning of the pulmonary artery model.

Footnote

Conflicts of Interest: The authors have no conflicts of interest to declare.

Ethical Statement: No ethical approval is required since this study is based on a phantom experiment.

Referenoes

1. Sherk WM, Stojanovska J. Role of clinical decision tools in the diagnosis of pulmonary embolism. AJR Am J Roentgenol 2017;208:W60-70.
2. Albrecht MH, Bickford MW, Nance JW Jr, Zhang L, De Cecco CN, Wichmann JL, Vogl TJ, Schoepf UJ. State-of-the-Art pulmonary CT angiography for acute pulmonary embolism. AJR Am J Roentgenol 2017;208:495-504.
3. Kligerman SJ, Mitchell JW, Sechrist JW, Meeks AK, Galvin JR, White CS. Radiologist performance in the detection of pulmonary embolism: Features that favor correct interpretation and risk factors for errors. J Thorac Imaging 2018. [Epub ahead of print].
4. Sun Z, Lei J. Diagnostic yield of CT pulmonary angiography in the diagnosis of pulmonary embolism: a single center experience. Interv Cardiol 2017;9:191-8.
5. Ong CW, Malipatil V, Lavercombe M, Teo MG, Coughlin PB, Leach D, Spanger MC, Thien F. Implementation of a clinical prediction tool for pulmonary embolism diagnosis in a tertiary teaching hospital reduces the number of computed tomography pulmonary angiograms performed. Intern Med J 2013;43:169-74.
6. Chen EL, Ross JA, Grant C, Wilbur A, Mehta N, Hart E, Mar WA. Improved image quality of low-dose CT pulmonary angiograms. J Am Coll Radiol 2017;14:648-53.
7. Wichmann JL, Hu X, Kerl JM, Schulz B, Frellesen C, Bodelle B, Kaup M, Scholtz JE, Lehnert T, Vogl TJ, Bauer RW. 70 kVp computed tomography pulmonary angiography: potential for reduction of iodine load and radiation dose. J Thorac Imaging 2015;30:69-76.
8. Martini K, Meier A, Higashhigaito K, Saltybaeva N, Alkadhi H, Frauenfelder T. Prospective randomized comparison of high-pitch CT at 80 kVp under free breathing with standard-pitch CT at 100 kVp under breath-hold for detection of pulmonary embolism. Acad Radiol 2016;23:1335-41.
9. Li X, Ni QQ, Schoepf UJ, Wichmann JL, Felmly LM, Qi L, Kong X, Zhou CS, Luo S, Zhang LJ, Lu GM. 70-kVp high-pitch computed tomography pulmonary angiography with 40 mL contrast agent: initial experience. Acad Radiol 2015;22:1562-70.
10. Kligerman S, Lahiji K, Weihe E, Lin CT, Terpenning S, Jeudy J, Frazier A, Pugatch R, Galvin JR, Mittal D, Kothari K, White CS. Detection of pulmonary embolism on computed tomography: improvement using a model-based iterative reconstruction algorithm compared with filtered back projection and iterative reconstruction algorithms. J Thorac Imaging 2015;30:60-8.
11. Bolen MA, Renapurkar RD, Popovic ZB, Popovic ZB, Heresi GA, Flamm SD, Lau CT, Lau CT, Halliburton SS. High-pitch ECG synchronized pulmonary CT angiography versus standard CT pulmonary angiography: a prospective randomized study. AJR Am J Roentgenol 2013;201:971-6.
12. Lu GM, Luo S, Meinel FG, McQuiston AD, Zhou CS, Kong X, Zhao YE, Zheng L, Schoepf UJ, Zhang LJ. High-pitch computed tomography pulmonary angiography with iterative reconstruction at 80 kVp and 20 mL contrast agent volume. Eur Radiol 2014;24:3260-8.
13. Sabel BO, Buric K, Karara N, Thierfelder KM, Dinkel J, Sommer WH, Meinel FG. High-pitch CT pulmonary angiography in third generation dual-source CT: image quality in an unselected patient population. PLoS ONE 2016;11:e0146949.
14. Boos J, Kropil P, Lanzman RS, Aissa J, Schleich C, Heusch P, Sawicki LM, Antoch G, Thomas C. CT pulmonary angiography: simultaneous low-pitch dual-source acquisition mode with 70 kVp and 40 ml of contrast medium and comparison with high-pitch spiral dual-source acquisition with automated tube potential selection. Br J Radiol 2016;89:20151059.
15. Laqmani A, Regier M, Veldhoen S, Backhaus A, Wassenberg F, Sehner S, Groth M, Nagel HD, Adam G, Henes FO. Improved image quality and low radiation dose with hybrid iterative reconstruction with 80 kV CT pulmonary angiography. Eur J Radiol 2014;83:1962-9.
16. Hu X, Ma L, Zhang J, Li Z, Shen Y, Hu D. Use of pulmonary CT angiography with low tube voltage and low-iodine-concentration contrast agent to diagnose pulmonary embolism. Sci Rep 2017;7:12741.
17. Aldosari S, Squelch A, Sun Z. Patient-specific 3D printed pulmonary artery model: A preliminary study. Digit Med 2017;3:170-7.
18. Olivieri LJ, Krieger A, Loke YH, Nath DS, Kim PC, Sable CA. Three-dimensional printing of intracardiac defects from three-dimensional echocardiographic images: feasibility and relative accuracy. J Am Soc Echocardiogr 2015;28:392-97.
19. Cantinotti M, Valverde I, Kutty S. Three-dimensional printed models in congenital heart disease. Int J Cardiovasc Imaging 2017;33:137-44.
20. Lau IW, Liu D, Xu L, Fan Z, Sun Z. Clinical value of patient-specific three-dimensional printing of congenital heart disease: Quantitative and qualitative Assessments. PLoS One 2018;13:e0194333.

21. Liu D, Sun Z, Chaichana T, Ducke W, Fan Z. Patient-specific 3D printed models of renal tumours using home-made 3D printer in comparison with commercial 3D printer. J Med Imaging Health Inf 2018;8:303-8.
22. Sun Z, Liu D. A systematic review of clinical value of three-dimensional printing in renal disease. Quant Imaging Med Surg 2018;8:311-25.
23. Lau I, Sun Z. Three-dimensional printing in congenital heart disease: A systematic review. J Med Radiat Sci 2018;65:226-36.
24. Shapeways. Frequently Asked Questions. Available online: https://www.shapeways.com/support/faq
25. 3D Printing Materials. Shapeways. Available online: https://www.shapeways.com/materials/
26. Xu L, Sun Z. Virtual intravascular endoscopy visualization of calcified coronary plaques: a novel approach of identifying plaque features for more accurate assessment of coronary lumen stenosis. Medicine 2015;94:e805.
27. Sun Z, Dosari SA, Ng C, al-Muntashari A, Almaliky S. Multislice CT virtual intravascular endoscopy for assessing pulmonary embolisms: a pictorial review. Korean J Radiol 2010;11:222-30.
28. Sun Z, Dimpudus FJ, Nugroho J, Adipranoto JD. CT virtual intravascular endoscopy assessment of coronary artery plaques: a preliminary study. Eur J Radiol 2010;75:e112-9.
29. Sun Z, Winder JR, Kelly BE, Ellis PK, Kennedy PT, Hirst DG. Assessment of VIE image quality using helical CT angiography: in vitro phantom study. Comput Med Imaging Graph 2004;28:3-12.
30. Sun Z, Gallagher E. Multislice CT virtual intravascular endoscopy for abdominal aortic aneurysm stent grafts. J Vasc Interv Radiol 2004;15:961-70.
31. McCollough CH, Primak AN, Braun N, Kofler J, Yu L, Christner J. Strategies for reducing radiation dose in CT. Radiol Clin North Am 2009;47:27-40.
32. Henzler T, Barraza JM, Nance JW, Jr, Costello P, Krissak R, Fink C, Schoepf UJ. CT imaging of acute pulmonary embolism. J Cardiovasc Comput Tomogr 2011;5:3-11.
33. Zhang LJ, Lu GM, Meinel FG, McQuiston AD, Ravenel JG, Schoepf UJ. Computed tomography of acute pulmonary embolism: state-of-the-art. Eur Radiol 2015;25:2547-57.
34. Bucher AM, Kerl MJ, Albrecht MH, Beeres M, Ackermann H, Wichmann JL, Vogl TJ, Bauer RW, Lehnert T. Systematic comparison of reduced tube current protocols for high-pitch and standard-pitch pulmonary CT angiography in a large single-center population. Acad Radiol 2016;23:619-27.

Cite this article as: Aldosari S, Jansen S, Sun Z. Optimization of computed tomography pulmonary angiography protocols using 3D printed model with simulation of pulmonary embolism. Quant Imaging Med Surg 2018. doi: 10.21037/qims.2018.09.15

A.1 Permission to reproduce published (Copyright forms)

AME Publishing Company LICENSE TERMS AND CONDITIONS

Dec 03, 2018

This is a License Agreement between sultan Ae aldosari ("You") and AME Publishing Company ("AME Publishing Company") provided by Copyright Clearance Center ("CCC"). The license consists of your order details, the terms and conditions provided by AME Publishing Company, and the payment terms and conditions.

All payments must be made in full to CCC. For payment instructions, please see information listed at the bottom of this form.

License Number	4481381235871
License date	Dec 03, 2018
Licensed content publisher	AME Publishing Company
Licensed content title	Quantitative imaging in medicine and surgery
Licensed content date	Jan 1, 2011
Type of Use	Thesis/Dissertation
Requestor type	Academic institution
Format	Print, Electronic
Portion	chart/graph/table/figure
Number of charts/graphs/tables/figures	6
The requesting person/organization is:	Sultan Rashed
Title or numeric reference of the portion(s)	Figures 1, 2,3,4,5, table 1
Title of the article or chapter the portion is from	Optimization of computed tomography pulmonary angiography protocols using 3D printed model with simulation of pulmonary embolism
Editor of portion(s)	n/a
Author of portion(s)	Aldosari S, Jansen S, Sun Z
Volume of serial or monograph.	n/a
Issue, if republishing an article from a serial	n/a
Page range of the portion	3-8
Publication date of portion	2018
Rights for	Main product
Duration of use	Life of current edition
Creation of copies for the disabled	no
With minor editing privileges	no
For distribution to	Worldwide
In the following language(s)	Original language of publication

With incidental promotional use	no
The lifetime unit quantity of new product	Up to 499
Title	Diagnostic Value of Multi-Slice CT Pulmonary Angiography in the Diagnosis of Pulmonary Embolism: An Investigation of Optimal Scanning Protocols in Terms of Image Quality, Contrast and Radiation Doses
Institution name	Curtin University
Expected presentation date	Dec 2018
Order reference number	cao2722
Billing Type	Invoice
Billing Address	sultan Ae aldosari 71 a mackie st vic park perth WA australia Perth, Australia Attn: sultan aldosari
Total (may include CCC user fee)	0.00 USD
Terms and Conditions	

TERMS AND CONDITIONS

The following terms are individual to this publisher:

It is the responsibility of the users' to identify the copyright holder of any materials. If the user has any doubts, please contact the publisher at permissions@amegrouops.com. For illustrations owned by Ms. Croce, please contact beth@bioperspective.com.

Other Terms and Conditions:

STANDARD TERMS AND CONDITIONS

1. Description of Service; Defined Terms. This Republication License enables the User to obtain licenses for republication of one or more copyrighted works as described in detail on the relevant Order Confirmation (the "Work(s)"). Copyright Clearance Center, Inc. ("CCC") grants licenses through the Service on behalf of the rightsholder identified on the Order Confirmation (the "Rightsholder"). "Republication", as used herein, generally means the inclusion of a Work, in whole or in part, in a new work or works, also as described on the Order Confirmation. "User", as used herein, means the person or entity making such republication.

2. The terms set forth in the relevant Order Confirmation, and any terms set by the Rightsholder with respect to a particular Work, govern the terms of use of Works in connection with the Service. By using the Service, the person transacting for a republication license on behalf of the User represents and warrants that he/she/it (a) has been duly authorized by the User to accept, and hereby does accept, all such terms and conditions on behalf of User, and (b) shall inform User of all such terms and conditions. In the event such person is a "freelancer" or other third party independent of User and CCC, such party shall be deemed jointly a "User" for purposes of these terms and conditions. In any event, User shall be deemed to have accepted and agreed to all such terms and conditions if User republishes the Work in any fashion.

3. Scope of License; Limitations and Obligations.

3.1 All Works and all rights therein, including copyright rights, remain the sole and exclusive property of the Rightsholder. The license created by the exchange of an Order Confirmation (and/or any invoice) and payment by User of the full amount set forth on that document includes only those rights expressly set forth in the Order Confirmation and in

these terms and conditions, and conveys no other rights in the Work(s) to User. All rights not expressly granted are hereby reserved.

3.2 General Payment Terms: You may pay by credit card or through an account with us payable at the end of the month. If you and we agree that you may establish a standing account with CCC, then the following terms apply: Remit Payment to: Copyright Clearance Center, 29118 Network Place, Chicago, IL 60673-1291. Payments Due: Invoices are payable upon their delivery to you (or upon our notice to you that they are available to you for downloading). After 30 days, outstanding amounts will be subject to a service charge of 1-1/2% per month or, if less, the maximum rate allowed by applicable law. Unless otherwise specifically set forth in the Order Confirmation or in a separate written agreement signed by CCC, invoices are due and payable on "net 30" terms. While User may exercise the rights licensed immediately upon issuance of the Order Confirmation, the license is automatically revoked and is null and void, as if it had never been issued, if complete payment for the license is not received on a timely basis either from User directly or through a payment agent, such as a credit card company.

3.3 Unless otherwise provided in the Order Confirmation, any grant of rights to User (i) is "one-time" (including the editions and product family specified in the license), (ii) is non-exclusive and non-transferable and (iii) is subject to any and all limitations and restrictions (such as, but not limited to, limitations on duration of use or circulation) included in the Order Confirmation or invoice and/or in these terms and conditions. Upon completion of the licensed use, User shall either secure a new permission for further use of the Work(s) or immediately cease any new use of the Work(s) and shall render inaccessible (such as by deleting or by removing or severing links or other locators) any further copies of the Work (except for copies printed on paper in accordance with this license and still in User's stock at the end of such period).

3.4 In the event that the material for which a republication license is sought includes third party materials (such as photographs, illustrations, graphs, inserts and similar materials) which are identified in such material as having been used by permission, User is responsible for identifying, and seeking separate licenses (under this Service or otherwise) for, any of such third party materials; without a separate license, such third party materials may not be used.

3.5 Use of proper copyright notice for a Work is required as a condition of any license granted under the Service. Unless otherwise provided in the Order Confirmation, a proper copyright notice will read substantially as follows: "Republished with permission of [Rightsholder's name], from [Work's title, author, volume, edition number and year of copyright]; permission conveyed through Copyright Clearance Center, Inc. " Such notice must be provided in a reasonably legible font size and must be placed either immediately adjacent to the Work as used (for example, as part of a by-line or footnote but not as a separate electronic link) or in the place where substantially all other credits or notices for the new work containing the republished Work are located. Failure to include the required notice results in loss to the Rightsholder and CCC, and the User shall be liable to pay liquidated damages for each such failure equal to twice the use fee specified in the Order Confirmation, in addition to the use fee itself and any other fees and charges specified.

3.6 User may only make alterations to the Work if and as expressly set forth in the Order Confirmation. No Work may be used in any way that is defamatory, violates the rights of third parties (including such third parties' rights of copyright, privacy, publicity, or other tangible or intangible property), or is otherwise illegal, sexually explicit or obscene. In addition, User may not conjoin a Work with any other material that may result in damage to the reputation of the Rightsholder. User agrees to inform CCC if it becomes aware of any infringement of any rights in a Work and to cooperate with any reasonable request of CCC or the Rightsholder in connection therewith.

4. Indemnity. User hereby indemnifies and agrees to defend the Rightsholder and CCC, and their respective employees and directors, against all claims, liability, damages, costs and expenses, including legal fees and expenses, arising out of any use of a Work beyond the

scope of the rights granted herein, or any use of a Work which has been altered in any unauthorized way by User, including claims of defamation or infringement of rights of copyright, publicity, privacy or other tangible or intangible property.

5. Limitation of Liability. UNDER NO CIRCUMSTANCES WILL CCC OR THE RIGHTSHOLDER BE LIABLE FOR ANY DIRECT, INDIRECT, CONSEQUENTIAL OR INCIDENTAL DAMAGES (INCLUDING WITHOUT LIMITATION DAMAGES FOR LOSS OF BUSINESS PROFITS OR INFORMATION, OR FOR BUSINESS INTERRUPTION) ARISING OUT OF THE USE OR INABILITY TO USE A WORK, EVEN IF ONE OF THEM HAS BEEN ADVISED OF THE POSSIBILITY OF SUCH DAMAGES. In any event, the total liability of the Rightsholder and CCC (including their respective employees and directors) shall not exceed the total amount actually paid by User for this license. User assumes full liability for the actions and omissions of its principals, employees, agents, affiliates, successors and assigns.

6. Limited Warranties. THE WORK(S) AND RIGHT(S) ARE PROVIDED "AS IS". CCC HAS THE RIGHT TO GRANT TO USER THE RIGHTS GRANTED IN THE ORDER CONFIRMATION DOCUMENT. CCC AND THE RIGHTSHOLDER DISCLAIM ALL OTHER WARRANTIES RELATING TO THE WORK(S) AND RIGHT(S), EITHER EXPRESS OR IMPLIED, INCLUDING WITHOUT LIMITATION IMPLIED WARRANTIES OF MERCHANTABILITY OR FITNESS FOR A PARTICULAR PURPOSE. ADDITIONAL RIGHTS MAY BE REQUIRED TO USE ILLUSTRATIONS, GRAPHS, PHOTOGRAPHS, ABSTRACTS, INSERTS OR OTHER PORTIONS OF THE WORK (AS OPPOSED TO THE ENTIRE WORK) IN A MANNER CONTEMPLATED BY USER; USER UNDERSTANDS AND AGREES THAT NEITHER CCC NOR THE RIGHTSHOLDER MAY HAVE SUCH ADDITIONAL RIGHTS TO GRANT.

7. Effect of Breach. Any failure by User to pay any amount when due, or any use by User of a Work beyond the scope of the license set forth in the Order Confirmation and/or these terms and conditions, shall be a material breach of the license created by the Order Confirmation and these terms and conditions. Any breach not cured within 30 days of written notice thereof shall result in immediate termination of such license without further notice. Any unauthorized (but licensable) use of a Work that is terminated immediately upon notice thereof may be liquidated by payment of the Rightsholder's ordinary license price therefor; any unauthorized (and unlicensable) use that is not terminated immediately for any reason (including, for example, because materials containing the Work cannot reasonably be recalled) will be subject to all remedies available at law or in equity, but in no event to a payment of less than three times the Rightsholder's ordinary license price for the most closely analogous licensable use plus Rightsholder's and/or CCC's costs and expenses incurred in collecting such payment.

8. **Miscellaneous.**

8.1 User acknowledges that CCC may, from time to time, make changes or additions to the Service or to these terms and conditions, and CCC reserves the right to send notice to the User by electronic mail or otherwise for the purposes of notifying User of such changes or additions; provided that any such changes or additions shall not apply to permissions already secured and paid for.

8.2 Use of User-related information collected through the Service is governed by CCC's privacy policy, available online here:
http://www.copyright.com/content/cc3/en/tools/footer/privacypolicy.html.

8.3 The licensing transaction described in the Order Confirmation is personal to User. Therefore, User may not assign or transfer to any other person (whether a natural person or an organization of any kind) the license created by the Order Confirmation and these terms and conditions or any rights granted hereunder; provided, however, that User may assign such license in its entirety on written notice to CCC in the event of a transfer of all or substantially all of User's rights in the new material which includes the Work(s) licensed under this Service.

8.4 No amendment or waiver of any terms is binding unless set forth in writing and signed by the parties. The Rightsholder and CCC hereby object to any terms contained in any writing prepared by the User or its principals, employees, agents or affiliates and purporting to govern or otherwise relate to the licensing transaction described in the Order Confirmation, which terms are in any way inconsistent with any terms set forth in the Order Confirmation and/or in these terms and conditions or CCC's standard operating procedures, whether such writing is prepared prior to, simultaneously with or subsequent to the Order Confirmation, and whether such writing appears on a copy of the Order Confirmation or in a separate instrument.

8.5 The licensing transaction described in the Order Confirmation document shall be governed by and construed under the law of the State of New York, USA, without regard to the principles thereof of conflicts of law. Any case, controversy, suit, action, or proceeding arising out of, in connection with, or related to such licensing transaction shall be brought, at CCC's sole discretion, in any federal or state court located in the County of New York, State of New York, USA, or in any federal or state court whose geographical jurisdiction covers the location of the Rightsholder set forth in the Order Confirmation. The parties expressly submit to the personal jurisdiction and venue of each such federal or state court.If you have any comments or questions about the Service or Copyright Clearance Center, please contact us at 978-750-8400 or send an e-mail to info@copyright.com.

v 1.1

Questions? customercare@copyright.com or +1-855-239-3415 (toll free in the US) or +1-978-646-2777.

Appendix II: Statements of contributions of others

Statement of Contribution of Others to (Patient-specific 3D printed pulmonary artery model with simulation of peripheral pulmonary embolism for developing optimal computed tomography pulmonary angiography protocols).

Aldosari S, Jansen S, Sun Z. Patient-specific 3D printed pulmonary artery model with simulation of peripheral pulmonary embolism for developing optimal computed tomography pulmonary angiography protocols. 2018 Quant Imaging Med Surg 2018 (Epub ahead of print). (IF=2.231)

To Whom It May Concern

I, Sultan Al-Dosari contributed (I designed the study and conducted image post-processing and segmentation of the CT imaging data; I performed measurements of dimensional accuracy of anatomical structures and image quality, and finally I wrote the manuscript) to the paper (Patient-specific 3D printed pulmonary artery model with simulation of peripheral pulmonary embolism for developing optimal computed tomography pulmonary angiography protocols).

Sultan Al-Dosari

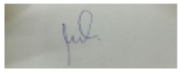

I, as a Co-Author, endorse that this level of contribution by the candidate indicated above is appropriate.

Jansen S (Signature of Co-Author 1)

Zhonghua Sun (Signature of Co-Author 2) 

Original Article

Patient-specific 3D printed pulmonary artery model with simulation of peripheral pulmonary embolism for developing optimal computed tomography pulmonary angiography protocols

Sultan Aldosari[1], Shirley Jansen[2,3,4,5], Zhonghua Sun[1]

[1]Discipline of Medical Radiation Sciences, School of Molecular and Life Sciences, Curtin University, Perth, Australia; [2]Department of Vascular and Endovascular Surgery, Sir Charles Gairdner Hospital, Perth, Australia; [3]Curtin Medical School, Curtin University, Perth, Australia; [4]Faculty of Health and Medical Sciences, University of Western Australia, Crawley, Australia; [5]Heart and Vascular Research Institute, Harry Perkins Medical Research Institute, Perth, Australia

Correspondence to: Professor Zhonghua Sun. Discipline of Medical Radiation Sciences, School of Molecular and Life Sciences, Curtin University, GPO Box U1987, Perth, Western Australia 6845, Australia. Email: z.sun@curtin.edu.au.

Background: Computed tomography pulmonary angiography (CTPA) is the preferred imaging modality for diagnosis of patients with suspected pulmonary embolism (PE). Radiation dose associated with CTPA has been significantly reduced due to the use of dose-reduction strategies, however, investigation of low-dose CTPA with use of different kVp and pitch values has not been systematically studied. The aim of this study was to utilize a 3D printed pulmonary model with simulation of small thrombus in the pulmonary arteries for development of optimal CTPA protocols.

Methods: Animal blood clots were inserted into the pulmonary arteries to simulate peripheral embolism based on a realistic 3D printed pulmonary artery model. The 3D printed model was scanned with 192-slice 3rd generation dual-source CT with 1 mm slice thickness and 0.5 mm reconstruction interval. All images were reconstructed with advanced modelled iterative reconstruction (IR) at a strength level of 3. CTPA scanning parameters were as follows: 70, 80, 100 and 120 kVp, 0.9, 2.2 and 3.2 pitch values. Quantitative assessment of image quality was determined by measuring signal-to-noise ratio (SNR) in both main pulmonary arteries, while qualitative analysis of images was scored by two experienced radiologists (score of 1 indicates poor visualization of thrombus with no confidence, and score of 5 excellent visualization of thrombus with high confidence) to determine the image quality in relation to different scanning protocols for detection of thrombus in the pulmonary arteries.

Results: No significant differences were found in SNR measurements among all CTPA protocols ($P>0.05$), regardless of kVp or pitch values used, although SNR was higher with 120 kVp and 0.9 and 2.2 pitch protocols than that in other protocols. The thrombi were detected in all images, with 70 kVp and 3.2 pitch protocol scored the lowest with a score of 3 by two observers, and images with other protocols were scored 4 or 5. Lowering kVp from 120 to 70 with use of high-pitch 2.2 or 3.2 protocol resulted in up to 80% dose reduction without significantly affecting image quality.

Conclusions: Low-dose CT pulmonary angiography protocols comprising 70 kVp and high pitch 2.2 or 3.2 allow for detection of peripheral PE with significant reduction in radiation dose while images are still considered diagnostic.

Keywords: Assessment; computed tomography pulmonary angiography (CTPA); pulmonary embolism (PE); optimization; pitch; reduction; three-dimensional printing

Submitted Oct 10, 2018. Accepted for publication Oct 26, 2018.
doi: 10.21037/qims.2018.10.13
View this article at: http://dx.doi.org/10.21037/qims.2018.10.13

Introduction

Computed tomography pulmonary angiography (CTPA) is increasingly used in the diagnosis of patients with suspected pulmonary embolism (PE) due to its high sensitivity and specificity for detecting segmental and subsegmental PE (1-5). However, the high radiation dose associated with the increased use of CTPA examinations has raised concerns leading to the paradigm shift of developing optimal CTPA protocols to lower radiation dose while still achieving diagnostic images. Low-dose CTPA protocols have been reported in some studies showing the feasibility of reducing tube voltage to 80 and 70 kVp with use of high pitch values with resultant effective dose of less than 2 mSv (6-13). The main disadvantage of lowering tube voltage during CTPA is associated with increased image noise, with noise further increased when a high pitch protocol is used. Use of iterative reconstruction (IR) algorithms have been shown to compensate for increased image noise arising from low kVp protocols, thus improving image quality for diagnosis of PE (14-17). This has created potential opportunities for developing low-dose CT protocols through combining low kVp and high pitch protocols with IR.

Testing different CT protocols on a 3D printed realistic anatomy model represents a new research direction for investigation of optimal CT angiography protocols as 3D printed models accurately replicate both normal anatomical structures and pathologies (18-23). In our previous papers, we reported how we developed a patient-specific 3D printed pulmonary artery model with high accuracy, and tested different CTPA protocols on the model with simulation of thrombus in the main pulmonary arteries (24,25). Through quantitative assessment of image quality, we concluded that low-dose CTPA is achievable with tube voltage lowering to 100 and 80 kVp and use of high pitch 3.2 with more than 80% radiation dose reduction without compromising image quality. In this study we extended our previous research by simulating thrombus in the peripheral pulmonary arteries and scanning the model with different parameters using the latest CT scanner, the 3rd generation dual-source CT, Siemens Force. Further, advanced modelled iterative reconstruction (ADMIRE) available with the Siemens Force system is the latest IR algorithm which offers higher radiation dose reduction while reducing image noise and minimizing artifacts. The purpose of this study was to determine optimal CTPA protocols for detection of small and peripheral thrombus in the pulmonary arteries with resulting low radiation dose and acceptable diagnostic images.

Methods

3D printed pulmonary artery model

This study used the same 3D printed pulmonary artery model as reported in our previous papers (24,25). The model was confirmed to be highly accurate in delineating anatomical structures of pulmonary arteries with successful simulation of PE in the main pulmonary arteries.

Simulation of thrombus in the peripheral pulmonary arteries

Animal blood clots were obtained from a local butcher with small amounts inserted into the peripheral pulmonary arteries to mimic PE. *Figure 1* shows selection of small thrombus for insertion into the distal pulmonary artery branches prior to CT scans.

CTPA scanning protocols

Similar to our previous papers, the 3D printed model with peripheral thrombus in the pulmonary arteries was immersed in a plastic container which was filled with diluted contrast medium to create a CT attenuation of 200 HU which is similar to that of CTPA examinations (*Figure 2*). CTPA scans were performed on a 3rd generation dual-source 192-slice CT scanner (Siemens Force, Siemens Healthcare, Forchheim, Germany) with beam collimation of 192 mm × 0.6 mm and gantry rotation of 250 ms. The CTPA scanning protocols were as follows: 70, 80, 100 and 120 kVp, pitch of 0.9, 2.2 and 3.2, resulting in a total of 12 datasets. The tube current was adjusted for CTPA protocols with pitch of 0.9 based on the kVp, with mAs of 121, 35, 42 and 52 corresponding to 70, 80, 100 and 120 kVp, respectively. For higher pitch values of 2.2 and 3.2, 80 mAs were used for the remaining protocols, regardless of the kVp values. All images were acquired with a slice thickness of 1.0 and 0.5 mm reconstruction interval, resulting in the voxel size of 0.31×0.31×0.31 mm^3 for volumetric data. All images were reconstructed with ADMIRE (Siemens Medical Solutions, Forchheim, Germany) at a strength level of 3, and a tissue convolution kernel of Br40d.

Qualitative assessment of image quality

Images were presented to two experienced thoracic radiologists (each with more than 5 years of experience in interpreting chest CT images) in a random order without

Figure 1 Procedure to insert blood clots in the 3D printed pulmonary artery model. (A) Blood clots which were obtained from a local butcher were broken into small pieces; (B) insertion of small blood clots in the peripheral segments of pulmonary arteries in the 3D printed model.

Figure 2 3D visualization of 3D printed pulmonary artery model which was placed inside the container filled with contrast medium. Since the model was immersed into the water with diluted contrast medium with similar CT attenuation to that of routine CT pulmonary angiography, surface voxel projection was used to create 3D view of the model.

showing any information about the scanning parameters. The two assessors were blinded to the scanning protocols and they assessed image quality independently using a 5-point Likert scale with a score of 3 or above indicating that image quality is diagnostic:

- 5: excellent visualization of thrombus with high confidence;
- 4: good visualization of thrombus with good confidence;
- 3: average visualization of thrombus with moderate confidence;
- 2: suboptimal visualization of thrombus with low confidence, and;
- 1: poor visualization of thrombus with no confidence.

Quantitative assessment of image quality

Quantitative assessment of image quality was determined by measuring the image noise in the main pulmonary arteries in terms of signal-to-noise ratio (SNR). A region of interest (ROI) with an area of >0.5 cm^2 (containing minimum 500 voxels) was placed in both main pulmonary arteries to measure the SNR. Due to the presence of air bubbles in the pulmonary arteries, ROI was placed in the central part of the main pulmonary arteries to avoid inclusion of any air bubbles which could affect the measurements. *Figure 3* shows SNR measurements in the main pulmonary arteries. Measurements at each location were repeated three times with the mean values used to reduce intra-observer variability. Two observers performed the measurements

Figure 3 Measurement of signal-to-noise ratio (SNR) in the main pulmonary arteries. (A,B) SNR measurements at the right and left main pulmonary arteries.

separately with excellent correlation between them (R=0.918, P<0.001). Mean values of measurements from these two observers were used as the final results.

Radiation dose calculation

Volume CT dose index (CTDIvol) and dose length product (DLP) were available on CT console after scans. These values were used to calculate effective dose based on a tissue conversion coefficient of 0.014 mSv/mGy/cm for chest CT dose calculation (26).

Statistical analysis

Data were analysed using SPSS 24.0 (IBM Corporation, Armonk, NY, USA). Mean and standard deviation were used to represent continuous variables. A paired sample Student T test was used to determine any significant differences in SNR measurements among different CTPA protocols. Inter-observer agreement for image quality assessment was assessed by kappa statistics: poor: k<0.20; fair: k=0.21–0.40; moderate: k=0.41–0.60; good: k=0.61–0.80, and excellent agreement k=0.81–1.00. A statistically significant difference was reached at a P value of less than 0.05.

Results

Insertion of small blood clots into the side or peripheral pulmonary was found to be challenging due to softness of the blood clots which were easily broken into small pieces during the insertion procedure (*Figure 1*). We managed to insert two small blood clots in the pulmonary arteries with one in the left segmental pulmonary arterial branch and another one in the distal segment of right main pulmonary artery simulating thrombus. CTPA scans with different protocols were successfully performed on the 3D printed model with simulation of PE.

Table 1 shows SNR measurements at the main pulmonary arteries corresponding to different CTPA protocols. Although low kVp 70 and 80 protocols were associated with increased image noise when compared to 100 and 120 kVp protocols, a high CT attenuation was found in these low kVp protocols in comparison with the high kVp protocols (340–440 *vs.* 210–260 HU). Thus, SNR measured with the 70 kVp protocols was found to be even higher than that with 80 or 100 kVp protocols as shown in *Table 1*. There were no significant differences in SNR measurements across all CTPA protocols (P>0.05), regardless of the pitch or kVp values. SNR was slightly higher in the 120 kVp with pitch 0.9 and 2.2 protocols, however, this did not reach statistical significance compared to other protocols (P>0.05).

Figures 4-7 show coronal reformatted images acquired with different CTPA protocols demonstrating pulmonary emboli in the pulmonary artery branches. Despite low kVp or high pitch protocols, thrombi are still visible in all images, although 100 and 120 kVp protocols allowed for better visualization of the small thrombus, especially at the left side. Inter-observer agreement was fair (k=0.333,

Table 1 Measurements of SNR in images acquired with different CTPA protocols and associated radiation dose

Pitch values/SNR and radiation dose	70 kVp			80 kVp			100 kVp			120 kVp		
	0.9	2.2	3.2	0.9	2.2	3.2	0.9	2.2	3.2	0.9	2.2	3.2
Right main pulmonary artery	39.69±4.39	29.75±0.10	31.66±1.49	31.33±0.50	37.84±2.57	35.83±1.04	26.48±2.12	37.44±1.72	39.17±1.85	40.17±0.61	43.35±1.55	38.92±2.00
Left main pulmonary artery	31.05±0.92	30.81±1.43	26.11±0.69	28.24±1.10	30.31±0.60	28.27±1.85	31.60±0.45	29.90±1.11	24.30±0.47	40.43±1.94	33.72±0.49	27.68±1.07
CTDIvol (mGy)	1.42	0.72	0.72	0.68	1.17	1.17	1.72	2.53	2.53	3.53	4.26	4.26
DLP (mGy/cm)	30.4	14.7	15.6	14.6	24	25.5	36.7	51.6	55	75.4	87.2	92.7
Effective dose (mSv)	0.42	0.20	0.21	0.20	0.33	0.35	0.51	0.72	0.77	1.05	1.22	1.29

CTPA, computed tomography pulmonary angiography; SNR, signal-to-noise ratio; CTDIvol, volume computed tomography dose index; DLP, dose length product.

P=0.118). The protocol of 70 kVp and pitch 3.2 was scored 3, the lowest score by these two assessors, indicating that images are still acceptable with the low-dose protocol. All of the remaining images were scored 4 or 5 by the two assessors.

Table 1 shows radiation dose values associated with these CTPA protocols. When kVp was reduced from 120 to 70 and pitch was increased from 0.9 to 2.2 or 3.2, radiation dose was reduced by up to 84% without compromising diagnostic image quality as evaluated by qualitative and quantitative assessments. It should be noted that CTDIvol remains the same for pitch of 2.2 and 3.2 protocols and this is due to the use of same mAs of 80 for these high pitch protocols. Therefore, as shown in *Table 1*, the effective dose of these high pitch protocols remains unchanged or even slightly increased. Further, due to selection of different mAs corresponding to kVp values in the low pitch 0.9 protocols, the CTPA protocol of 80 kVp and 0.9 pitch resulted in the lowest dose compared to other protocols. This needs to be interpreted with caution.

Discussion

In this phantom study, we further confirmed the feasibility of low-dose CTPA protocols with simulation of thrombus in peripheral pulmonary arteries. Quantitative assessment of image quality did not show any significant differences among these CTPA protocols with 70 kVp protocols even producing higher SNR than that of 80 or 100 kVp protocols. Qualitative analysis of image quality by experienced observers showed that all of the images are acceptable for detection of small thrombus, despite lowering kVp to 70 or increasing pitch to 3.2. Radiation dose reduction by more than 80% could be achieved with use of low-dose CTPA protocol while maintaining diagnostic image quality.

Low-dose CTPA has been reported in the literature with radiation dose down to 2 mSv or even less than 1.0 mSv (7-12). Lu *et al.* compared 80 kVp and 2.2 pitch protocol with 100 kVp and pitch 1.2 in 100 patients with suspected PE with 50 cases in each group (8). No significant difference was found in subjective scoring of image quality between the two groups, while quantitative measurements of image quality were significantly higher in the low-dose protocol than the standard group, with significant dose reduction achieved in the low kVp and high pitch protocol (0.9 *vs.* 1.7 mSv). Li and colleagues reported similar findings by using 70 kVp and high pitch 3.2 CTPA protocol in 80 patients with 40 in each group (9). Their results showed no significant difference in the subjective image quality

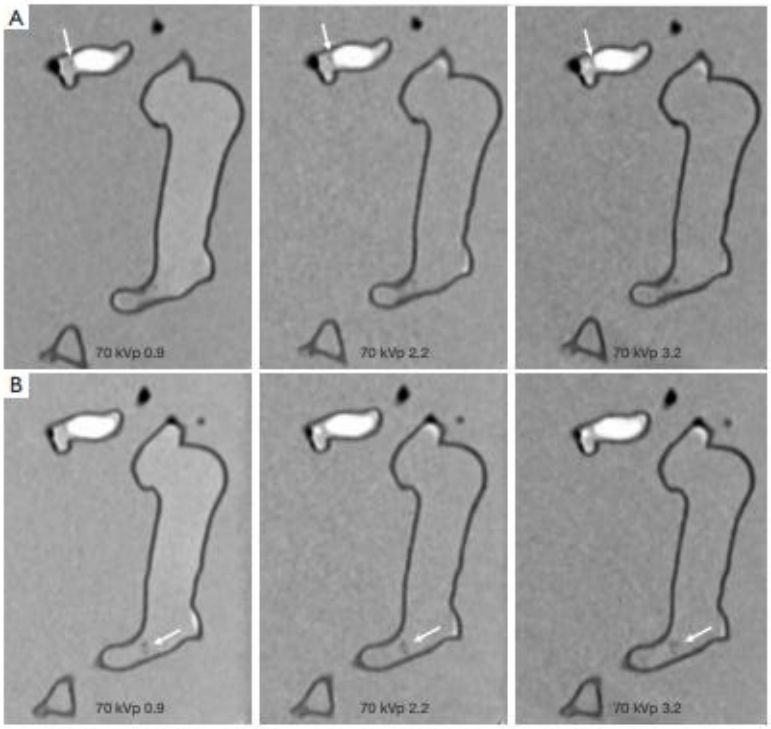

Figure 4 CTPA protocols with use of 70 kVp and different pitch values. (A) Visualization of small thrombus in the left segmental pulmonary artery with low-attenuation filling defect (arrows). Thrombus was more clearly visualized in pitch 0.9 and 2.2 protocols when compared to the high pitch 3.2 protocol. (B) Visualization of small thrombus in the distal part of right main pulmonary artery with filling defect (arrows) detected in all of the protocols. CTPA, computed tomography pulmonary angiography.

but with significantly higher quantitative assessments in the low-dose group. Up to 80% dose reduction was noted in the 70 kVp and 3.2 protocol (0.4 *vs.* 2.0 mSv). Our results are consistent with these findings. Low-dose CTPA protocol comprising 70 kVp and 3.2 pitch was scored to be acceptable for detection of small thrombus in the pulmonary arteries, with more than 80% dose reduction. The effective dose of the low-dose protocol in our study is between 0.20 and 0.21 mSv, almost half of what has been reported by Li's study. Thus, our study validates the feasibility of using lower kVp and high pitch CTPA protocol with further dose reduction.

Despite the great benefit of reducing radiation dose with a high-pitch CT protocol, the disadvantage of increasing pitch is associated with increased image noise which could affect diagnostic quality. This was noticed in our recent paper with increased image noise in the 70 kVp protocol with a pitch of 3.2 affecting visualization of thrombus and pulmonary arterial wall (25). With the latest CT scanners, advanced IR algorithms are developed to improve image quality by reducing image noise associated with the use of low-dose CT protocols (27,28). This is confirmed by findings in our study as the IR available with the Siemens Force scanner represents the latest algorithm used in image reconstruction for reducing image noise. A combination of low-dose protocol with advanced IR resulted in increased quantitative image quality, with low kVp 70 and high pitch 2.2 and 3.2 protocols still producing diagnostic images, but with much lower radiation dose.

3D printed models derived from patient's imaging data

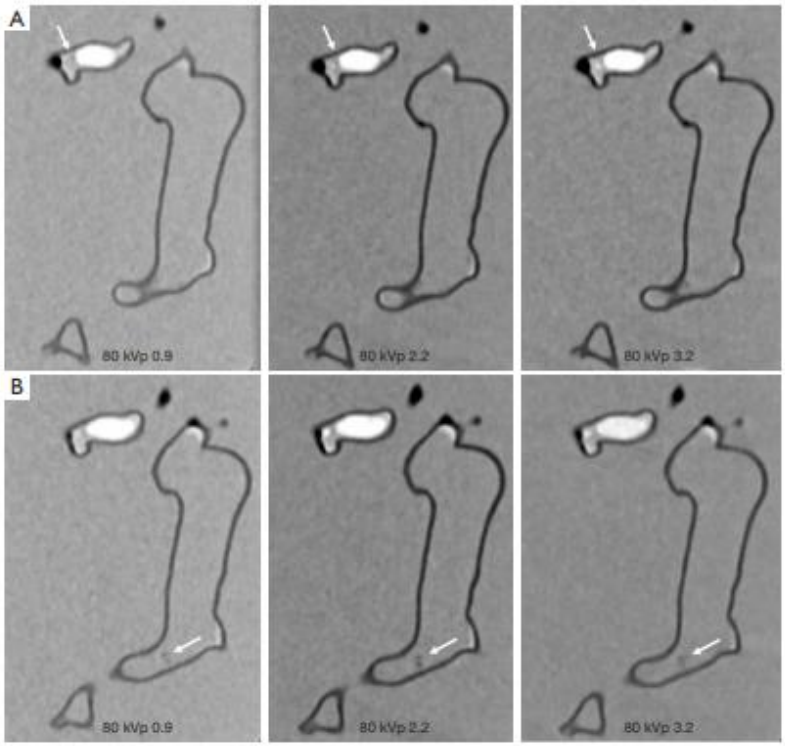

Figure 5 CTPA protocols with use of 80 kVp and different pitch values. (A,B) The small thrombus is viewed as low-attenuation filling defect in the left segmental pulmonary artery (arrows in A) and right pulmonary artery (arrows in B) and thrombi are visible in all protocols, regardless of pitch values used. CTPA, computed tomography pulmonary angiography.

are increasingly used in medical applications, with most of the studies focusing on the clinical value of patient-specific 3D printed models such as pre-surgical planning and simulation, medical education and patient-doctor communication (18-23,29,30). A new research direction of clinical application of 3D printed models is to develop optimal CT scanning protocols for radiation dose reduction. Abdullah *et al.* created a 3D printed cardiac phantom based on CT images of anthropomorphic chest phantom and inserted filling materials into the phantom to simulate different anatomical structures (31). CT scans of the 3D printed model showed that CT attenuations of these filling materials were similar to those from patient's CT images (contrast medium, air, oil/fat and jelly/muscle). Despite the novel design of this cardiac insert phantom, testing different scanning protocols on the 3D printed model remains to be investigated.

Our recent papers have addressed this limitation by developing a realistic pulmonary artery model with different CTPA protocols tested on the model with simulation of PE (24,25). With model's accuracy validated in the first paper, we scanned the model with a combination of different kVp and pitch values on a 128-slice dual-source CT scanner by inserting thrombus in the main pulmonary arteries. A dose reduction of 80% was achieved with use of low kVp 80 and high pitch 3.2 protocol when compared to the standard 100 or 120 kVp protocols, while low-dose 70 kVp and high pitch 3.2 was not recommended due to high image noise (25). In the current study, we simulated small thrombus in peripheral pulmonary arteries and

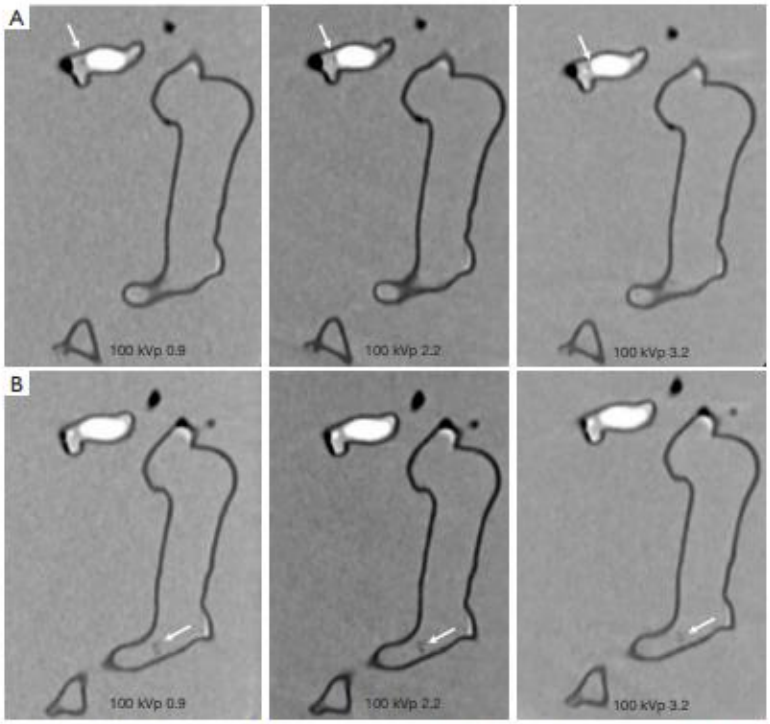

Figure 6 CTPA protocols with use of 100 kVp and different pitch values. (A,B) The small thrombus is viewed as low-attenuation filling defect in the left segmental pulmonary artery (arrows in A) and right pulmonary artery (arrows in B) and they are visible in all protocols, regardless of pitch values used. CTPA, computed tomography pulmonary angiography.

scanned the 3D printed model using the same CTPA protocols as in our previous paper, but on a latest CT scanner with use of advanced IR algorithm for image reconstruction. No significant differences were found in SNR measurements among all the protocols, with all images scored as diagnostic by two observers. Therefore, low-dose CTPA with 70 kVp and high pitch 2.2 or 3.2 is acceptable for detection of small PE with dose reduction up to 80%. Findings of this study further advanced our previous research and others, thus contributing to the current literature by recommending low-dose CTPA protocols with significant dose reduction.

Some limitations in this study should be acknowledged. Limitations that have been addressed in our previous papers still apply to the current study, such as the necessity of simulating a realistic anatomical environment with lungs, ribs, heart and other thoracic structures. Although small thrombus was inserted into in the left peripheral pulmonary artery branch, we failed to insert the thrombus in other small branches of the right pulmonary artery due to difficulty with handling the soft blood clots during the procedure. This could be addressed in future studies by simulating peripheral PE which is made of materials with similar attenuation to that of blood but with solid properties which can be easily deployed in the 3D printed models. Finally, air bubbles which are present in the pulmonary artery branches could affect the visualization and assessment of image quality to some extent (*Figure 8*). This needs to be considered in further experiments with approaches undertaken to reduce the negative impact of air bubbles.

In conclusion, we have simulated the small PE in the 3D printed pulmonary model and scanned the model with

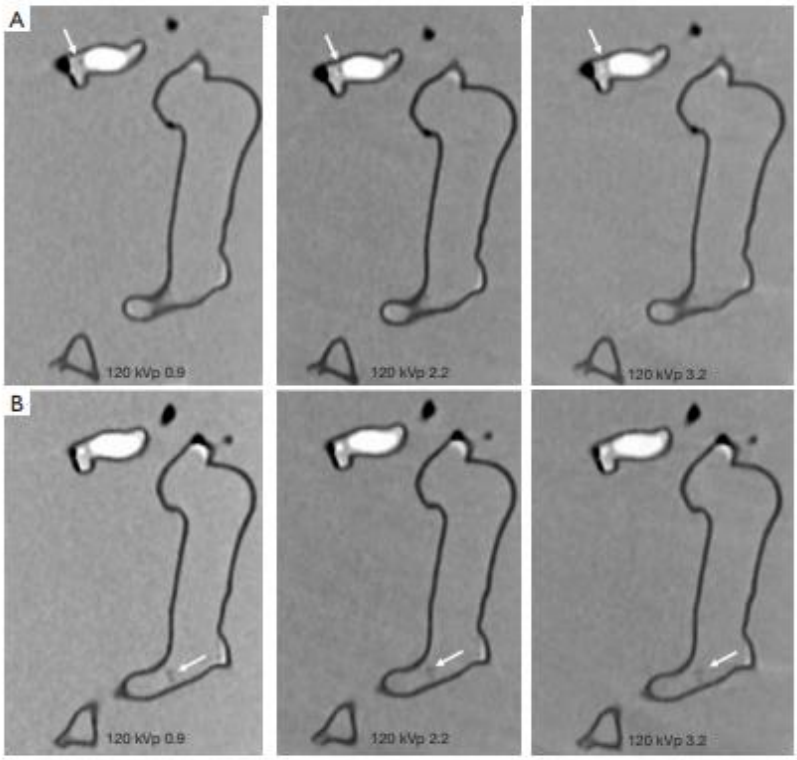

Figure 7 CTPA protocols with use of 120 kVp and different pitch values. (A,B) The small thrombus is viewed as low-attenuation filling defect in the left segmental pulmonary artery (arrows in A) and right pulmonary artery (arrows in B) and they are visible in all protocols, regardless of pitch values used. CTPA, computed tomography pulmonary angiography.

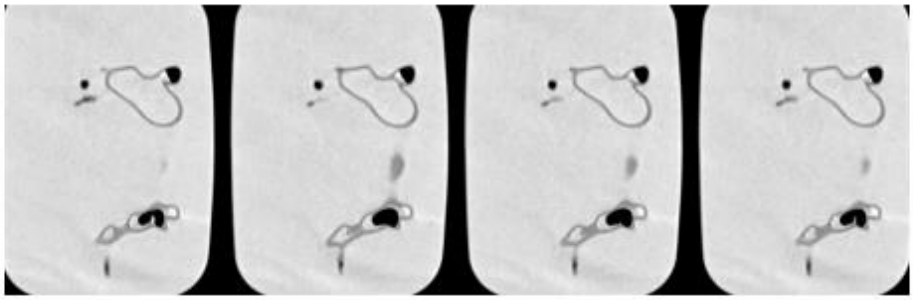

Figure 8 Air bubbles in the pulmonary arteries. Multiple air bubbles with different sizes are present in main and side branches of both pulmonary arteries which could affect assessment of image quality.

different CT pulmonary angiography protocols using the latest 3rd generation dual-source CT scanner with images reconstructed using the advanced IR algorithm. Low-dose CTPA protocols comprising low kVp 70 and high pitch of 2.2 or 3.2 result in more than 80% dose reduction, but still producing acceptable image quality as determined by quantitative and qualitative assessments. The small PE can still be detected on this low-dose CTPA protocol, further validating the feasibility of lowering kVp to 70 and increasing pitch up to 3.2 for diagnosis of patients with suspected PE. Findings of this study could stimulate further similar research to develop optimal CT scanning protocols in other areas based on realistic 3D printed models.

Acknowledgements

Authors would like to thank Mr Tom Tiang from Perth Children's Hospital for his assistance in CT scanning of the pulmonary artery model. We think Mr Gil Stevenson for his assistance in the statistical analysis.

Footnote

Conflicts of Interest: The authors have no conflicts of interest to declare.

Ethical Statement: Ethical approval was waived in this study as it is based on a phantom experiment.

References

1. Albrecht MH, Bickford MW, Nance JW Jr, Zhang L, De Cecco CN, Wichmann JL, Vogl TJ, Schoepf UJ. State-of-the-Art pulmonary CT angiography for acute pulmonary embolism. AJR Am J Roentgenol 2017;208:495-504.
2. Sun Z, Lei J. Diagnostic yield of CT pulmonary angiography in the diagnosis of pulmonary embolism: a single center experience. Interv Cardiol 2017;9:191-8.
3. Chen EL, Ross JA, Grant C, Wilbur A, Mehta N, Hart E, Mar WA. Improved image quality of low-dose CT pulmonary angiograms. J Am Coll Radiol 2017;14:648-53.
4. Devaraj A, Sayer C, Sheard S, Grubnic S, Nair A, Vlahos I. Diagnosing acute pulmonary embolism with computed tomography: imaging update. J Thorac Imaging 2015;30:176-92.
5. Henzler T, Barraza JM, Nance JW, Jr, Costello P, Krissak R, Fink C, Schoepf UJ. CT imaging of acute pulmonary embolism. J Cardiovasc Comput Tomogr 2011;5:3-11.
6. Wichmann JL, Hu X, Kerl JM, Schulz B, Frellesen C, Bodelle B, Kaup M, Scholtz JE, Lehnert T, Vogl TJ, Bauer RW. 70 kVp computed tomography pulmonary angiography: potential for reduction of iodine load and radiation dose. J Thorac Imaging 2015;30:69-76.
7. Martini K, Meier A, Higashhigaito K, Saltybaeva N, Alkadhi H, Frauenfelder T. Prospective randomized comparison of high-pitch CT at 80 kVp under free breathing with standard-pitch CT at 100 kVp under breath-hold for detection of pulmonary embolism. Acad Radiol 2016;23:1335-41.
8. Lu GM, Luo S, Meinel FG, McQuiston AD, Zhou CS, Kong X, Zhao YE, Zheng L, Schoepf UJ, Zhang LJ. High-pitch computed tomography pulmonary angiography with iterative reconstruction at 80 kVp and 20 mL contrast agent volume. Eur Radiol 2014; 24:3260-8.
9. Li X, Ni QQ, Schoepf UJ, Wichmann JL, Felmly LM, Qi L, Kong X, Zhou CS, Luo S, Zhang LJ, Lu GM. 70-kVp high-pitch computed tomography pulmonary angiography with 40 mL contrast agent: initial experience. Acad Radiol 2015;22:1562-70.
10. Bolen MA, Renapurkar RD, Popovic ZB, Popovic ZB, Heresi GA, Flamm SD, Lau CT, Lau CT, Halliburton SS. High-pitch ECG synchronized pulmonary CT angiography versus standard CT pulmonary angiography: a prospective randomized study. AJR Am J Roentgenol 2013;201:971-6.
11. Sabel BO, Buric K, Karara N, Thierfelder KM, Dinkel J, Sommer WH, Meinel FG. High-pitch CT pulmonary angiography in third generation dual-source CT: image quality in an unselected patient population. PLoS ONE 2016;11:e0146949.
12. Boos J, Kropil P, Lanzman RS, Aissa J, Schleich C, Heusch P, Sawichi LM, Antoch G, Thomas C. CT pulmonary angiography: simultaneous low-pitch dual-source acquisition mode with 70 kVp and 40 ml of contrast medium and comparison with high-pitch spiral dual-source acquisition with automated tube potential selection. Br J Radiol 2016;89:20151059.
13. Bucher AM, Kerl MJ, Albrecht MH, Beeres M, Ackermann H, Wichmann JL, Vogl TJ, Bauer RW, Lehnert T. Systematic comparison of reduced tube current protocols for high-pitch and standard-pitch pulmonary CT angiography in a large single-center population. Acad Radiol 2016;23:619-27.
14. Kligerman S, Lahiji K, Weihe E, Lin CT, Terpenning S, Jeudy J, Frazier A, Pugatch R, Galvin JR, Mittal D, Kothari K, White CS. Detection of pulmonary embolism

on computed tomography: improvement using a model-based iterative reconstruction algorithm compared with filtered back projection and iterative reconstruction algorithms. J Thorac Imaging 2015;30:60-8.
15. Laqmani A, Regier M, Veldhoen S, Backhaus A, Wassenberg F, Sehner S, Groth M, Nagel HD, Adam G, Henes FO. Improved image quality and low radiation dose with hybrid iterative reconstruction with 80 kV CT pulmonary angiography. Eur J Radiol 2014;83:1962-9.
16. McLaughlin PD, Liang T, Homiedan M, Louis LJ, O'Connell TW, Krzymyk K, Nicolaou S, Mayo JR. High pitch, low voltage dual source CT pulmonary angiography: assessment of image quality and diagnostic acceptability with hybrid iterative reconstruction. Emerg Radiol 2015;22:117-23.
17. Wortman JR, Adduci AJ, Sodickson AD. Synergistic radiation dose reduction by combining automatic tube voltage selection and iterative reconstruction. J Thorac Imaging 2016;31:111-8.
18. Olivieri LJ, Krieger A, Loke YH, Nath DS, Kim PC, Sable CA. Three-dimensional printing of intracardiac defects from three-dimensional echocardiographic images: feasibility and relative accuracy. J Am Soc Echocardiogr 2015;28:392-7.
19. Cantinotti M, Valverde I, Kutty S. Three-dimensional printed models in congenital heart disease. Int J Cardiovasc Imaging 2017;33:137-44.
20. Lau IW, Liu D, Xu L, Fan Z, Sun Z. Clinical value of patient-specific three-dimensional printing of congenital heart disease: Quantitative and qualitative Assessments. PLoS One 2018;13:e0194333.
21. Liu D, Sun Z, Chaichana T, Ducke W, Fan Z. Patient-specific 3D printed models of renal tumours using home-made 3D printer in comparison with commercial 3D printer. J Med Imaging Health Inf 2018;8:303-8.
22. Sun Z, Liu D. A systematic review of clinical value of three-dimensional printing in renal disease. Quant Imaging Med Surg 2018;8:311-25.
23. Lau I, Sun Z. Three-dimensional printing in congenital heart disease: A systematic review. J Med Radiat Sci 2018;65:226-36.
24. Aldosari S, Squelch A, Sun Z. Patient-specific 3D printed pulmonary artery model: A preliminary study. Digit Med 2017;3:170-7.
25. Aldosari S, Jansen S, Sun Z. Optimization of computed tomography pulmonary angiography using 3D printed model with simulation of pulmonary embolism. Quant Imaging Med Surg 2018. [Epub ahead of print]. doi: 10.21037/qims.2018.09.15
26. McCollough CH, Primak AN, Braun N, Kofler J, Yu L, Christner J. Strategies for reducing radiation dose in CT. Radiol Clin North Am 2009;47:27-40.
27. Leithner D, Gruber-Rouh T, Beeres M, Wichmann JL, Mahmoudi S, Martin SS, Lenga L, Albrecht MH, Booz C, Vogl TJ, Scholtz JE. 90-kVp low-tube-voltage CT pulmonary angiography in combination with advanced modeled iterative reconstruction algorithm: effects on radiation dose, image quality and diagnostic accuracy for the detection of pulmonary embolism. Br J Radiol 2018;91:20180269.
28. Leithner D, Wichmann JL, Mahmoudi S, Martin SS, Albrecht MH, Vogl TJ, Scholtz JE. Diagnostic yield of 90-kVp low-tube-voltage carotid and intracerebral CT-angiography: effects on radiation dose, image quality and diagnostic performance for the detection of carotid stenosis. Br J Radiol 2018;91:20170927.
29. White SC, Sedler J, Jones TW, Seckeler M. Utility of three-dimensional models in resident education on simple and complex intracardiac congenital heart defects. Congenit Heart Dis 2018. [Epub ahead of print]. doi: 10.1111/chd.12673
30. Loke YH, Harahsheh AS, Krieger A, Olivieri LJ. Usage of 3D models of tetralogy of Fallot for medical education: impact on learning congenital heart disease. BMC Med Educ 2017;17:54.
31. Abdullah KA, McEntee MF, Reed W, Kench PL. Development of an organ-specific insert phantom generated using a 3D printer for investigations of cardiac computed tomography protocols. J Med Radiat Sci 2018;65:175-83.

Cite this article as: Aldosari S, Jansen S, Sun Z. Patient-specific 3D printed pulmonary artery model with simulation of peripheral pulmonary embolism for developing optimal computed tomography pulmonary angiography protocols. Quant Imaging Med Surg 2018. doi: 10.21037/qims.2018.10.13

A.2 Permission to reproduce published (Copyright forms)

AME Publishing Company LICENSE TERMS AND CONDITIONS

Dec 03, 2018

This is a License Agreement between sultan Ae aldosari ("You") and AME Publishing Company ("AME Publishing Company") provided by Copyright Clearance Center ("CCC"). The license consists of your order details, the terms and conditions provided by AME Publishing Company, and the payment terms and conditions.

All payments must be made in full to CCC. For payment instructions, please see information listed at the bottom of this form.

License Number	4481381237245
License date	Dec 03, 2018
Licensed content publisher	AME Publishing Company
Licensed content title	Quantitative imaging in medicine and surgery
Licensed content date	Jan 1, 2011
Type of Use	Thesis/Dissertation
Requestor type	Academic institution
Format	Print, Electronic
Portion	chart/graph/table/figure
Number of charts/graphs/tables/figures	9
The requesting person/organization is:	Sultan Rashed
Title or numeric reference of the portion(s)	Figures 1,2,3,4,5,6,7,8 table 1
Title of the article or chapter the portion is from	article Patient-specific 3D printed pulmonary artery model with simulation of peripheral pulmonary embolism for developing optimal computed tomography pulmonary angiography protocols
Editor of portion(s)	n/a
Author of portion(s)	Aldosari S, Jansen S, Sun Z
Volume of serial or monograph.	n/a
Issue, if republishing an article from a serial	n/a
Page range of the portion	3-9
Publication date of portion	2018
Rights for	Main product
Duration of use	Life of current edition
Creation of copies for the disabled	no
With minor editing privileges	no
For distribution to	Worldwide
In the following language(s)	Original language of publication

With incidental promotional use	no
The lifetime unit quantity of new product	Up to 499
Title	Diagnostic Value of Multi-Slice CT Pulmonary Angiography in the Diagnosis of Pulmonary Embolism: An Investigation of Optimal Scanning Protocols in Terms of Image Quality, Contrast and Radiation Doses
Institution name	Curtin University
Expected presentation date	Dec 2018
Order reference number	cao2722
Billing Type	Invoice
Billing Address	sultan Ae aldosari 71 a mackie st vic park perth WA australia Perth, Australia Attn: sultan Ae aldosari
Total (may include CCC user fee)	0.00 USD

Terms and Conditions

TERMS AND CONDITIONS

The following terms are individual to this publisher:

It is the responsibility of the users' to identify the copyright holder of any materials. If the user has any doubts, please contact the publisher at permissions@amegrouops.com. For illustrations owned by Ms. Croce, please contact beth@bioperspective.com.

Other Terms and Conditions:

STANDARD TERMS AND CONDITIONS

1. Description of Service; Defined Terms. This Republication License enables the User to obtain licenses for republication of one or more copyrighted works as described in detail on the relevant Order Confirmation (the "Work(s)"). Copyright Clearance Center, Inc. ("CCC") grants licenses through the Service on behalf of the rightsholder identified on the Order Confirmation (the "Rightsholder"). "Republication", as used herein, generally means the inclusion of a Work, in whole or in part, in a new work or works, also as described on the Order Confirmation. "User", as used herein, means the person or entity making such republication.

2. The terms set forth in the relevant Order Confirmation, and any terms set by the Rightsholder with respect to a particular Work, govern the terms of use of Works in connection with the Service. By using the Service, the person transacting for a republication license on behalf of the User represents and warrants that he/she/it (a) has been duly authorized by the User to accept, and hereby does accept, all such terms and conditions on behalf of User, and (b) shall inform User of all such terms and conditions. In the event such person is a "freelancer" or other third party independent of User and CCC, such party shall be deemed jointly a "User" for purposes of these terms and conditions. In any event, User shall be deemed to have accepted and agreed to all such terms and conditions if User republishes the Work in any fashion.

3. Scope of License; Limitations and Obligations.

3.1 All Works and all rights therein, including copyright rights, remain the sole and exclusive property of the Rightsholder. The license created by the exchange of an Order Confirmation (and/or any invoice) and payment by User of the full amount set forth on that document includes only those rights expressly set forth in the Order Confirmation and in

these terms and conditions, and conveys no other rights in the Work(s) to User. All rights not expressly granted are hereby reserved.

3.2 General Payment Terms: You may pay by credit card or through an account with us payable at the end of the month. If you and we agree that you may establish a standing account with CCC, then the following terms apply: Remit Payment to: Copyright Clearance Center, 29118 Network Place, Chicago, IL 60673-1291. Payments Due: Invoices are payable upon their delivery to you (or upon our notice to you that they are available to you for downloading). After 30 days, outstanding amounts will be subject to a service charge of 1-1/2% per month or, if less, the maximum rate allowed by applicable law. Unless otherwise specifically set forth in the Order Confirmation or in a separate written agreement signed by CCC, invoices are due and payable on "net 30" terms. While User may exercise the rights licensed immediately upon issuance of the Order Confirmation, the license is automatically revoked and is null and void, as if it had never been issued, if complete payment for the license is not received on a timely basis either from User directly or through a payment agent, such as a credit card company.

3.3 Unless otherwise provided in the Order Confirmation, any grant of rights to User (i) is "one-time" (including the editions and product family specified in the license), (ii) is non-exclusive and non-transferable and (iii) is subject to any and all limitations and restrictions (such as, but not limited to, limitations on duration of use or circulation) included in the Order Confirmation or invoice and/or in these terms and conditions. Upon completion of the licensed use, User shall either secure a new permission for further use of the Work(s) or immediately cease any new use of the Work(s) and shall render inaccessible (such as by deleting or by removing or severing links or other locators) any further copies of the Work (except for copies printed on paper in accordance with this license and still in User's stock at the end of such period).

3.4 In the event that the material for which a republication license is sought includes third party materials (such as photographs, illustrations, graphs, inserts and similar materials) which are identified in such material as having been used by permission, User is responsible for identifying, and seeking separate licenses (under this Service or otherwise) for, any of such third party materials; without a separate license, such third party materials may not be used.

3.5 Use of proper copyright notice for a Work is required as a condition of any license granted under the Service. Unless otherwise provided in the Order Confirmation, a proper copyright notice will read substantially as follows: "Republished with permission of [Rightsholder's name], from [Work's title, author, volume, edition number and year of copyright]; permission conveyed through Copyright Clearance Center, Inc. " Such notice must be provided in a reasonably legible font size and must be placed either immediately adjacent to the Work as used (for example, as part of a by-line or footnote but not as a separate electronic link) or in the place where substantially all other credits or notices for the new work containing the republished Work are located. Failure to include the required notice results in loss to the Rightsholder and CCC, and the User shall be liable to pay liquidated damages for each such failure equal to twice the use fee specified in the Order Confirmation, in addition to the use fee itself and any other fees and charges specified.

3.6 User may only make alterations to the Work if and as expressly set forth in the Order Confirmation. No Work may be used in any way that is defamatory, violates the rights of third parties (including such third parties' rights of copyright, privacy, publicity, or other tangible or intangible property), or is otherwise illegal, sexually explicit or obscene. In addition, User may not conjoin a Work with any other material that may result in damage to the reputation of the Rightsholder. User agrees to inform CCC if it becomes aware of any infringement of any rights in a Work and to cooperate with any reasonable request of CCC or the Rightsholder in connection therewith.

4. Indemnity. User hereby indemnifies and agrees to defend the Rightsholder and CCC, and their respective employees and directors, against all claims, liability, damages, costs and expenses, including legal fees and expenses, arising out of any use of a Work beyond the

scope of the rights granted herein, or any use of a Work which has been altered in any unauthorized way by User, including claims of defamation or infringement of rights of copyright, publicity, privacy or other tangible or intangible property.

5. Limitation of Liability. UNDER NO CIRCUMSTANCES WILL CCC OR THE RIGHTSHOLDER BE LIABLE FOR ANY DIRECT, INDIRECT, CONSEQUENTIAL OR INCIDENTAL DAMAGES (INCLUDING WITHOUT LIMITATION DAMAGES FOR LOSS OF BUSINESS PROFITS OR INFORMATION, OR FOR BUSINESS INTERRUPTION) ARISING OUT OF THE USE OR INABILITY TO USE A WORK, EVEN IF ONE OF THEM HAS BEEN ADVISED OF THE POSSIBILITY OF SUCH DAMAGES. In any event, the total liability of the Rightsholder and CCC (including their respective employees and directors) shall not exceed the total amount actually paid by User for this license. User assumes full liability for the actions and omissions of its principals, employees, agents, affiliates, successors and assigns.

6. Limited Warranties. THE WORK(S) AND RIGHT(S) ARE PROVIDED "AS IS". CCC HAS THE RIGHT TO GRANT TO USER THE RIGHTS GRANTED IN THE ORDER CONFIRMATION DOCUMENT. CCC AND THE RIGHTSHOLDER DISCLAIM ALL OTHER WARRANTIES RELATING TO THE WORK(S) AND RIGHT(S), EITHER EXPRESS OR IMPLIED, INCLUDING WITHOUT LIMITATION IMPLIED WARRANTIES OF MERCHANTABILITY OR FITNESS FOR A PARTICULAR PURPOSE. ADDITIONAL RIGHTS MAY BE REQUIRED TO USE ILLUSTRATIONS, GRAPHS, PHOTOGRAPHS, ABSTRACTS, INSERTS OR OTHER PORTIONS OF THE WORK (AS OPPOSED TO THE ENTIRE WORK) IN A MANNER CONTEMPLATED BY USER; USER UNDERSTANDS AND AGREES THAT NEITHER CCC NOR THE RIGHTSHOLDER MAY HAVE SUCH ADDITIONAL RIGHTS TO GRANT.

7. Effect of Breach. Any failure by User to pay any amount when due, or any use by User of a Work beyond the scope of the license set forth in the Order Confirmation and/or these terms and conditions, shall be a material breach of the license created by the Order Confirmation and these terms and conditions. Any breach not cured within 30 days of written notice thereof shall result in immediate termination of such license without further notice. Any unauthorized (but licensable) use of a Work that is terminated immediately upon notice thereof may be liquidated by payment of the Rightsholder's ordinary license price therefor; any unauthorized (and unlicensable) use that is not terminated immediately for any reason (including, for example, because materials containing the Work cannot reasonably be recalled) will be subject to all remedies available at law or in equity, but in no event to a payment of less than three times the Rightsholder's ordinary license price for the most closely analogous licensable use plus Rightsholder's and/or CCC's costs and expenses incurred in collecting such payment.

8. **Miscellaneous.**

8.1 User acknowledges that CCC may, from time to time, make changes or additions to the Service or to these terms and conditions, and CCC reserves the right to send notice to the User by electronic mail or otherwise for the purposes of notifying User of such changes or additions; provided that any such changes or additions shall not apply to permissions already secured and paid for.

8.2 Use of User-related information collected through the Service is governed by CCC's privacy policy, available online here:
http://www.copyright.com/content/cc3/en/tools/footer/privacypolicy.html.

8.3 The licensing transaction described in the Order Confirmation is personal to User. Therefore, User may not assign or transfer to any other person (whether a natural person or an organization of any kind) the license created by the Order Confirmation and these terms and conditions or any rights granted hereunder; provided, however, that User may assign such license in its entirety on written notice to CCC in the event of a transfer of all or substantially all of User's rights in the new material which includes the Work(s) licensed under this Service.

8.4 No amendment or waiver of any terms is binding unless set forth in writing and signed by the parties. The Rightsholder and CCC hereby object to any terms contained in any writing prepared by the User or its principals, employees, agents or affiliates and purporting to govern or otherwise relate to the licensing transaction described in the Order Confirmation, which terms are in any way inconsistent with any terms set forth in the Order Confirmation and/or in these terms and conditions or CCC's standard operating procedures, whether such writing is prepared prior to, simultaneously with or subsequent to the Order Confirmation, and whether such writing appears on a copy of the Order Confirmation or in a separate instrument.

8.5 The licensing transaction described in the Order Confirmation document shall be governed by and construed under the law of the State of New York, USA, without regard to the principles thereof of conflicts of law. Any case, controversy, suit, action, or proceeding arising out of, in connection with, or related to such licensing transaction shall be brought, at CCC's sole discretion, in any federal or state court located in the County of New York, State of New York, USA, or in any federal or state court whose geographical jurisdiction covers the location of the Rightsholder set forth in the Order Confirmation. The parties expressly submit to the personal jurisdiction and venue of each such federal or state court.If you have any comments or questions about the Service or Copyright Clearance Center, please contact us at 978-750-8400 or send an e-mail to info@copyright.com.

v 1.1

Questions? customercare@copyright.com or +1-855-239-3415 (toll free in the US) or +1-978-646-2777.

Appendix III: Statements of contributions of others

Statement of Contribution of Others to (Patient-specific three-dimensional printed pulmonary artery model: A preliminary study).

Aldosari S, Squelch A, Sun Z. Patient-specific three-dimensional printed pulmonary artery model: A preliminary study. Digital Med 2017;3(4):170-7.

To Whom It May Concern

I, Sultan Al-Dosari contributed (I designed the study and conducted image postprocessing and segmentation of the CT imaging data; I performed measurements of dimensional accuracy of anatomical structures and image quality, and finally I wrote the manuscript) to the paper (Patient-specific three-dimensional printed pulmonary artery model: A preliminary study).

Sultan Al-Dosari

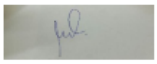

I, as a Co-Author, endorse that this level of contribution by the candidate indicated above is appropriate.

Squelch Andrew (Signature of Co-Author 1)

Zhonghua Sun (Signature of Co-Author 2)

ORIGINAL ARTICLE

Patient-specific three-dimensional printed pulmonary artery model: A preliminary study

Sultan Aldosari[1], Andrew Squelch[2,3], Zhonghua Sun[1]*

[1]Department of Medical Radiation Sciences, Curtin University, [2]Department of Exploration Geophysics, Western Australian School of Mines, Curtin University, [3]Curtin Institute for Computation, Curtin University, Perth, Western Australia, Australia

ABSTRACT

Background and Objectives: Three-dimensional (3D) printing has potential value in medical applications with increasing reports in the diagnostic assessment of cardiovascular diseases. The use of 3D printing in replicating pulmonary artery anatomy and diagnosing pulmonary embolism is very limited. The purpose of this study was to develop a 3D printed pulmonary artery model and test different computed tomography (CT) scanning protocols for determination of an optimal protocol with acceptable image quality but low radiation dose. **Materials and Methods:** A patient-specific 3D printed pulmonary artery model was created based on contrast-enhanced CT images in a patient with suspected pulmonary embolism. Different CT pulmonary angiography protocols consisting of 80, 100, and 120 kVp, pitch 0.7, 0.9, and 1.2 with 1 mm slice thickness, and 0.6 mm reconstruction interval were tested on the phantom. Quantitative assessment of image quality in terms of signal-to-noise ratio (SNR) was measured in the images acquired with different protocols. Measurements in pulmonary artery diameters were conducted and compared between pre- and post-3D printed images and 3D printed model. **Results:** The 3D printed model was found to replicate normal pulmonary artery with high accuracy. The mean difference in diameter measurements was <0.8 mm (<0.5% deviation in diameter). There was no significant difference in SNR measured between these CT protocols (P = 0.96–0.99). Radiation dose was reduced by 55% and 75% when lowering kVp from 120 to 100 and 80 kVp, without affecting image quality. **Conclusions:** It is feasible to produce a 3D printed pulmonary artery model with high accuracy in replicating normal anatomy. Different CT scanning protocols are successfully tested on the model with 80 kVp and pitch 0.9 being the optimal one with resultant diagnostic images but at much lower radiation dose.

Keywords: Diagnosis, image quality, model, pulmonary artery, three-dimensional printing

INTRODUCTION

Three-dimensional (3D) printing is a rapidly developing technique showing increasing interest and great potential in medicine.[1-5] The diagnostic application of using patient-specific 3D printed models has been reported in the diagnostic assessment of cardiovascular disease, presurgical planning and simulation, as well as medical education.[6-13] These studies created 3D printed realistic models using either computed tomography (CT) or magnetic resonance imaging or echocardiography data with accurate replication of anatomical structures and pathological changes. A recent systematic review of 48 studies has demonstrated the usefulness of 3D printed models in replicating complex cardiovascular anatomy with high accuracy, serving as a valuable tool for presurgical planning and simulation of cardiovascular disease and medical education to healthcare professionals and medical students.[14]

*Address for correspondence:
Prof. Zhonghua Sun, Department of Medical Radiation Sciences, Curtin University, GPO Box U1987, Perth, Western Australia 6845, Australia.
E-mail: z.sun@curtin.edu.au

Access this article online

Quick Response Code

Website: www.digitmedicine.com

DOI: 10.4103/digm.digm_42_17

How to cite this article: Aldosari S, Squelch A, Sun Z. Patient-specific three-dimensional printed pulmonary artery model: A preliminary study. Digit Med 2017;3:170-7.

To the best of our knowledge, very few research studies have been conducted in the diagnostic assessment of 3D printed models in pulmonary artery diseases.[15] CT pulmonary angiography (CTPA) is the preferred imaging modality in the diagnosis of pulmonary embolism.[16-20] Although CTPA has high diagnostic value in detecting pulmonary embolism, it has disadvantages of the associated high radiation dose. Further, administration of contrast medium during CTPA represents another limitation with a potential risk of contrast-induced nephropathy.[21,22] Therefore, reduction of both radiation and contrast medium doses during CTPA is the current research direction with promising results achieved.

According to these studies, there is still potential for further lowering of the radiation and contrast medium doses during CTPA. To test the feasibility of different protocols, a realistic anatomic phantom is an ideal option, and a 3D printed model serves this purpose. Thus, the primary aim of this study was to use a patient-specific 3D printed pulmonary artery model to test different CTPA protocols with the aim of identifying optimal CTPA protocol. Further, potential factors including image segmentation, editing, and 3D printing processes could affect the dimensional accuracy of 3D printed models.[23,24] Witowski *et al.* in their recent systematic review indicate the lack of quantitative methods to validate liver model accuracy.[25] Similarly, no studies have reported the quantitative assessment of 3D printed pulmonary model accuracy. Therefore, the secondary aim of this study was to quantitatively assess the model accuracy of 3D printed pulmonary artery model in delineating anatomical structures.

MATERIALS AND METHODS

Sample image selection

CTPA images from a 53-year-old female with suspected pulmonary embolism were selected in this study to generate 3D reconstructed pulmonary artery model for 3D printing. CTPA showed normal pulmonary artery without any sign of pulmonary embolism. The CT scan was performed on a 128-slice scanner (Siemens Definition Flash, Siemens Healthcare, Forchheim, Germany) with slice thickness of 1.0 mm and reconstruction interval of 0.6 mm.

Image postprocessing and segmentation for three-dimensional printing

Original digital imaging and communications in medicine (DICOM) of CTPA images was transferred to a separate workstation equipped with analyze 12.0 (AnalyzeDirect, Inc., Lexana, KS, USA) for image processing and segmentation. Semiautomatic approach was used to perform image postprocessing and segmentation of 3D volume data. A CT number thresholding technique was first used to produce 3D volume rendering images with inclusion of the pulmonary trunk, left main, and right main pulmonary arteries. In brief, CT attenuation in the pulmonary arteries was measured (around 150 Hounsfield unit [HU]) and applied as the lowest threshold to demonstrate only contrast-enhanced pulmonary arteries and cardiac chambers, while soft tissue, pulmonary veins, and other structures with CT attenuation <150 HU were removed as the focus of this study was pulmonary arteries. Bony structures and cardiac chambers have high CT attenuation (>300 HU); thus, removal of these structures was conducted by the function of object separator that is available with analyze 12.0. Some manual editing was applied to ensure the accuracy of 3D model in the delineation of pulmonary arterial tree. This involved further removal of some structures that were still included in the 3D volume data such as overlapping tissues and presence of artifacts and applying a median filter to remove some image noise for better definition of pulmonary arteries with side branches. The generated model of the segmented pulmonary arteries was subsequently exported to the standard tessellation language (STL) file format which is commonly used for 3D printing. Figure 1 shows the steps of image postprocessing and segmentation from original 2D DICOM images to generation of segmented volume data and STL file to the final step of 3D printed model.

The STL file of 3D segmented pulmonary artery was uploaded to Shapeways, an online 3D printing service.[26] The model was printed in "elastoplastic" material, which has material property closest to that of arterial wall.[27]

Computed tomography pulmonary angiography scanning protocols for three-dimensional printed model

To determine the accuracy of the 3D printed model in replicating anatomical structures, a series of CTPA scans were conducted on the 3D printed pulmonary artery model with different scanning protocols. A total of nine scans were performed, in which three tube voltages of 80, 100, and 120 kVp and three pitch values of 0.7, 0.9, and 1.2 were tested. The 3D printed model was placed in a plastic box filled with a contrast medium (Omnipaque 370) [Figure 2], and scans were performed on a 64-slice CT scanner (Siemens Definition AS, Siemens Healthcare, Forchheim, Germany) with slice thickness

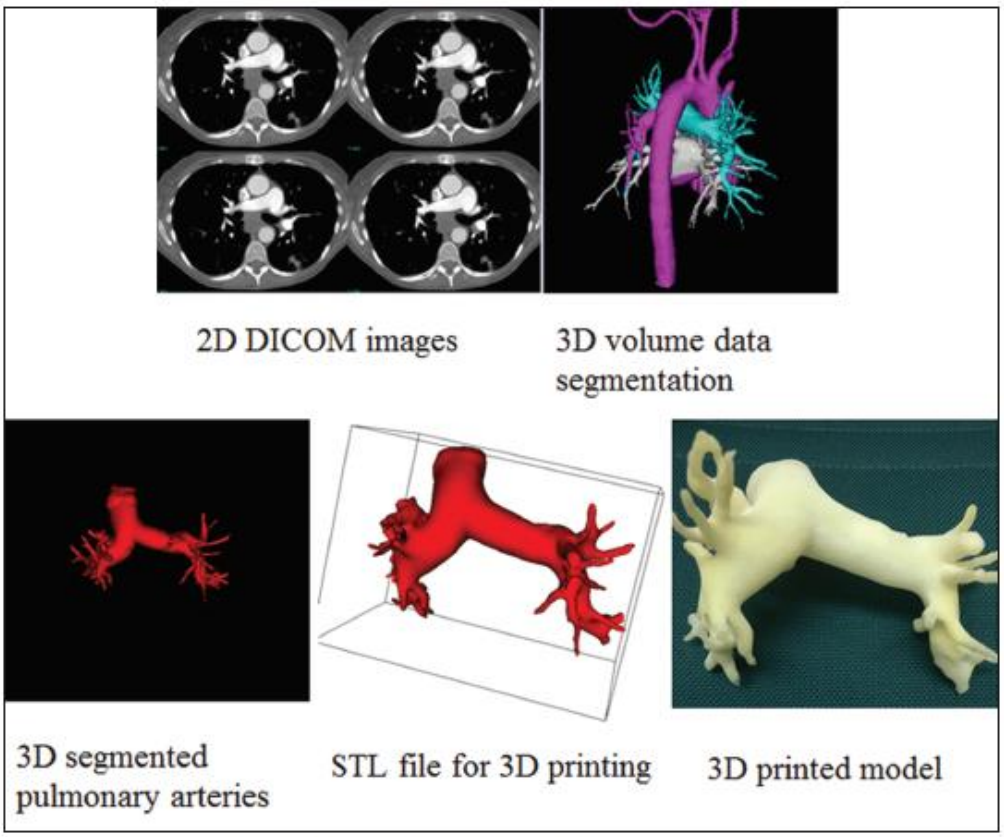

Figure 1: Flow diagram shows the image postprocessing and segmentation steps from two-dimensional computed tomography images to creation of three-dimensional printed model. Original two-dimensional digital imaging and communications in medicine images were used to create three-dimensional volume-rendering image with use of computed tomography number thresholding technique to display contrast-enhanced vessels (blue color - pulmonary arteries, pink color - aorta and its branches, white color - left atrium and pulmonary veins). Three-dimensional volume rendering of pulmonary artery tree is segmented through semiautomatic segmentation and manual editing. Standard tessellation language file of three-dimensional segmented volume data was generated for three-dimensional printing of patient-specific three-dimensional printed model

of 1.0 mm and reconstruction interval of 0.6 mm. The contrast medium was diluted to 6% resulting in CT attenuation of 150 HU which is similar to that of clinical CTPA examination. DICOM images of the scanned model were transferred to a workstation for measurements of pulmonary artery diameters and image quality.

Measurements of pulmonary artery diameters

Diameter measurements at the pulmonary trunk, right, and left main pulmonary arteries were performed on original CTPA images, STL file, 3D printed model, and post-3D printing scanned CT images. Measurements were performed by two observers with >10 years of experience in CT imaging, with each measurement repeated three times. The two observers performed measurements separately, and the results showed a very high correlation between these two observers ($r = 0.99–1.0$, $P < 0.001$). Figure 3 shows an example of measuring the pulmonary trunk using an electronic caliper.

Quantitative measurements of image quality

Image quality was assessed by measuring the image noise, which is defined as standard deviation (SD) of CT attenuation (HU) in the pulmonary arteries. A circular region of interest (ROI) with a diameter of 50 mm^2 (containing 300 voxels within the ROI) was placed at the pulmonary trunk, left main, and right

Figure 2: Three-dimensional printed pulmonary model is placed in a plastic box which is used to be filled with contrast medium for computed tomography scans

Figure 3: Measurement of the diameter of pulmonary trunk using an electronic caliper

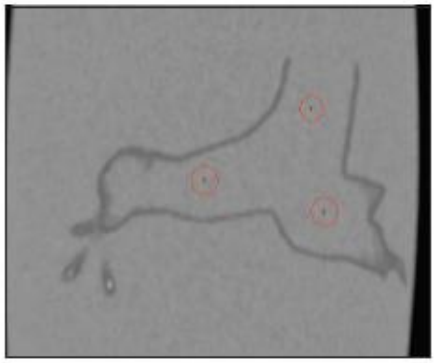

Figure 4: Region of interest is placed at the pulmonary trunk, right, and left main pulmonary arteries for measurement of image quality

main pulmonary arteries to measure the signal-to-noise ratio (SNR) which is defined as:

SNR = CT attenuation in the pulmonary artery/SD

Figure 4 is an example showing measurement of image quality (SNR) at the pulmonary trunk, left main, and right main pulmonary arteries. Contrast-to-noise ratio was not measured in this study due to lack of background tissue since 3D printed model was immersed into the contrast medium. The two observers performed measurements separately, and the results showed a high correlation between these two observers ($r = 0.99–1.0$, $P < 0.05$).

Radiation dose

Radiation dose values in terms of volume CT dose index (CTDIvol) and dose length product (DLP) were available on the CT console. Effective dose (ED) was calculated by multiplying the DLP by a tissue coefficient factor, which is 0.014 mSv/mGy/cm for chest CT scan.[28]

Statistical analysis

Data were entered into MS Excel for analysis. Continuous variables were presented as mean ± SD. A two-sided Student's *t*-test was used to determine any significant differences between measurements performed at original CT, STL, 3D printed model, and post-3D printing scanned images, with $P < 0.05$ indicating statistical significance.

RESULTS

CT scans of the 3D printed pulmonary artery model were successfully performed. Table 1 shows measurements of the main pulmonary arteries made with different scanning protocols when compared to the original CTPA images with differences <0.8 mm, indicating high accuracy of 3D printed model in replicating anatomical structures. There was also very good correlation between measurements on STL file in comparison to those on original CT images, post-3D printed CT images, and 3D printed model, with the mean difference <0.5 mm as shown in Table 2.

Table 3 shows SNR measurements at different CTPA protocols with corresponding radiation dose values. With 80 and 100 kVp protocols, SNR was slightly decreased when the pitch was increased from 0.7 to 0.9 and 1.2 although this did not reach significant difference in measurements with these protocols ($P = 0.96–0.99$). With 120 kVp protocol, SNR was slightly increased with the increase of pitch in most of the measurements, with no statistical significance difference noted ($P = 0.97–0.99$).

Table 3 also shows radiation dose values associated with these CTPA protocols. As shown in Table 3, CTDIvol

Table 1: Diameters of pulmonary arteries measured on computed tomography scanned three-dimensional printed model

Measurement locations	80 kVp protocol (mean mm)			100 kVp protocol (mean mm)			120 kVp protocol (mean mm)		
	Pitch 0.7	Pitch 0.9	Pitch 1.2	Pitch 0.7	Pitch 0.9	Pitch 1.2	Pitch 0.7	Pitch 0.9	Pitch 1.2
Pulmonary trunk	25.44	25.97	25.59	25.77	25.13	25.1	25.97	25.86	25.94
LMPA	26.57	26.11	26.88	26.25	26.72	26.31	26.22	26.79	26.86
RMPA	21.77	21.88	21.45	21.66	21.07	21.41	21.23	21.23	21.45

LMPA: Left main pulmonary artery, RMPA: Right main pulmonary artery

Table 2: Diameters of pulmonary arteries measured on original CT images, STL images and 3D printed model

Measurements on datasets	Pulmonary trunk (mean mm)	Left main pulmonary artery (mean mm)	Right main pulmonary artery (mean mm)
Original CT images	25.93	26.20	21.63
STL images	25.98	26.03	21.90
3D printed model	25.85	26.02	21.84

3D: Three-dimensional, CT: Computed tomography, STL: Standard tessellation language

Table 3: Quantitative measurement of image quality and radiation dose in different computed tomography scanning protocols

Measurement locations	80 kVp protocol			100 kVp protocol			120 kVp protocol		
	Pitch 0.7	Pitch 0.9	Pitch 1.2	Pitch 0.7	Pitch 0.9	Pitch 1.2	Pitch 0.7	Pitch 0.9	Pitch 1.2
SNR at pulmonary trunk	13.28	12.79	11.41	20.29	14.68	13.36	17.18	19.46	18.99
SNR at left main pulmonary artery	13.44	12.16	10.59	14.81	14.73	10.97	14.18	16.28	16.27
SNR at right main pulmonary artery	10.25	10.84	10.08	15.11	10.97	11.19	15.21	17.35	15.72
CTDIvol (mGy)	5.81	5.73	5.62	12.96	12.84	12.64	23.12	22.90	22.61
DLP (mGy/cm)	128	128	128	286	286	286	510	511	514
ED (mSv)	1.79	1.79	1.79	4.04	4.04	4.04	7.14	7.15	7.19

SNR: Signal-to-noise ratio, DLP: Dose-length product, ED: Effective dose, CTDIvol: Volume CT dose index

and DLP remained almost the same despite the use of different pitch values, mainly due to the use of tube current modulation. With 80 kVp as the selected protocol, the ED was reduced by 55% and 75% when kVp was lowered from 100 and 120 kVp to 80 kVp, respectively, while still maintaining diagnostic image quality. Figure 5 shows coronal reformatted CT images acquired with 9 different protocols with good visualization of the pulmonary trunk and left and right main pulmonary arteries.

DISCUSSION

This preliminary study has two main findings: first, 3D printed pulmonary artery model has high accuracy in replicating anatomical structures; thus, it can be used as a reliable tool for testing CT scans. Second, an optimal CTPA protocol can be developed through testing different scanning protocols on the 3D printed model, with a protocol of 80 kVp and pitch 0.9 being the optimal one with resultant low radiation dose but maintaining diagnostic image quality.

3D printed models have been shown to enhance understanding of the complexity of cardiovascular disease by demonstrating the accuracy of delineating anatomical structures and pathologies, preoperative planning and simulation, and medical education.[6-15] Case reports and case series studies have proved successful applications of 3D printed models in assisting diagnosis and clinical management of congenital heart diseases including pulmonary artery abnormalities.[29-35] A recent case report discussing the 3D printed model of ventricular septal defect (VSD) and pulmonary atresia showed that 3D printing assisted the development of preoperative planning and treatment approach for managing this complex case.[30] Sahayaraj *et al.* further confirmed the clinical value of using 3D printed model in managing complex cardiovascular cases involving great vessels.[31] The 3D printed model was found to have great value in improving understanding of the spatial relationship between cardiac chambers, VSD, and great arteries, with biventricular physiologic repair successfully performed owing to the increased spatial perception provided by the 3D printed model.

Biglino *et al.* provided an insight into the clinical applications of 3D printed heart model based on the

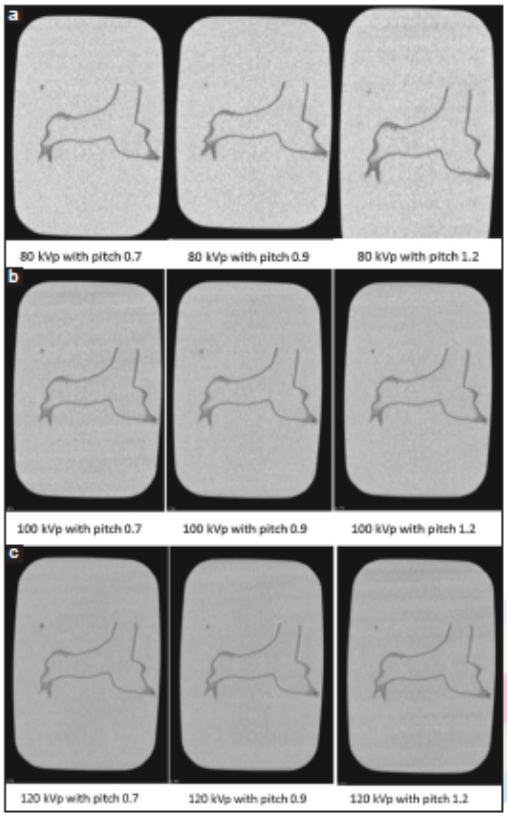

Figure 5: Computed tomography pulmonary angiography scanning protocols in the three-dimensional printed model. Two-dimensional coronal reformatted images showing main pulmonary trunk, right, and left main pulmonary arteries with 80 kVp, pitch 0.7, 0.9, and 1.2 (a), 100 kVp, pitch 0.7, 0.9 ,and 1.2 (b), 120 kVp, pitch 0.7, 0.9, and 1.2 (c)

perspective from different stakeholders.[29] The 3D printed model was considered by surgeon and cardiologist to improve understanding of the 3D relationship of different structures, such as better demonstrating the narrowed pulmonary artery and the dilated ascending aorta. Medical imaging specialist considered that 3D printed model improved communication in multidisciplinary meetings, thus allowing better decision-making in patient treatment. Further, a medical student indicated the great potential of 3D printed models in teaching anatomy and pathology.[29]

Despite promising results about the clinical value of 3D printed models, reports on the dimensional accuracy of 3D printed pulmonary artery model are scarce. Most of the current studies focus on the accuracy of 3D printed heart models, in particular, congenital heart disease with good correlation between 3D printed models and original source images.[5-9] However, in their recent study, Ho *et al.* reported the mean difference of >1.0 mm in aortic vessel diameters between contrast-enhanced CT images before and after 3D printing.[34] The variance in dimensional accuracy was also demonstrated by Lan *et al.* who showed that the mean diameter difference between 3D printed model of brain tumor and original images being 0.98%, which exceeds the recommended 0.5% deviation.[35] Findings in this study showed high accuracy of the 3D printed pulmonary artery model with the mean difference <0.5% deviation in measurements between pre- and post-3D printing images. Thus, results of CT scans based on the 3D printed model could be used as a reliable source for determining optimal scanning protocols in terms of acquiring diagnostic images with radiation dose reduction.

Increased use of CTPA in clinical practice has raised concerns because of its associated high radiation exposure and potential risk of contrast-induced nephropathy.[16,20] Therefore, optimization of CTPA protocol is a hot topic in the current literature with successful reductions in both radiation dose and contrast medium dose achieved. Findings of this study are in line with these previous reports on patient's data.[16-20] Low tube voltage and low pitch value such as 80 kVp and 0.9 are preferred with acquisition of acceptable diagnostic images (similar SNR values) but low radiation dose when compared to the protocol of 100 or 120 kVp and high pitch value. The current multislice CT scanners are equipped with latest dose-reduction protocols, such as automatic tube current or tube potential modulation; therefore, high pitch is not recommended. The pitch of 0.9 as recommended by this study is consistent with Boos *et al.* who also proposed the 70 kVp and pitch of 0.9 CTPA protocol.[36] We did not include 70 kVp in this study as 100 or 120 kVp is commonly used in CTPA. Further, due to 3D printed model being static instead of having hemodynamic flow features, we did not assess the effect of changing contrast medium volume on image quality. This could be addressed in further studies.

Despite promising results, this study has several limitations which need to be acknowledged. First, the 3D printed model was based on a normal case without showing any sign of pulmonary embolism. Thus, no subjective assessment of image quality was conducted. Experiments on the optimal CTPA protocols in the detection of pulmonary embolism with use of 3D

printed model are under investigation. Second, although the 3D printed model was made with elastic material, it still does not represent the real tissue properties of vascular wall. Further, the phantom was scanned in a static condition instead of representing realistic CTPA with blood circulating to the pulmonary arteries. Finally, due to including only one case, we did not perform Bland–Altman assessment of degree of agreement in measurements between pre- and post-3D printing images. Further studies should include more cases for generating 3D printed models, which would allow for more reliable detection of trends in bias.

CONCLUSIONS

We have shown the feasibility of generating patient-specific 3D printed pulmonary artery model with high accuracy in replicating normal anatomical structures. The 3D printed model is used to test different CTPA protocols with the protocol of 80 kVp, pitch 0.9 with 1 mm slice thickness, and reconstruction interval of 0.6 mm being the optimal one. Future research based on simulation of pulmonary embolism with different CT scanning parameters is needed to determine the clinical value of 3D printed model in the detection of pulmonary embolism with lower radiation dose while still maintaining diagnostic image quality.

Acknowledgments

This work was supported by The Pawsey Supercomputing Centre through the use of advanced visualization resources located at The Australian Resources Research Centre with funding from the Australian Government and the Government of Western Australia. The authors would also like to acknowledge the assistance of Dr. Lionel Esteban, Manager, NGL medical XCT facility, CSIRO, oil, gas and fuels program in the acquisition of the CT scans of the pulmonary artery model.

Financial support and sponsorship

Nil.

Conflicts of interest

There are no conflicts of interest.

REFERENCES

1. Valverde I, Gomez G, Gonzalez A, Suarez-Mejias C, Adsuar A, Coserria JF, *et al.* Three-dimensional patient-specific cardiac model for surgical planning in Nikaidoh procedure. Cardiol Young 2015;25:698-704.
2. Ebert J, Ozkol E, Zeichner A, Uibel K, Weiss O, Koops U, *et al.* Direct inkjet printing of dental prostheses made of zirconia. J Dent Res 2009;88:673-6.
3. Ploch CC, Mansi CS, Jayamohan J, Kuhl E. Using 3D printing to create personalized brain models for neurosurgical training and preoperative planning. World Neurosurg 2016;90:668-74.
4. Martelli N, Serrano C, van den Brink H, Pineau J, Prognon P, Borget I, *et al.* Advantages and disadvantages of 3-dimensional printing in surgery: A systematic review. Surgery 2016;159:1485-500.
5. Bartel T, Rivard A, Jimenez A, Mestres CA, Müller S. Medical three-dimensional printing opens up new opportunities in cardiology and cardiac surgery. Eur Heart J 2017;Feb 16. doi: 10.1093/eurheartj/ehx016. [Epub ahead of print].
6. Schmauss D, Haeberle S, Hagl C, Sodian R. Three-dimensional printing in cardiac surgery and interventional cardiology: A single-centre experience. Eur J Cardiothorac Surg 2015;47:1044-52.
7. Biglino G, Koniordou D, Gasparini M, Capelli C, Leaver LK, Khambadkone S, *et al.* Piloting the use of patient-specific cardiac models as a novel tool to facilitate communication during cinical consultations. Pediatr Cardiol 2017;38:813-8.
8. Cantinotti M, Valverde I, Kutty S. Three-dimensional printed models in congenital heart disease. Int J Cardiovasc Imaging 2017;33:137-44.
9. Giannopoulos AA, Mitsouras D, Yoo SJ, Liu PP, Chatzizisis YS, Rybicki FJ, *et al.* Applications of 3D printing in cardiovascular diseases. Nat Rev Cardiol 2016;13:701-18.
10. Bhatla P, Tretter JT, Chikkabyrappa S, Chakravarti S, Mosca RS. Surgical planning for a complex double-outlet right ventricle using 3D printing. Echocardiography 2017;34:802-4.
11. Lim KH, Loo ZY, Goldie SJ, Adams JW, McMenamin PG. Use of 3D printed models in medical education: A randomized control trial comparing 3D prints versus cadaveric materials for learning external cardiac anatomy. Anat Sci Educ 2016;9:213-21.
12. Costello JP, Olivieri LJ, Krieger A, Thabit O, Marshall MB, Yoo SJ, *et al.* Utilizing three-dimensional printing technology to assess the feasibility of high-fidelity synthetic ventricular septal defect models for simulation in medical education. World J Pediatr Congenit Heart Surg 2014;5:421-6.
13. Costello JP, Olivieri LJ, Su L, Krieger A, Alfares F, Thabit O, *et al.* Incorporating three-dimensional printing into a simulation-based congenital heart disease and critical care training curriculum for resident physicians. Congenit Heart Dis 2015;10:185-90.
14. Sun Z, Lee SY. A systematic review of 3-D printing in cardiovascular and cerebrovascular diseases. Anatol J Cardiol 2017;17:423-35.
15. Giannopoulos AA, Steigner ML, George E, Barile M, Hunsaker AR, Rybicki FJ, *et al.* Cardiothoracic applications of 3-dimensional printing. J Thorac Imaging 2016;31:253-72.
16. Mayo J, Thakur Y. Pulmonary CT angiography as first-line imaging for PE: Image quality and radiation dose considerations. AJR Am J Roentgenol 2013;200:522-8.
17. Wittram C. How I do it: CT pulmonary angiography. AJR Am J Roentgenol 2007;188:1255-61.
18. den Exter PL, van der Hulle T, Klok FA, Huisman MV. Advances in the diagnosis and management of acute pulmonary embolism. Thromb Res 2014;133 Suppl 2:S10-6.
19. Righini M, Le Gal G, Aujesky D, Roy PM, Sanchez O, Verschuren F, *et al.* Diagnosis of pulmonary embolism by multidetector CT alone or combined with venous ultrasonography of the leg: A randomised non-inferiority trial. Lancet 2008;371:1343-52.
20. Sun Z, Lei J. Diagnostic yield of CT pulmonary angiography in the diagnosis of pulmonary embolism: A single center experience. Interv Cardiol 2017;9:191-8.
21. Ong CW, Malipatil V, Lavercombe M, Teo KG, Coughlin PB, Leach D, *et al.* Implementation of a clinical prediction tool for pulmonary embolism diagnosis in a tertiary teaching hospital reduces the number of computed tomography pulmonary angiograms performed. Intern Med J 2013;43:169-74.
22. Newman DH, Schriger DL. Rethinking testing for pulmonary

embolism: Less is more. Ann Emerg Med 2011;57:622-7.e3.

23. Mitsouras D, Liacouras P, Imanzadeh A, Giannopoulos AA, Cai T, Kumamaru KK, *et al.* Medical 3D printing for the radiologist. Radiographics 2015;35:1965-88.
24. Madurska MJ, Poyade M, Eason D, Rea P, Watson AJ. Development of a patient-specific 3D-printed liver model for preoperative planning. Surg Innov 2017;24:145-50.
25. Witowski JS, Coles-Black J, Zuzak TZ, Pędziwiatr M, Chuen J, Major P, *et al.* 3D printing in liver surgery: A systematic review. Telemed J E Health 2017;23:943-7.
26. Shapeways. Frequently Asked Questions. Available from: http://www.shapeways.com/support/faq?li=footer#faq-whatisshapeways. [Last accessed on 2017 Nov 29].
27. Available from: https://www.shapeways.com/materials/elasto-plastic. [Last accessed on 2017 Nov 29].
28. McCollough CH, Primak AN, Braun N, Kofler J, Yu L, Christner J, *et al.* Strategies for reducing radiation dose in CT. Radiol Clin North Am 2009;47:27-40.
29. Biglino G, Moharem-Elgamal S, Lee M, Tulloh R, Caputo M. The perception of a three-dimensional-printed heart model from the perspective of different stakeholders: A complex case of truncus arteriosus. Front Pediatr 2017;5:209.
30. Jaworski R, Haponiuk I, Chojnicki M, Olszewski H, Lulewicz P. Three-dimensional printing technology supports surgery planning in patients with complex con-genital heart defects. Kardiol Pol 2017;75:185.
31. Sahayaraj RA, Ramanan S, Subramanyan R, Cherian KM. 3D printing to model surgical repair of complex congenitally corrected transposition of the great arteries. World J Pediatr Congenit Heart Surg 2017;2017 Jan 1:2150135117704655. doi: 10.1177/2150135117704655. [Epub ahead of print].
32. Jones TW, Seckeler MD. Use of 3D models of vascular rings and slings to improve resident education. Congenit Heart Dis 2017;12:578-82.
33. Kappanayil M, Koneti NR, Kannan RR, Kottayil BP, Kumar K. Three-dimensional-printed cardiac prototypes aid surgical decision-making and preoperative planning in selected cases of complex congenital heart diseases: Early experience and proof of concept in a resource-limited environment. Ann Pediatr Cardiol 2017;10:117-25.
34. Ho D, Squelch A, Sun Z. Modelling of aortic aneurysm and aortic dissection through 3D printing. J Med Radiat Sci 2017;64:10-7.
35. Lau I, Squelch A, Wan YL, Wong A, Ducke W, Sun Z. Patient-specific 3D printed model in delineating brain glioma and surrounding structures in a pediatric patient. Digit Med 2017;3:86-92.
36. Boos J, Kröpil P, Lanzman RS, Aissa J, Schleich C, Heusch P, *et al.* CT pulmonary angiography: Simultaneous low-pitch dual-source acquisition mode with 70 kVp and 40 ml of contrast medium and comparison with high-pitch spiral dual-source acquisition with automated tube potential selection. Br J Radiol 2016;89:20151059.

Appendix IV Statements of contributions of others

Statement of Contribution of Others to (A systematic review of double low-dose CT pulmonary angiography in pulmonary embolism).

Aldosari S, Sun Z. A systematic review of double low-dose CT pulmonary angiography in pulmonary embolism. Curr Med Imaging Rev 2018 (Epub ahead of print) (IF=0.299)

To Whom It May Concern

I, Sultan Al-Dosari contributed (I designed the study and conducted image post-processing and segmentation of the CT imaging data; I performed measurements of dimensional accuracy of anatomical structures and image quality, and finally I wrote the manuscript) to the paper (Patient-specific 3D printed pulmonary artery model with simulation of peripheral pulmonary embolism for developing optimal computed tomography pulmonary angiography protocols).

Sultan Al-Dosari

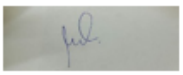

I, as a Co-Author, endorse that this level of contribution by the candidate indicated above is appropriate.

Zhonghua Sun (Signature of Co-Author 1)

"I warrant that I have obtained, where necessary, permission from the copyright owners to use any third party copyright material reproduced in the thesis or to use any of my own published work (e.g. journal articles) in which the copyright is held by another party (e.g. publisher, co-author)."

Signature 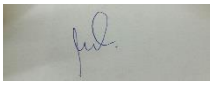

December 2018

“Every reasonable effort has been made to acknowledge the owners of copyright material. I would be pleased to hear from any copyright owner who has been omitted or incorrectly acknowledged”

Signature 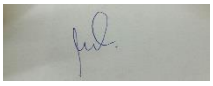

December 2018